CHARACTERISTICS OF THE ROCKET MOTOR AND FLIGHT ANALYSES OF THE SOUNDING ROCKET

Thesis

by

Frank J. Malina

In Partial Fulfilment of the Requirements for

the Degree of Doctor of Philosophy

California Institute of Technology

Pasadena, California

1940

ACKNOWLEDGEMENT:

I wish to express my sincere gratitude to Dr. Theodore von Kármán for permitting me to carry on work on the problem of rocket propulsion, a problem that is still trying to outgrow the realm of fantasy woven around it. His intellect and colorful personality have inspired in me a patience for work and a happy philosophical outlook on life.

I also wish to thank again the various men who have been connected with the work described in this thesis and especially Dr. Hsue-Shen Tsien who contributed the main ideas in Part IV and has made many valuable suggestions in the other parts.

TABLE OF CONTENTS

PART I.

CHARACTERISTICS OF THE ROCKET MOTOR UNIT BASED ON THE THEORY OF PERFECT GASES

(Accepted for publication by the Journal of The Franklin Institute).

Introduction

Recently a descriptive survey of reaction propulsion was presented by A. Ananoff[1] which gives a clear perspective of the progress that has been made during the last twenty years. During this period a number of investigators, among them Goddard[2], Esnault-Pelterie[3], Oberth[4], Sänger[5], Rinin[6], Buckingham[7], Africano[8], Vogelpohl[9], and others have studied at length the general theory of operation of the constant pressure rocket motor unit. Most of these authors have confined their analyses within the bounds of the theory of perfect gases; there remain a number of important characteristics of this propulsive unit that can be usefully discussed within these bounds before a study, based on actual operating conditions, is made.

It is found that if the formulae expressing the operation of the ideal rocket motor are transformed into dimensionless form, a universal thrust diagram can be constructed corresponding to the fixed value chosen for the ratio of the specific heats of the products of combustion. From the diagram the thrust characteristics of the motor unit can be determined for any divergent type nozzle when the rocket is operated at an arbitrary altitude.

It must be realized that the results obtained on the basis of perfect gas theory will be subject to some

alteration when the roles of such phenomena as vaporization of the propellants within the combustion chamber, variation of specific heats with temperature, dissociation of the products of combustion, heat losses, friction, and turbulence are taken into account.

In this study the general formulae that appear will be evaluated for the propellants liquid oxygen and gasoline. This combination of propellants has been accepted by most experimentors as the one that is most favorable when all factors affecting the choice of propellants are considered. They have been chosen by Goddard, who has made a large number of experiments with them, both in static test stands and in flight.

General

The term, rocket motor, has been attached to a device which liberates the available heat energy of combustion of a fuel and converts it into kinetic energy of flow in the products of combustion. Two types of rocket motors have been developed: (a) The constant pressure rocket motor uses propellants such as gases, liquids, or slow burning dry fuels, which are burned in a combustion chamber at constant or nearly constant pressure. The thrust force is delivered as long as propellants are supplied to the motor. (b) The constant volume rocket motor uses as a propellant a fast burning powder in the form of single charges fed to the combustion chamber.

The duration of combustion is so short that the burning process can be assumed to take place at constant volume and the thrust force is an impulsive force (See Ref. 10). In this paper no further mention will be made of the constant volume rocket motor.

To obtain reaction propulsion from the two propellants, liquid oxygen and gasoline, an apparatus consisting of propellant tanks, feed system, mixture control, combustion chamber, and exhaust nozzle are required. The constant pressure rocket motor unit is made up of the combustion chamber and exhaust nozzle. The thermal efficiency of reaction propulsion must take into account each component of the complete system. In the past it has been common to regard the thermal efficiency of the motor unit alone as the efficiency of the propulsive system, which helps to account for the exceedingly favorable comparisons obtained with respect to other thermal engines. The assumption that the motor efficiency is the principal propulsive parameter is justified if the propellants are fed to the combustion chamber by pressure cells that are charged before flight is begun. However, the work required to charge the cells should not be neglected if comparison is made with other types of heat engines. If feed pumps must be used during flight, the work necessary to operate them cannot be overlooked in calculating the overall thermal efficiency of the system.

It is important to stress the significance of the thermal efficiency of the motor unit in rocket

propulsion. If the reaction system is to be used to propel a sounding rocket, the overall thermal efficiency of a system using pressure-cell feed can be replaced by the thermal efficiency of the motor unit, especially if the sounding rocket is to reach as high an altitude as possible. In this case the performance of the rocket will not depend on the efficiency of the work done on the ground, but only on the efficient transformation of the heat energy into as high an effective exhaust velocity as possible.

The Propellants

The constant pressure rocket motor system appears to possess advantages over other forms of propulsion in being able: first, to deliver a large thrust, which can be varied with great flexibility; second, to operate *in vacuo* as long as an oxidizer is carried to burn the fuel, which is a characteristic of all reaction propulsion systems.

The first characteristic has caused the suggestion to be made that the rocket motor be used to improve certain phases of heavier-than-air performance, such as take-off and climb. To deliver a large thrust large quantities of combustibles must be consumed-- a requirement that practically eliminates the use of the gaseous form of combustibles, as the supply tanks would be excessively large and heavy. If the second characteristic of the rocket motor is to be exploited in the

sounding rocket, performance studies show that it is necessary that supply tanks be as small and as light as possible. For these reasons liquid propellants are the ones most likely to be useful.

The fuel used should have a high heat content and require a minimum of oxidizer to burn it completely. In other words, the heat content per pound of fuel and oxidizer necessary for its combustion should be high.

A liquid fuel can be chosen from a number of cheap, easily handled, and readily obtainable hydrocarbons. Gasoline appears to be the most general choice. To burn the fuel liquid oxygen is the most desirable oxidizer.

The characteristics of gasoline vary considerably depending on the nature of the crude oil and the process of preparation. Gasoline consists principally of a mixture of three different series of hydrocarbons:

a) Paraffins,

b) Naphthenes,

c) Aromatics,

For thermodynamic analysis it has been found that gasoline can be closely represented by octane, therefore this chemical formula will henceforth be used. A value of 18,800 B.t.u./lb has been chosen for the lower heat of combustion of the fuel.

Theory of the Rocket Motor with Perfect Gases

Throughout this analysis it is assumed that

the perfect gas relations apply to the processes encountered in the rocket motor unit, that is, the specific heats of the products of combustion once chosen are considered constant. Furthermore, it is assumed that none of the heat liberated in the chamber is lost through dissociation or by conduction and radiation through the walls of the chamber and of the nozzle or through friction, turbulence, and condensation of the gases in the nozzle. The heat of vaporization is also neglected.

On the basis of these assumptions the chemical equation for the combustion process can be written:

$$C_8H_{18} + 12.5\,O_2 \longrightarrow 8\,CO_2 + 9\,H_2O \qquad (1)$$

To burn one pound of gasoline 3.51 pounds of oxygen are required. The products of combustion consist of 3.09 pounds of carbon dioxide and 1.42 pounds of water vapor. During this reaction the heat of combustion of the fuel is liberated and appears in the form of increased temperature in the products of combustion.

The specific heats of the products of combustion vary greatly with the temperature. A study of their variation with temperature shows that their values increase with the temperature. Since the gas is at high temperature during most of its stay in the rocket motor, a fairly low value of the ratio of $c_p/c_v = \gamma$ can be expected. For the propellants oxygen and gasoline a value of 1.2 has been chosen for γ. Furthermore it is assumed that the values of c_p and c_v in B.t.u./mol/°F are

the same for both CO_2 and H_2O . Therefore for the products of combustion $8CO_2$ and $9H_2O$ with $\gamma = 1.2$ and R = 1.986 B.t.u./mol/°F = 0.0658 B.t.u./lb./°F

We obtain

$$C_p = 11.916 \text{ B.t.u./mol/°F} = 0.395 \text{ B.t.u./lb./°F}$$
$$C_v = 9.930 \text{ B.t.u./mol/°F} = 0.329 \text{ B.t.u./lb./°F}$$

The second law of thermodynamics states that of a given quantity of heat applied to a working substance only a part can be transformed into useful energy. Before attempting to use the heat energy available in the gasoline it is, therefore, desirable first to determine the maximum possible efficiency obtainable in the ideal case of the engine. An aid to the understanding of the operation of a heat engine is found in discussing its cycle of operations.

The diagram in Fig. 1a shows the components of the reaction propulsion system. Consider a mass of propellant, m, composed of gasoline and sufficient oxygen to burn it completely, flowing per second from the supply tanks at a. Between a and b' the pressure of the propellants is increased and vaporization is completed. At b' the propellants are fed into the combustion chamber in the state p_b', V_b' and T_b' . From b' to c the mixture is burned at constant pressure and the available heat of the gasoline is liberated. The state of the products of combustion, CO_2 and H_2O, is determined by p_c, V_c and T_c . At c the burned gases enter the

exhaust nozzle and the liberated heat is transformed into kinetic energy of flow by an adiabatic expansion process. The jet energy acquired will be equal to the adiabatic drop in heat content of the products of combustion. If the expansion is complete, the state of the gases at e is determined by p_e, V_e and T_e. The remainder of the cycle can be imagined to be completed by nature. The cycle is made up of two adiabatic processes and two constant pressure processes (Fig.1b). The work done during the cycle is represented by the area enclosed by ab'ce in the temperature-entropy diagram. The available heat liberated during the combustion process is expressed by:

$$H_p = m g c_p (T_c - T_{b'}) = m g c_p \Delta T \qquad (2)$$

where H_p = lower heat of combustion of a unit weight of propellant mixture, B.t.u. per lb. at constant pressure,

c_p = specific heat constant of the products of combustion at constant pressure, B.t.u. per lb. per degree Fahrenheit,

T = temperature, ° F. abs.

For the propellants considered

$$\Delta T = 10,560 \ ^\circ F \qquad (3)$$

Heat is rejected from e to a at constant pressure so that

$$H_c = m g c_p (T_e - T_a) \qquad (4)$$

The ideal cycle efficiency is given by the relation

$$\eta_i = \frac{\text{Work done in B.t.u.}}{\text{Heat available in B.t.u.}} = \frac{H_p - H_e}{H_p} = 1 - \frac{T_e - T_a}{T_c - T_{b'}} \qquad (5)$$

If it is assumed that $T_a \ll T_e$ and $T_{b'} \ll T_c$ so that T_a and $T_{b'}$ can be neglected, then

$$\eta_i = \frac{T_c - T_e}{T_c} \tag{6}$$

but the ideal gas law $pV = RT$ gives

$$T_c = \frac{p_c V_c}{R} \quad \text{and} \quad T_e = \frac{p_e V_e}{R} \tag{7}$$

Therefore, $$\eta_i = \frac{p_c V_c - p_e V_e}{p_c V_c} \tag{8}$$

Since the expansion from c to e is adiabatic, the following relation holds:

$$p_c V_c^{\gamma} = p_e V_e^{\gamma} \tag{9}$$

and finally $$\eta_i = 1 - \left(\frac{p_e}{p_c}\right)^{\frac{\gamma-1}{\gamma}} \tag{10}$$

For the products of combustion of gasoline and oxygen with $$\gamma = 1.2 \tag{11}$$

it follows that $$\eta_i = 1 - \left(\frac{p_e}{p_c}\right)^{0.167} \tag{12}$$

This relation for the ideal cycle efficiency shows that the efficiency increases with the expansion ratio, i.e., with an increasing chamber pressure and a decreasing back pressure. In Fig.2 the variation of the ideal cycle efficiency with the pressure ratio is shown.

The experimenter has found it more convenient to define a thermal efficiency η_{th} of the rocket motor unit in terms of the kinetic energy of the outflowing products of combustion and the available heat energy of

the fuel, thus the familiar form is:

$$\eta_{th} = \frac{A\,(w_f + w_{o_2})\,c^2}{2g\,w_f\,H_{p_f}} \qquad (13)$$

where A = mechanical equivalent of heat $\frac{1}{777.6}$ ft.lb/B.t.u.

w_f = weight of fuel in lbs. burned per second

w_{o_2} = " " oxygen in lbs. used " "

c = effective exhaust velocity, ft. per second (The quantity c will be discussed later)

H_{p_f} = lower heat of combustion of fuel, B.t.u. per lb. at constant pressure

In Fig.3 the thermal efficiency η_{th} is plotted against the effective exhaust velocity c for the ideal oxygen-gasoline motor.

Ideal Transformation of Available Heat Energy

The first correct treatment of the elementary theory of the discharge of gases under high pressure was published by Saint-Venant and Wantzel. The theory has since been extended and applied in the de Laval nozzle. The de Laval divergent nozzle converts the available heat energy liberated in the combustion chamber into kinetic energy of flow of the exhaust gases. (See Ref.11).

This conversion of energy is most complete when an adiabatic expansion takes place in the nozzle. The theory of the de Laval nozzle is so well known that the formulae employed will not be derived. However, the

formulae will be expressed in dimensionless form which will make possible the construction of a universal thrust diagram for the ideal rocket motor unit using any chosen propellants. The diagram is universal in that from the diagram constructed for the fixed value of γ the propulsive characteristics of the motor unit with any de Laval type nozzle can be immediately determined.

In Fig. 4 a diagram of a divergent type nozzle is shown with the notation used for its dimensions. The rate of flow of the products of combustion under a pressure p_c in the combustion chamber is controlled by the existence of a critical pressure p_t at the nozzle throat. The throat is the narrowest cross-section through which the gas flows. It is known that the rate of flow of a gas through the throat will increase up to the point that the exit pressure reaches the critical pressure at the throat, thereafter the rate of flow will remain constant. It will be assumed that the critical pressure always prevails in the throat. The ratio of the critical pressure to the chamber pressure is given by:

$$\frac{p_t}{p_c} = \left(\frac{2}{\gamma+1}\right)^{\frac{\gamma}{\gamma-1}} \tag{14}$$

If the critical pressure prevails at the throat, the velocity of flow of the gas through it will be equal to the sonic velocity of the gas corresponding to its state in the throat. The velocity of flow through the throat can also be expressed in terms of the conditions in the combustion chamber:

$$v_t = \sqrt{\frac{2gR\gamma T_c}{\gamma+1}} \tag{15}$$

The velocity of sound corresponding to the conditions in combustion chamber is expressed by the relation:

$$a_c = \sqrt{g\gamma R T_c} \tag{16}$$

so that eq. (15) can be written in dimensionless form:

$$\frac{v_t}{a_c} = \sqrt{\frac{2}{\gamma+1}} \tag{17}$$

The rate of flow of propellants is given by:

$$W = \frac{f_t v_t}{V_t} = \left(\frac{2}{\gamma+1}\right)^{\frac{\gamma+1}{2(\gamma-1)}} \frac{f_t p_c a_c}{R T_c} \tag{18}$$

where f_t = area of cross-section of the nozzle throat.

As the flow in the nozzle has been assumed to follow an adiabatic process, the following expression can be written for the conservation of energy:

$$C_p T_c = \frac{v_x^2}{2g} + c_p T_x \tag{19}$$

so that the velocity at any cross-section is given by:

$$v_x = \sqrt{2g c_p T_c (1 - T_x/T_c)} \tag{20}$$

or

$$\frac{v_x}{a_c} = \sqrt{\frac{2}{\gamma-1}\left(1 - \frac{T_x}{T_c}\right)} \tag{21}$$

also

$$\frac{v_x}{a_c} = \sqrt{\frac{2}{\gamma-1}\left[1 - \left(\frac{p_x}{p_c}\right)^{\frac{\gamma-1}{\gamma}}\right]} \tag{22}$$

This equation shows that the liberated heat energy will be completely transformed into kinetic energy of flow when the pressure at the exhaust section is zero. Thus the ideal transformation of the heat energy is the optimum when the rocket motor is operated in vacuo.

Heretofore it has been assumed that the gas flowing through the exhaust nozzle has either been completely expanded to the external pressure or that expansion has not been completed so that the gas passes the exit cross-

section at a pressure higher than the external pressure. If, however, the expansion ratio $\frac{f_x}{f_t}$ is too great, overexpansion of the gas will result and if the overexpansion is continued a shock wave may occur.

It is possible that before overexpansion takes place the jet will separate from the walls of the nozzle, in which case the most efficient transformation of the available heat energy into velocity will not be effected. It will be assumed that the jet does not separate; hence overexpansion to some pressure below the external pressure is possible.

Experiments with gases flowing at high velocity in an expanding nozzle show that if overexpansion is continued, when the external pressure p_0 is greater than zero, at some pressure p_{x_s} a sudden change in the characteristics of the gas flow will result. The flow characteristics again reach a steady state after passing through a narrow transition layer. The thickness of the transition layer is extremely small so that it can be assumed that there is a discontinuity in the flow characteristics. The transition layer is known as a "shock wave." (For the basis of this discussion and of the following analysis see Ref.12).

If the divergence angle of the nozzle is small, it can be assumed that the shock wave is a "plane shock wave", i.e., the change in flow characteristics takes place across a plane perpendicular to the nozzle axis.

Denoting for all points on the inner side of

the wave the velocity, pressure, and mass density by v_{s_1}, p_{s_1}, and ρ_{s_1}, $(\rho = \frac{1}{Vg})$, and on the outer side by v_{s_2}, p_{s_2}, and ρ_{s_2}, the equation of continuity can be written:

$$\rho_{s_1} v_{s_1} = \rho_{s_2} v_{s_2} = m_a \tag{23}$$

where m_a is the mass which crosses a unit area of the shock wave per second. The equation for the conservation of momentum is

$$p_{s_1} - p_{s_2} = m_a (v_{s_1} - v_{s_2}) \tag{24}$$

and the condition of the conservation of energy is

$$p_{s_1} v_{s_1} - p_{s_2} v_{s_2} - \frac{1}{2} m_a (v_{s_2}^2 - v_{s_1}^2) = \frac{m_a}{\gamma - 1} \left(\frac{p_{s_2}}{\rho_{s_2}} - \frac{p_{s_1}}{\rho_{s_1}} \right) \tag{25}$$

Making use of eq. (23) and eq. (24) the energy equation can be written in the form:

$$\frac{1}{2} (p_{s_1} + p_{s_2}) \left(\frac{1}{\rho_{s_1}} - \frac{1}{\rho_{s_2}} \right) = \frac{1}{\gamma - 1} \left(\frac{p_{s_2}}{\rho_{s_2}} - \frac{p_{s_1}}{\rho_{s_2}} \right) \tag{26}$$

This relation is known as the Rankine-Hugoniot equation. Solving for ρ_{s_1} / ρ_{s_2} the equation is obtained in the form:

$$\frac{\rho_{s_1}}{\rho_{s_2}} = \frac{(\gamma - 1) p_{s_1} + (\gamma + 1) p_{s_2}}{(\gamma - 1) p_{s_2} + (\gamma + 1) p_{s_1}} \tag{27}$$

From eq. (23):

$$\frac{v_{s_1}}{v_{s_2}} = \frac{\rho_{s_2}}{\rho_{s_1}} \tag{28}$$

and

$$\frac{p_{s_2}}{p_{s_1}} = \frac{2\gamma}{\gamma + 1} \left(\frac{v_{s_1}}{a_{s_1}} \right)^2 - \frac{\gamma - 1}{\gamma + 1} \tag{29}$$

where

$$a_{s_1} = \sqrt{\frac{p_{s_1} \gamma}{\rho_{s_1}}} = \text{velocity of sound corresponding to the conditions of the gas on the inner side of the shock wave.} \tag{30}$$

Since an adiabatic process has been assumed up to the point that the shock wave occurs, equation (26) can be expressed in terms of the chamber pressure:

$$\frac{p_{s_2}}{p_{s_1}} = \frac{4\gamma}{\gamma^2-1}\left[\left(\frac{p_c}{p_{s_1}}\right)^{\frac{\gamma-1}{\gamma}} - 1\right] - \frac{\gamma-1}{\gamma+1} \qquad (31)$$

By means of eq. (31) the pressure p_{s_1} to which the gas must be expanded to cause a shock wave with the pressure p_{s_2} on the outer side can be determined. Further, the pressure p_{s_2} cannot exceed the external pressure. For the rocket motor unit p_{s_2} cannot be greater than the pressure p_o that prevails at the altitude at which the rocket is being operated. The value of p_{s_1} will be the greatest when $p_{s_2} = p_o$ is the atmospheric pressure at sea level. Therefore at sea level the shock wave will occur the closest to the nozzle throat. The cross-section at which the shock wave first occurs will be called the "critical shock cross-section".

To determine the area of the "critical shock cross-section" $f_{x_s}^*$, the pressure p_{s_1} is calculated for $p_{s_2} = p_o$ (this is done most easily graphically). Then $f_{x_s}^*$ is obtained from the relation:

$$\frac{f_x}{f_t} = \frac{\left(\frac{2}{\gamma+1}\right)^{\gamma+1/2(\gamma-1)}}{\left(\frac{p_x}{p_c}\right)^{\frac{1}{\gamma}}\sqrt{\frac{2}{\gamma-1}\left[1-\left(\frac{p_x}{p_c}\right)^{\frac{\gamma-1}{\gamma}}\right]}} \qquad (32)$$

by putting $f_x = f_{x_s}^*$ and $p_x = p_{s_1}$. Equation (32) can be derived from the equation of state

$$f_x = \frac{w R T_x}{v_x p_x} \qquad (33)$$

and the relations for an adiabatic expansion.

If $f_{x_s}^*$ is greater than the area of the exit section f_e, of the nozzle, the shock wave will occur outside of the nozzle and the characteristics of the flow in the nozzle are those corresponding to an adiabatic expansion from the combustion chamber. If $f_{x_s}^* = f_e$ the characteristics of the flow will be effected at the exit cross-section. If $f_{x_s}^* < f_e$ the gas will expand further, disregarding the possibility of separation, and give rise to a shock wave for which $p_{s_2} < p_0$ so that the gas will be compressed after the shock wave has been passed. The compression of the gas cannot, however, raise the pressure at the exit cross-section above the external pressure. With compression after the shock wave the shock wave will occur closest to the throat when the gas is just compressed to the external pressure at the exit cross section. In Fig. 5 a diagram shows the various regions discussed. (See Ref.11).

The characteristics of the flow in the region following a shock wave can be determined by making use of the relations for adiabatic compression. The velocity of flow at the exit section if $f_e > f_{x_s}^*$ is simply determined using the equation of state:

$$v_{x_s} = v_e = \frac{w R T_e}{f_e p_0} \tag{34}$$

and the equation for the conservation of energy:

$$c_p T_c = c_p T_e + \frac{1}{2g} v_e^2 \tag{35}$$

which gives upon evaluating T_e in eq. (34) from eq. (35), substituting eq. (18) for w, and remembering the relation for a_c :

$$v_e^2 + \frac{2 a_c f_e p_o}{(\gamma-1)\left(\frac{2}{\gamma+1}\right)^{\gamma+1/2(\gamma-1)} f_t p_c} v_e - \frac{2 a_c^2}{\gamma-1} = 0 \tag{36}$$

Solving for v_e and writing it in dimensionless form:

$$\frac{v_e}{a_c} = - \frac{\left(\frac{\gamma+1}{2}\right)^{\frac{\gamma+1}{2(\gamma-1)}}}{\gamma-1} \frac{f_e p_o}{f_t p_c} + \left[\frac{\left(\frac{\gamma+1}{2}\right)^{\frac{\gamma+1}{\gamma-1}}}{(\gamma-1)^2} \left(\frac{f_e p_o}{f_t p_c} \right)^2 + \frac{2}{\gamma-1} \right]^{\frac{1}{2}} \tag{37}$$

The solution of the quadratic relation (36) gives for the second term a $\pm$ sign. If the minus sign is chosen, the velocity v_e, will be supersonic, which is not possible in the flow with compression after the shock wave. Therefore the positive sign has been retained, which assures a subsonic flow.

The transformation of heat energy into kinetic energy of flow and into pressure causes a force to act in the direction opposite to the flow of the exhaust gases. By application of the momentum theorem to the flow through the nozzle the following relation between the pressure forces and the force due to the change in momentum of the gases can be written:

$$\int p \, dS - \int (p_e - p_o) \, df_e = \int v_{e_x} \, dm \tag{38}$$

where p = absolute pressure acting on the walls of the

exhaust nozzle and combustion chamber, lbs. per sq. in.

dS = elementary surface area of the walls of the exhaust nozzle and combustion chamber, sq.in.

v_{e_x} = axial component of the exhaust velocity at the exit cross-section of the nozzle, ft. per sec.

dm = element of mass of propellant flowing through the exit section of the nozzle per second, slugs per second.

The first integral is to be taken over the whole surface area of the exhaust nozzle and combustion chamber. The second and third integrals are taken over the exit section of the nozzle only.

The first integral corresponds to the thrust of the rocket motor which is designated by $F = \int p\, dS$, and third integral is given by $(p_e - p_o) f_e$, so that

$$F = \int_{f_e} v_{e_x}\, dm + (p_e - p_o) f_e \tag{39}$$

If it is assumed that the flow at the exit section is uniformly radial* (see Fig.6), then

$$v_{e_x} = v_e \cos\Theta \tag{40}$$

The mass of propellants flowing through a ring of width $R\,d\Theta$ on the spherical surface f_e' is expressed by

$$dm = \rho v_e\, df_e' \tag{41}$$

Therefore,

$$\int_{f_e} v_{e_x}\, dm = 2\pi R^2 \rho v_e^2 \int_0^{\alpha} \sin\Theta\cos\Theta\, d\Theta \tag{42}$$

* I am indebted to Dr.H.S. Tsien for this analysis.

integrating and expressing R in terms of f_e',

$$\int_{f_e} v_{e_x}\, dm = \rho v_e f_e' \cdot v_e \cdot \frac{1-\cos 2\alpha}{4(1-\cos\alpha)} \qquad (43)$$

However, $\rho v_e f_e' = m$, the mass of propellant flowing through the exit section per second, and if we write $\lambda = \frac{1-\cos 2\alpha}{4(1-\cos\alpha)}$, then

$$\int_{f_e} v_{e_x}\, dm = \lambda m v_e \qquad (44)$$

Hence, the thrust of the rocket motor can be written in the form:

$$F = \lambda m v_e + (p_e - p_0) f_e \qquad (45)$$

It is seen that only the momentum term is affected by the angle of divergence of the nozzle. In Fig. 7 the variation of λ with the nozzle angle α, is shown. The small decrease in λ up to divergent angles of 35° is worthy of notice as it may permit an efficient use of shorter nozzles for a correct expansion ratio. This makes possible a reduction in the weight of the nozzle and in the surface area of the nozzle through which heat losses occur. Therefore an optimum nozzle for the rocket motor will probably have a much larger divergent angle than is usual in the design of the de Laval steam nozzle.

Eq.(30) for the thrust developed by a constant pressure rocket motor is seen to consist of two parts; the first part can be called the "velocity thrust" F_v, and the second part the "pressure thrust" F_p, that is,

$$F = F_v + F_p \qquad (46)$$

also

$$F = mc \qquad (47)$$

where $c = \lambda v_e + \frac{(p_e - p_0)}{m} f_e$ = effective exhaust velocity.

The latter form is most generally used, as the value of the effective exhaust velocity c can be easily calculated if the thrust delivered by the motor and the rate of flow of combustibles are known. The thermal efficiency η_{th} expressed by eq. (13) is evaluated in terms of c.

The thrust delivered by an ideal rocket motor unit can now be expressed for the regimes of flow discussed before and illustrated in Fig. 5. For the case in which the area of the exit is smaller than $f_{x_s}^*$ the thrust F_x for a motor whose nozzle is cut at any section $x \geq x_t$, where x_t is the throat location, is obtained in dimensionless form from eqs. (45), (18), and (22):

$$\frac{F_x}{F_t} = \frac{\lambda \sqrt{\frac{2\gamma^2}{\gamma-1}\left(\frac{2}{\gamma+1}\right)^{\frac{\gamma+1}{\gamma-1}}\left[1-\left(\frac{p_x}{p_c}\right)^{\frac{\gamma-1}{\gamma}}\right]} + \left(\frac{p_x}{p_c} - \frac{p_0}{p_c}\right)\frac{f_x}{f_t}}{2\left(\frac{2}{\gamma+1}\right)^{\frac{1}{\gamma-1}} - \frac{p_0}{p_c}} \qquad (48)$$

where

$$F_t = \left[2\left(\frac{2}{\gamma+1}\right)^{\frac{1}{\gamma-1}} p_c - p_0\right] f_t \qquad (49)$$

is the thrust that would be delivered by the motor unit if the nozzle terminated at the throat, i.e., there is no divergent nozzle part.

If the exit area is equal or greater than $f_{x_s}^*$, then a shock wave will occur and the thrust, F_{x_s}, is obtained in dimensionless form with respect to F_t from

eqs. (45), (18), and (37):

$$\frac{F_{x_s}}{F_t} = \frac{\lambda\gamma}{\gamma-1} \frac{-\frac{p_o f_{x_s}}{p_c f_t} + \sqrt{\left(\frac{p_o f_{x_s}}{p_c f_t}\right)^2 + 2(\gamma-1)\left(\frac{2}{\gamma+1}\right)^{\frac{\gamma+1}{\gamma-1}}}}{2\left(\frac{2}{\gamma+1}\right)^{\frac{1}{\gamma-1}} - \frac{p_o}{p_c}} \qquad (50)$$

In Fig. 8 a universal ideal thrust diagram has been constructed for an ideal rocket motor unit for $\gamma = 1.2$ and for $\lambda = 1$. As the preceding theory predicted, the efficiency and, therefore, the maximum thrust corresponding to complete expansion to p_o increases as the ratio p_o/p_c decreases. The curve of maximum thrust is indicated by a dotted line.

The fact that over-expansion, if jet separation does not occur, can seriously affect the thrust delivered by the motor, is clearly evident. The possibility of a shock wave occurring in the nozzle is remote unless very low chamber pressures, of the order of 200 to 300 pounds per square inch, are used when p_o is large, or unless the nozzle is built with much too large an expansion ratio

.

The diagram brings out another important fact. If a nozzle is designed to give the maximum thrust at sea level then the thrust delivered at other altitudes, where the external pressure is much lower, will be less than the amount that can theoretically be obtained. If on the other hand the nozzle is designed to give the maximum possible thrust at a high altitude, then the loss in thrust at lower altitudes may be so great that operation

of the rocket will be seriously impaired.

In drawing these conclusions it must be remembered that several simplifying assumptions have been made. It is planned to extend this study of the ideal rocket motor to learn to what extent the effects predicted will be valid for an actual rocket motor.

To illustrate the use of the universal ideal thrust diagram, the characteristics of the following rocket motor unit will be determined:

p_c = 1470 lb/sq. in.abs. $\quad d_t$ = throat diameter = 1 inch

p_o = 14.7 lb/sq.in.abs. $\quad f_t$ = 0.786 sq.in.

$\frac{p_o}{p_c}$ = 0.01 $\quad \alpha$ = 15

T_c = 11,970 °F abs. $\quad \lambda$ = 0.985

γ = 1.2

Since λ for this example differs from 1 by only a small amount, the diagram in Fig. 8 for $\lambda = 1$ can be used. From Fig. 8 it is found that the maximum thrust along the curve $p_o/p_c = 0.01$ is obtained for an expansion ratio of :

$$\frac{f_x}{f_t} = \frac{f_e}{f_t} = 11.85$$

The thrust ratio corresponding to this expansion ratio is:

$$\frac{F}{F_t} = 1.338$$

and eq. 49 gives $F_t = 1395$ lb. , therefore,

$$F = 1865 \text{ lb.}$$

Conclusion

This analysis of the ideal constant pressure rocket motor was made to bring out most of its operating characteristics and to determine the relative importance of various factors that affect its operation. The assumptions introduced greatly reduced the complexity of the mathematical analysis. However, the main features of operation of the actual constant pressure rocket motor will still be the same as for the ideal motor, therefore, the simple general theory presented can be used as a guide by the designer.

The author has been fortunate that during the conduction of this study he has been able to discuss many of its parts with Dr. Theodore de Kármán and especially with Dr. Hsue-shen Tsien. Also, an expression of indebtedness is due to Messrs. J.W. Parsons, A.M.O. Smith, E.S. Forman, and J.W. Braithwaite- members of the rocket research group of the Guggenheim Aeronautical Laboratory at the California Institute of Technology.

References

1. Ananoff, A.: "Comment fonctionne une fusee a combustible et comburant liquide", L'Aerophile, Vol. 46, pp. 157-161, 181-185, 204-208, 1938.

2. Goddard,R.H.:"Liquid-Propellant Rocket Development", Smithsonian Miscellaneous Collections, Vol. 95, No.3, 1936.

3. Esnault-Pelterie,R.: "L'Astronautique", pp. 109-151,Imrimerie A. Lahure, Pub., Paris, 1930.

4. Oberth, H. : "Wege zur Raumschiffahrt", pp. 23-36, R. Oldenbourg, Pub., München, 1929.

5. Sänger, E. : "Raketen-Flugtechnik", pp. 4-75, R. Oldenbourg, Pub., München, 1933.

6. Rinin, N.A.: "Propulsione a reazione senza utilizzazione dell' aria", Quinto Convegno Volta, Roma, pp. 628-636, 1935.

7. Buckingham,E.:"Jet Propulsion for Airplanes", N.A.C.A. Rep. 159, 1923.

8. Africano, A.: "Rocket Motor Efficiency", Astronautics, No. 37, pp. 13-16, 1937.

9. Vogelpohl, G.:"Uber den Impulssatz der Strömungslehre", Forschung aug dem Gebiete des Ingenieurwesens, Vol.8, pp. 35-41, 1937.

10. Tsien, H.S. and Malina, F.J.: "Flight Analysis of a Sounding Rocket with Special Reference to Propulsion by Successive Impulses", Jour. of Aero. Sciences, Vol. 6, No.2, pp. 50-58, 1938.

11. Stodola, A. : "Steam and Gas Turbines", Vol. 1,pp. 36 -48, 102-104; Vol II, pp. 1012-1016, 1173-1178, McGraw-Hill, New York 1927.

12. Durand,W.F.: "Aerodynamic Theory", Vol.III, Div.H, pp. 209-229, pp. 234-241, by G.I. Taylor and J.W. Maccoll, J. Springer, Pub., Berlin, 1935.

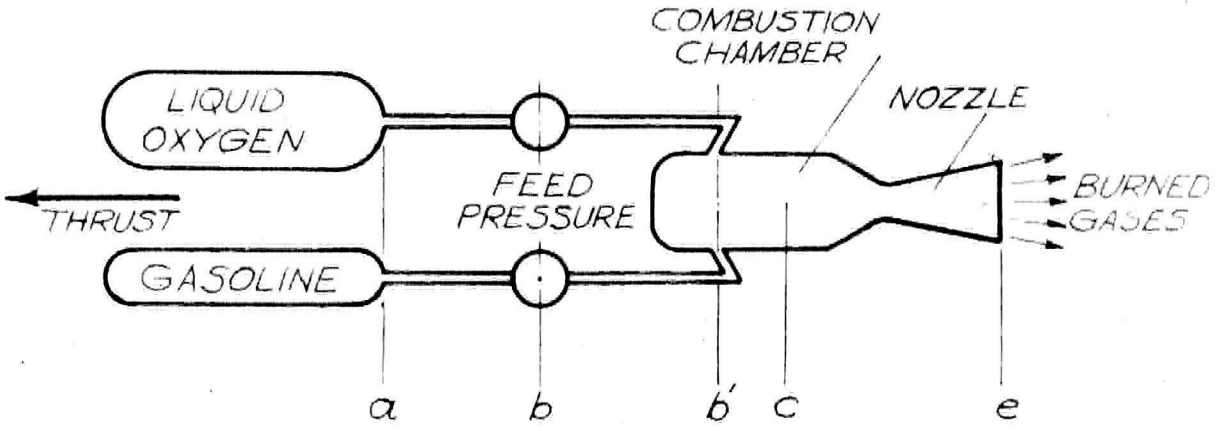
COMBUSTION
CHAMBER
NOZZLE
LIQUID
OXYGEN
FEED
PRESSURE
BURNED
GASES
THRUST
GASOLINE
a
b
b'
c
e

(a)

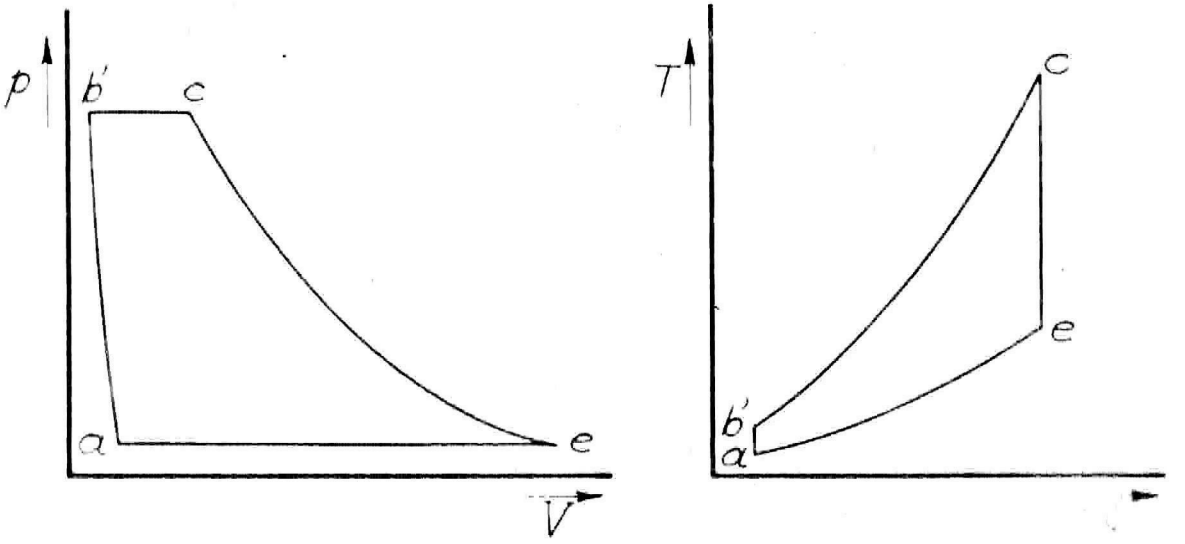
p
b'
c
a
e
V
T
c
e
b'
a

(b)

FIG. 1

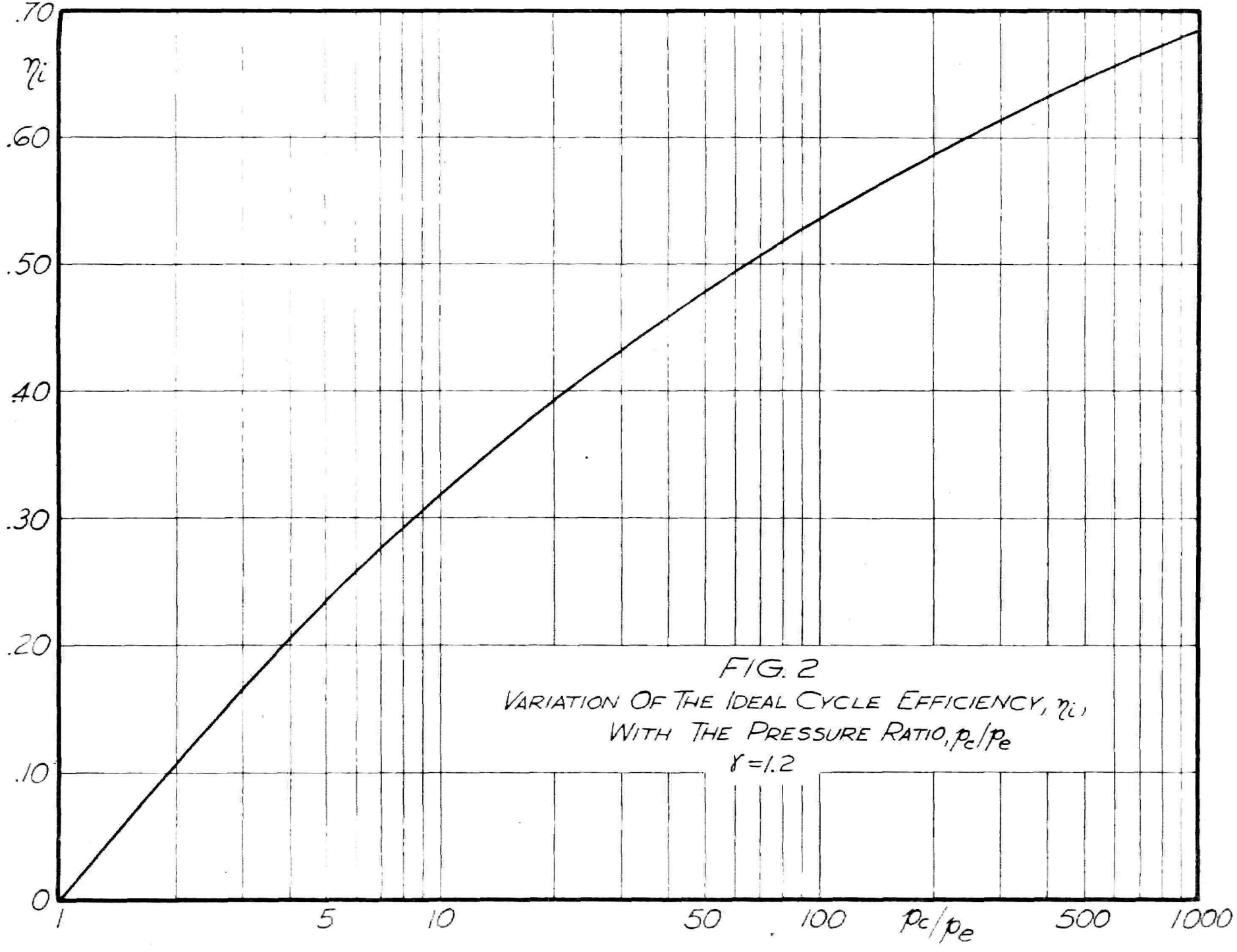

FIG. 2
VARIATION OF THE IDEAL CYCLE EFFICIENCY, η_i,
WITH THE PRESSURE RATIO, p_c/p_e
$\gamma = 1.2$

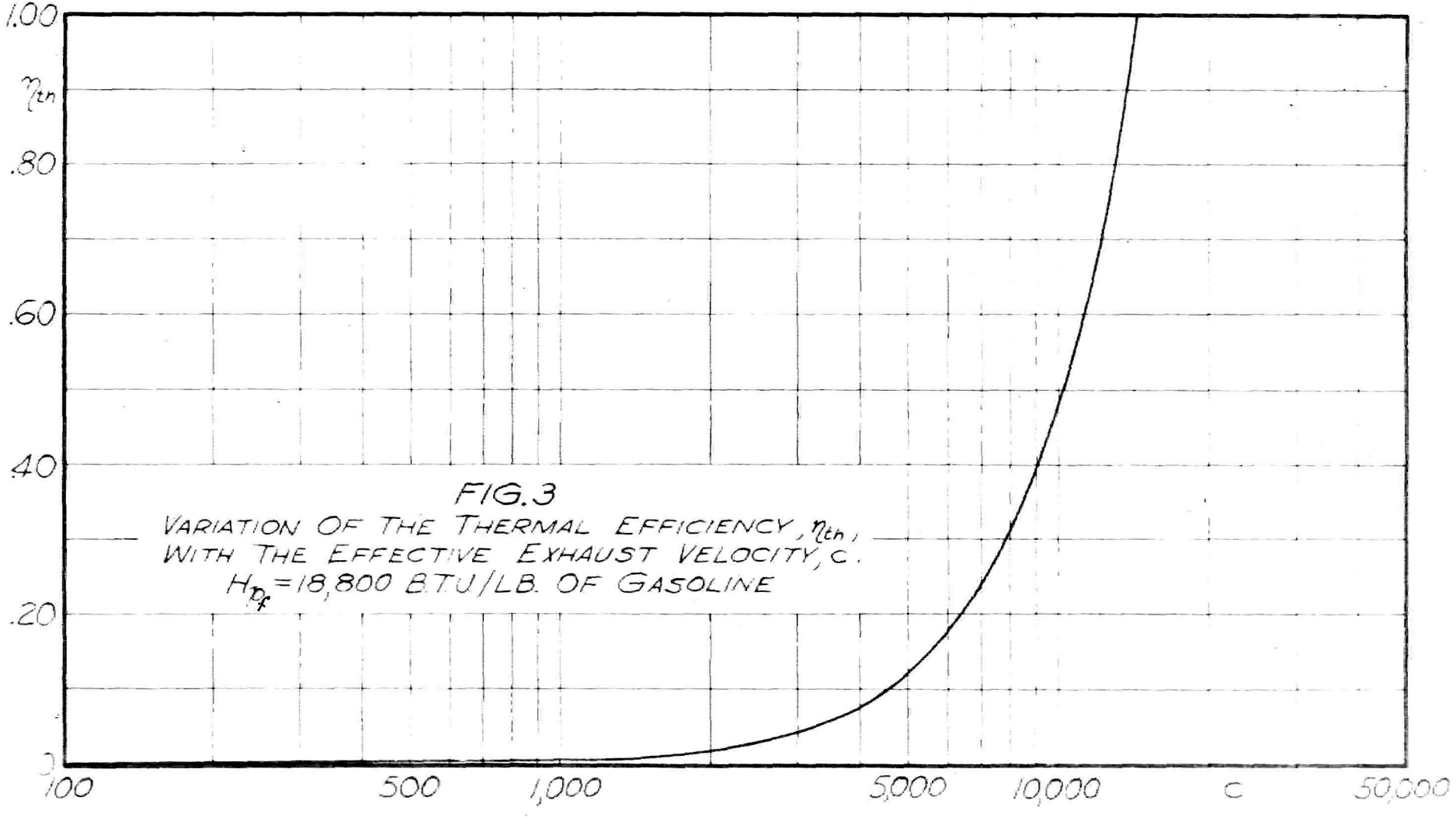

FIG. 3
VARIATION OF THE THERMAL EFFICIENCY, η_{th}, WITH THE EFFECTIVE EXHAUST VELOCITY, c.
H_{p_f} = 18,800 B.T.U/LB. OF GASOLINE

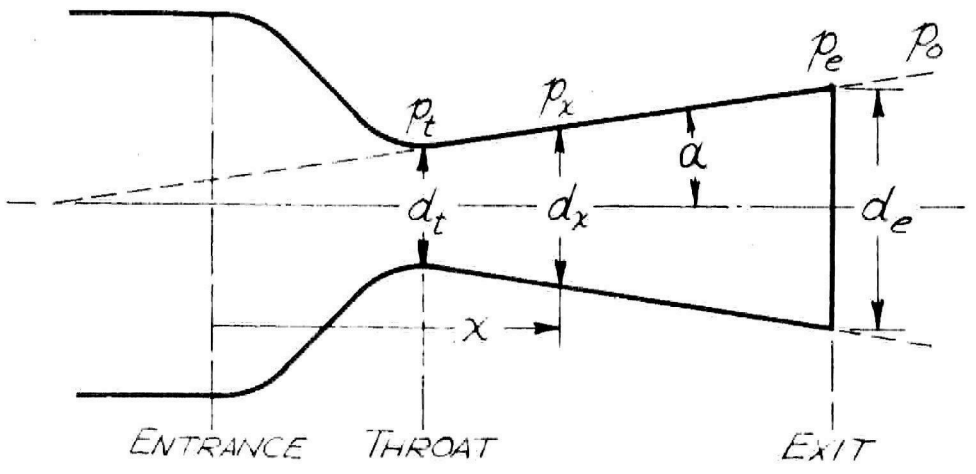

FIG. 4

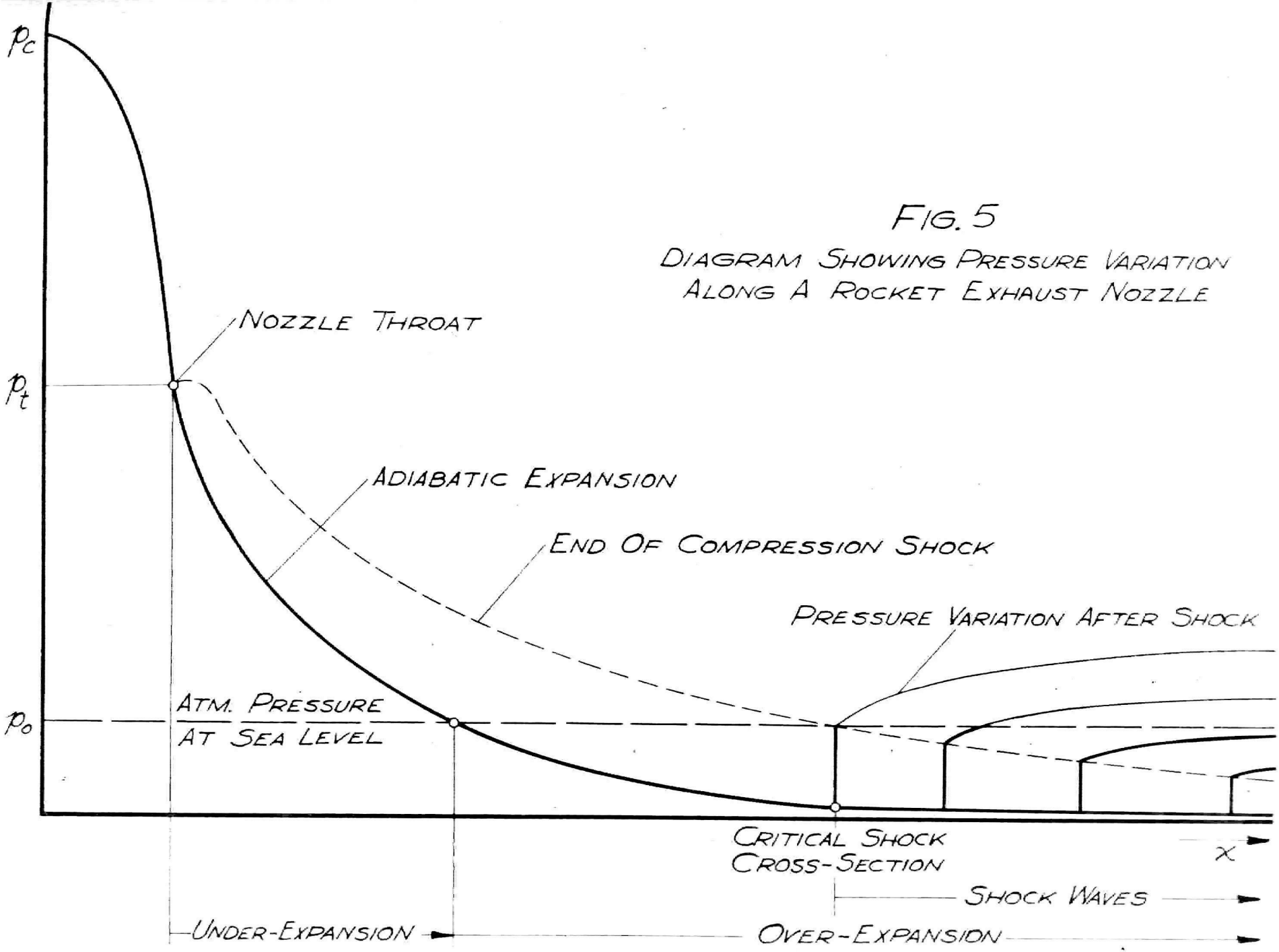

FIG. 5

DIAGRAM SHOWING PRESSURE VARIATION
ALONG A ROCKET EXHAUST NOZZLE

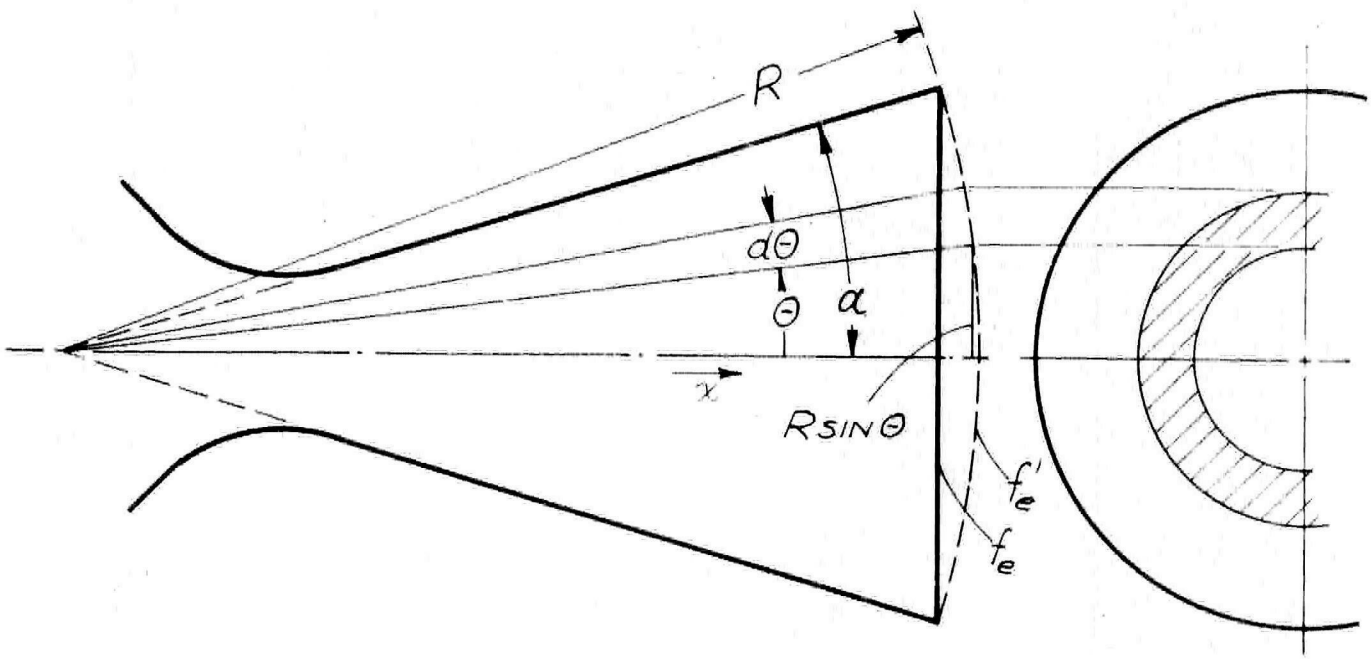

FIG. 6

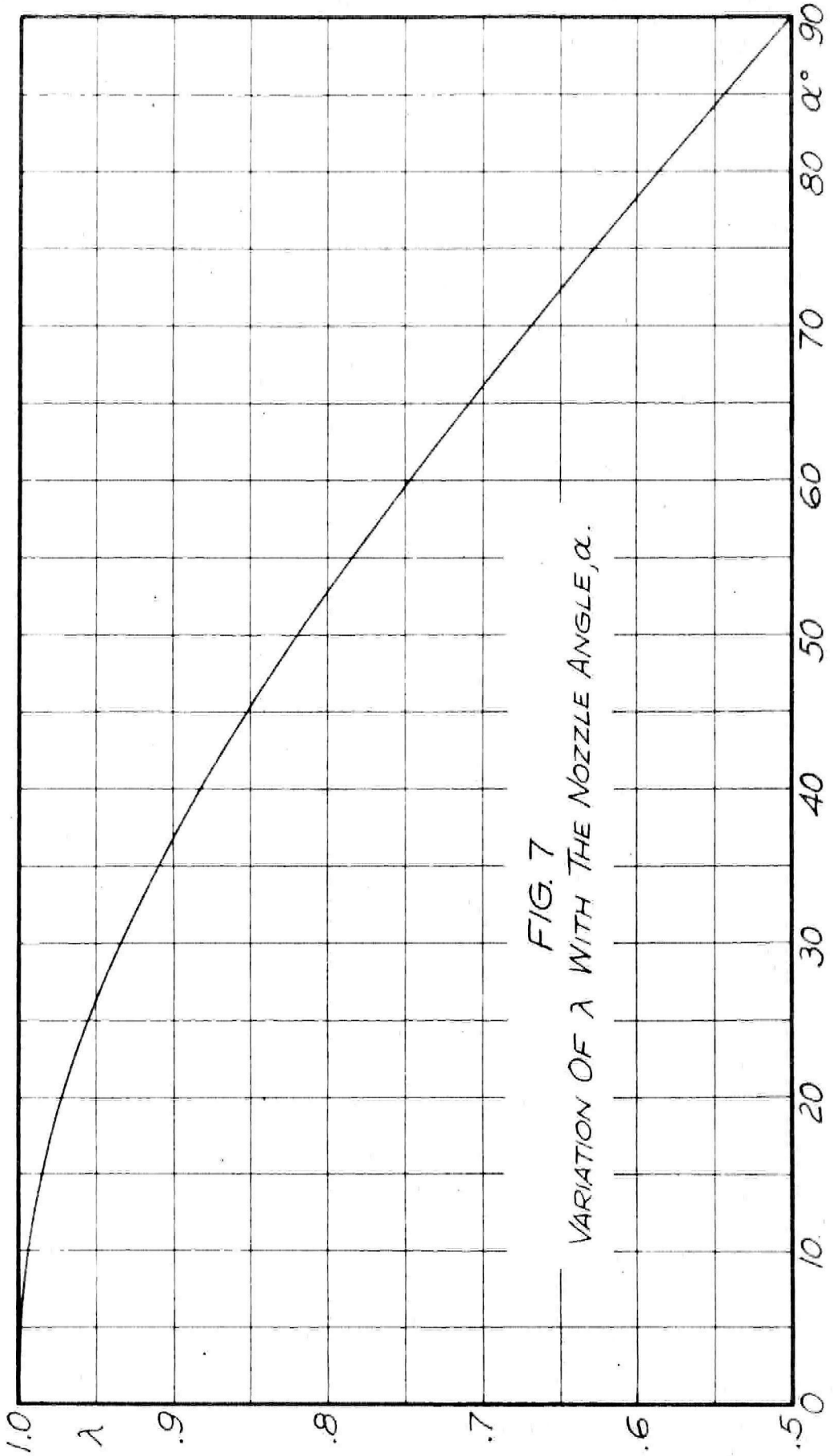

FIG. 7
VARIATION OF λ WITH THE NOZZLE ANGLE, α.

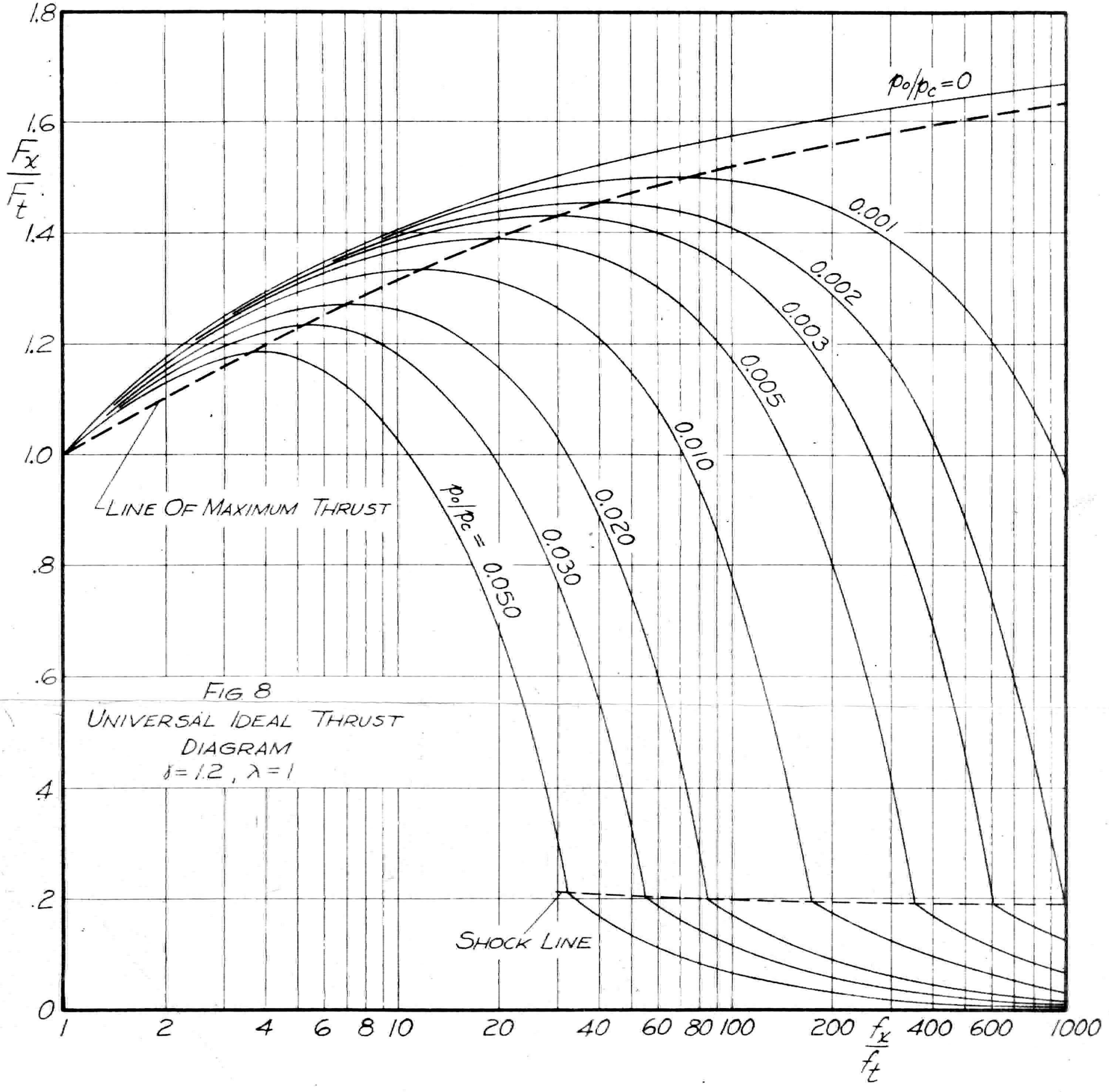

FIG 8
UNIVERSAL IDEAL THRUST DIAGRAM
$\gamma = 1.2$, $\lambda = 1$

PART II.

CHARACTERISTICS OF THE ACTUAL ROCKET MOTOR UTILIZING A GASEOUS PROPELLANT

by

F. J. Malina, E. S. Forman, and J. W. Parsons
California Institute of Technology

The design of a successful liquid propellant rocket motor has been handicapped by an insufficiency of experimental information on its behavior. Predictions of its characteristics have been made mainly on the basis of simplified theoretical analyses and on extensions of results borrowed from the investigations of turbines. This description of the status of the problem does not intend to ignore the published results of motor tests carried out by E. Sänger, R. H. Goddard, the American Rocket Society, and R. C. Truax. Unfortunately, the results, as far as available, are very small in number and for some of these the data is difficult to explain. The experiments of Sänger appear to be the most complete, however, the method of presentation obscures the factors needed for the formulation of a rational design theory. A. Africano, in 1936 set up some empirical design formulae on the basis of the American Rocket Society tests which were limited to chamber pressures in the neighborhood of 200 lb. per. sq. in.

The impatient desire to construct a successful rocket motor has no doubt contributed to the present impasse. Experiments have been attempted on a motor requiring the solution of many separate problems, e. g., propellant combinations,

propellant supply and injection, chamber and nozzle design, cooling and materials, weight reduction, etc.

The results described herein have been obtained after an attempt had been made to simplify and reduce the number of problems to a minimum. In brief, this was done by using gaseous propellants burned in a motor of large combustion volume and of sufficiently high heat capacity to permit tests of 60 seconds or more. The nozzle dimensions were chosen to permit low rates of propellant consumption. Every effort was directed to designing a laboratory apparatus that would give fairly accurate results as quickly and easily as possible.

1. Description of the apparatus and testing procedure.

Propellant

To simplify the problem of propellant supply and injection and to assure more complete combustion a gaseous propellant was used in all tests. The components of the propellant were gaseous oxygen and ethylene which were obtained in cylinders at high pressure. The specifications of the two gases are listed in Table I.

Motor

A cross section of the motor designed for the tests is shown in Fig.1. A hollow steel cylinder of $\frac{1}{2}$" wall thickness encircles a graphite lined combustion chamber and a copper nozzle block, which are held together by two steel

TABLE I

Propellant Component	Cylinder Capacity Lb.	Initial Cylinder Pressure lb/sq.in.	Lower Heat of Combustion B.t.u./lb. of fuel	Ratio of specific heats at 590 °F abs.	Gas Constant R Ft.lb/lb/ °F
Oxygen, O_2 Analysis O_2-99.5% by volume Rare Gases } 0.5% " "	18	2,000		1.40	48.25
Ethylene, C_2H_4 Analysis C_2H_4-96% by volume $C_2H_6+CH_4$-3.5% " " C_2H_2-0.5% by volume	28	1,200	20,032	1.26	55.08

Theoretically correct mixture ratio of O_2/C_2H_4 = 3.42

Theoretical maximum exhaust velocity = 15,100 ft/sec.

end plates. The end-plates also served to make the unit pressure tight.

The graphite liner had a wall thickness of 1" and surrounded a combustion volume of about 36 cubic inches. The combustion volume was made large to improve combustion.

The oxygen and ethylene were injected into the combustion chamber separately through injection nozzles opposite each other, which directed the incoming gases toward the end of the chamber opposite the exhaust nozzle. The mixture was ignited by an ordinary automobile spark plug.

The burnt gases flowed from the chamber through a convergent-divergent Laval nozzle machined in the exhaust nozzle block (cf. Fig.1).

The combustion chamber was tapped for the measurement of the chamber pressure.

Test stand

The schematic diagram in Fig. 2 shows the arrangement of the test stand. The oxygen cylinders were suspended in a cradle hung at one end of a beam (Fig.3) and balanced by a counterweight and tension coil-spring on the other end. The beam was free to see-saw on knife edges located as close to the tank cradle as possible to reduce the amount of counterweight. The free motion of the beam was restrained by a coil-spring under tension and was damped by a viscous damper. The unbalance of the beam due to the loss of gas in

the tanks was measured by a dial gage operated by an extension arm attached to the spring-suspended end of the beam. The dial gage reading was calibrated to give the weight of gas used during a test. A similar scale was used to determine the amount of ethylene used.

The gases were supplied to the combustion chamber through pressure regulators and both the mixture ratio of oxygen to ethylene and chamber pressure were governed by varying the settings on the regulators. As a measure of safety each line was provided with two check valves and blow-out valves.

The measurement of the thrust developed by the motor was accomplished as follows: The motor was supported on tubes extending from a torsion member rigidly supported in a steel frame (Fig.4). The motor weight was balanced by a counterweight hung from a box beam built out from the opposite side of the torsion member. The oscillation of the motor about the torsion member was damped by a viscous damper attached to the box beam. An extension arm attached to the balance beam operated a dial gage which was calibrated to give the thrust delivered by the motor.

The instruments for measuring the thrust, chamber pressure, weight of oxygen and ethylene used, the duration of the test and all controls were mounted on a central panel (Fig.5). The operators were protected by a sheet steel panel board, a wooden barricade around the motor, and a sandbag

barricade around the propellant cylinders.

A record of the instruments was made by means of a motion picture camera provided with a finger attachment for taking frames at any rate desired.

2. Experimental and Data Reduction Procedure.

During each run a photographic record of the thrust gage, pressure gages, oxygen and ethylene weight gages and stop watch was taken at intervals of 1 to 3 seconds. After collecting the data from the film it was plotted as shown in Fig. 6. Before each test a calibration was made of the thrust gage and of the two gas weighing scales by applying known weights. A set of calibration curves is shown in Fig. 7.

To calibrate the apparatus as a whole a series of experiments were made with oxygen alone and the results checked with those obtained by A. Bartocci. (These results will be discussed in another section). These are called "coldthrust" runs. The runs with combustion are called "hot thrust" runs.

Before commencing a cold thrust run the regulator was set to approximately the chamber pressure desired with the valve on the motor side of the regulator closed. Then the valve was opened and the chamber pressure brought to the desired value by manipulating the regulator.

A similar procedure was followed in the hot thrust runs, separately for the two propellant components. The mixture ratio was difficult to set before a run so that a

technique was evolved of making three tests at different mixture ratios in the one continuous run. Each test had a duration of about 30 seconds so that a continuous run lasted about 90 seconds plus the time required to vary the mixture ratio by reducing the flow of ethylene through the regulator. The camera was stopped while the mixture was being brought to a new value.

The experimentally determined quantities were:

$F \equiv$ thrust, lb.

$w_f \equiv$ rate of flow of fuel, lb/sec.

$w_o \equiv$ " " " " oxidizer, lb/sec.

$w = w_f + w_o \equiv$ rate of flow of propellant, lb/sec.

$p_c \equiv$ chamber pressure, lb/sq.in., abs.

$p_o \equiv$ atmospheric pressure, lb/sq.in.

$T_o \equiv$ atmospheric temperature, °F.

$t \equiv$ time, sec.

Before and after each test the throat of the exhaust nozzle was measured. The diameter of the exit section was taken as constant as no change could be measured. The nozzle dimensions are symbolized as follows (cf. Fig.8):

$d_t \equiv$ diameter of the throat, in.

$f_t \equiv$ area " " " , sq. in.

$d_e \equiv$ diameter " " exit section, in.

$f_e \equiv$ area " " " " , sq. in.

$\epsilon = \frac{f_e}{f_t} \equiv$ expansion ratio

$\mathcal{l} \equiv$ distance between throat and exit section

$\alpha \equiv$ nozzle angle, degrees

$\beta \equiv$ nozzle entrance angle, degrees

From these the following basic quantities and coefficients were calculated:

$c = \frac{Fg}{w} \equiv$ effective exhaust velocity, ft/sec.
where $g = 32.2$ ft/sec^2

$r = \frac{w_o}{w_f} \equiv$ mixture ratio

$\eta_{th} = \frac{A(1+r)c^2}{2g H_{p_f}} \equiv$ thermal efficiency, %
where

$A = \frac{1}{778} \equiv$ mechanical equivalent of heat

$H_{p_f} \equiv$ lower heat of combustion at constant pressure, B.t.u./lb. of fuel

$p_o/p_c \equiv$ pressure ratio

$C_F = \frac{F}{p_c f_t} \equiv$ thrust coefficient

$C_m = \frac{w}{g p_c f_t v_s} \equiv$ propellant flow coefficient, sec/ft. where $v_s = 1120$ ft/sec., velocity of sound in air at standard conditions.

$\frac{C_F}{C_m} = c \equiv$ effective exhaust velocity, ft/sec.

$w_{sp} = \frac{C_m}{C_F} \frac{g}{v_s} = \frac{g}{c} \equiv$ specific propellant consumption, lb/sec./lb of thrust.

3. Experimental Errors

The following table gives an estimate of the magnitude of the errors that entered into the more important quantities observed:

TABLE II

Quantity	Range of Measurement	Probable Maximum Error
Thrust	0- 10 lb.	3%
Chamber pressure Low pressure gage	0-400 lb/sq.in.	2%
High " "	400-1000 lb/sq.in.	5%
Nozzle dimensions		2%
Rate of flow of propellants	0.005 - 0.2 lb/sec.	5%

4. Discussion of basic quantities and coefficients

The design of a rocket motor to meet certain specifications, e.g., to deliver a thrust F, for a length of time t, with a propellant supply W requires first, a knowledge of the variation of thrust with the pressure ratio p_o/p_c , the expansion ratio ϵ , and the chamber pressure p_c ; second, variation of the rate of flow of propellant with chamber pressure p_c and the nozzle throat area, f_t .

On the assumption of a complete adiabatic expansion through the exhaust nozzle with the critical pressure existing in the nozzle throat and no heat losses in the combustion

chamber the thrust can be written in the form:

$$F = 2\sqrt{\left(\frac{2}{\gamma+1}\right)^{\frac{2}{\gamma-1}}\frac{\gamma^2}{\gamma^2-1}}\sqrt{1-\left(\frac{p_0}{p_c}\right)^{\frac{\gamma-1}{\gamma}}}\,p_c f_t \qquad (1)$$

R. Uddenberg has suggested writing this expression in the form:

$$F = C_F p_c f_t \qquad (2)$$

where

$$C_F = 2\sqrt{\left(\frac{2}{\gamma+1}\right)^{\frac{2}{\gamma-1}}\frac{\gamma^2}{\gamma^2-1}}\sqrt{1-\left(\frac{p_0}{p_c}\right)^{\frac{\gamma-1}{\gamma}}} \qquad (3)$$

so that C_F is a function of γ and $\frac{p_0}{p_c}$. This simplification of the expression for the thrust of an actual motor by forcing the thrust coefficient to account for the deviation from an adiabatic process, for the under-or over-expansion of the jet and for the combustion efficiency seems almost too great to expect reliability in predicting the thrust for rocket motors of different size. However, at the present time this method of presenting experimental data appears the best. The dependence of the coefficient on the specific heat ratio is equivalent to a dependence on the components making up the propellant mixture and the temperature variation during the process.

The expression for the thrust indicates that tests on a small scale made at the same value of $p_c f_t$ should give the same value of the thrust coefficient as resulting

on large scale. Factors tending to lead to a deviation are (1) the difference in heat losses, (2) the sensitivity of the expansion ratio of small nozzles to unavoidable small changes in the throat and exit dimensions, (3) the difference in frictional losses in the nozzle, (4) the difference in completeness of combustion in the combustion chamber. The four factors can be grouped under combustion efficiency and nozzle efficiency. Hence the usefulness of small scale experiments is dependent on the possibility of duplicating large scale combustion efficiency and nozzle efficiency.

The rate of flow of propellants can be expressed on the basis of similar assumptions in the form:

$$W = \left(\frac{2}{\gamma+1}\right)^{\frac{\gamma+1}{2(\gamma-1)}} \sqrt{\frac{\gamma g}{RT_c}}\, p_c f_t \qquad (4)$$

If this is written in such a way that all but $p_c f_t$ is absorbed in a coefficient and the coefficient is expressed in terms of mass and divided by v_s, the velocity of sound in air at standard conditions, to make it dimensionless, then

$$w = C_m \frac{g}{v_s} p_c f_t \qquad (5)$$

where $$C_m = \left(\frac{2}{\gamma+1}\right)^{\frac{\gamma+1}{2(\gamma-1)}} \sqrt{\frac{\gamma}{gRT_c}}\, v_s \qquad (6)$$

The evaluation of the coefficient in terms of mass makes possible the calculation of the effective exhaust

velocity from the ratio of C_F to C_m, thus

$$c = \frac{C_F}{C_m} v_s \tag{7}$$

The propellant flow coefficient is seen to be a function of the specific heat ratio γ, the gas constant R, and the chamber temperature T_c. It is to be noted that C_m is independent of the pressure ratio and of the history of the jet after the nozzle throat is passed. Therefore, the flow coefficient is affected only by the combustion efficiency and the entrance condition to the throat and the throat itself.

From an engineering point of view it is convenient to use the specific propellant consumption w_{sp}. A given application of a rocket motor specifies the thrust required and the duration of its action. The total propellant supply needed can then be immediately evaluated if the specific propellant consumption is known.

The merit of a rocket motor is determined by the value of the effective exhaust velocity developed. This is equivalent to the statement that the propellant consumption for a given thrust is lowest for a motor giving the highest exhaust velocity. The merit of a rocket motor can also be evaluated on the basis of the thermal efficiency.

$$\eta_{th} = \frac{A\,(1+\kappa)\,c^2}{2g\,H_{p_f}} \tag{8}$$

The expression for the thermal efficiency in this form brings out a factor that plays an important role in

determining the quantities and coefficients characterising the rocket motor. This factor is the mixture ratio r . The assignment of an exhaust velocity or thermal efficiency without mention of the mixture ratio actually employed gives very little information on the merit of a particular motor design. Although the mixture ratio does not appear explicitly in the thrust and propellant flow coefficients it nevertheless influences them, for it affects the chamber temperature, the specific heat ratio and the heat losses.

The experimental results that follow will be presented in terms of the quantities and coefficients discussed above.

5. Results of the Cold Thrust Experiments

The simplest method of checking the dependability of the test stand was to make experiments without combustion in the motor. The results of A. Bartocci on the reactive force of oxygen were available as a base of comparison so that data was first obtained on motor characteristics with oxygen alone. The results of the cold thrust experiments are listed in Table II.

The nozzle used in these experiments is illustrated in Fig. 9. The nozzle was machined from a block of graphite and the same nozzle was used in all cold thrust tests as no erosion was encountered.

The curves in Fig. 10 compare the variation of the

effective exhaust velocity with chamber pressure for three exhaust nozzle expansion ratios. The curve obtained for an expansion ratio of 6.26 is seen to fall correctly between Bartocci's curves for expansion ratios of 1.66 and 10.

Fig. 11 shows the variation of the propellant flow coefficient with the pressure ratio p_o/p_c. The critical pressure prevailed at the nozzle throat for the whole range of pressures. Bartocci's results for two different nozzle throat areas are drawn in. As he did not give the value of p_o at which his experiments were made a value of 14.4 lb/sq.in. sq.in. was used. According to Eq.(4) the propellant flow coefficient should be independent of the pressure ratio after the critical pressure is reached in the nozzle throat. The deviation of the experimental results from the theoretical prediction can be charged to the fact that the gas does not enter the nozzle entrance from rest, the presence of turbulence in the chamber, and non-constancy of the chamber temperature.

In Fig. 12 are plotted the values of the thrust coefficient obtained as function of the pressure ratio. The dotted curve drawn in corresponds to Eq. (3) for $\gamma = 1.4$, i.e., to an adiabatic and complete expansion in the nozzle.

The results of Bartocci's tests for expansion ratios of 1.66 and 10.00 are included and again a value of 14.4 lb. sq.in. was assumed for p_o. The effect of over-expansion is

brought out by the decrease in the thrust coefficient with increasing pressure ratio and increasing expansion ratio. The expansion ratio of 6.26 used in the present tests is theoretically correct for a pressure ratio if about 0.023 so that the jet was over-expanded over the whole range. The first author showed in Reference 8 that the thrust should be markedly affected by over-expansion.

6. Results of the Hot Thrust Experiments

The following problems were selected for investigation under conditions of combustion of the gaseous oxygen-ethylene propellant: Variation of the motor characteristics, i.e., thrust, propellant consumption, and effective exhaust velocity with:

1. Pressure ratio
2. Mixture ratio
3. Exhaust nozzle design

The results of the hot thrust experiments made to determine these effects are tabulated in Table III and Table IV.

In Fig. 13 drawings of the nozzles used are shown. The graphite exhaust nozzle employed in the cold thrust tests was found unsuitable for the hot thrust runs as at chamber pressures above 100 lb./sq.in. with an oxidizing mixture excessive errosion was encountered. The use of a copper block for the nozzle was found to be satisfactory. The

high heat capacity of the copper block and its high heat conductivity were, it is believed, factors that prevented serious erosion.

The experimental values of C_{m_f} and C_{m_o} are plotted against the chamber pressure in Fig. 14 and Fig. 15 respectively. Curves have been faired in for various mixture ratios. The fairing of the curves of constant mixture ratio was somewhat arbitrary as the experimental points had very large scatter. The scatter was probably due mainly to variations in the state of combustion and also to some extent to the difference in the motor wall temperature from test to test. From these curves cross-plots has been constructed in Fig. 16 and Fig. 17 of C_{m_f} and C_{m_o} against mixture ratio for various chamber pressures.

In Fig. 18 the propellant flow coefficient C_m has been plotted against mixture ratio for various chamber pressures. This set of curves was obtained from Fig. 16 and Fig. 17. It shows that the propellant flow coefficient for a given chamber pressure is a minimum around the theoretically correct mixture ratio of 3.42 and increases more slowly on the rich side of the curve. The latter effect is favorable to the life of motor materials which in general cannot resist oxidizing flames. Furthermore, C_m decreases with increasing chamber pressure as it should, for the chamber temperature increases with increasing chamber

pressure due to decreasing dissociation, i.e., a greater percentage of the available heat energy in the fuel is liberated at higher pressures. In conjunction with this effect more complete combustion should bring about a lower value of the ratio of specific heats which Eq. (6) shows will give a lower value of C_m.

The values of C_F obtained experimentally for the nozzles tested are plotted in Fig. 19, Fig. 20, and Fig. 21. The expansion ratios are 2.00, 2.45,and 5.38 respectively. The expansion remained constant for the two larger expansion ratios, whereas for the smallest it varied from 2.14 to 1.95 due to progressive erosion in the nozzle throat.

Because of the inconsistent experimental values a curve has been faired in for each case only for the theoretically correct mixture ratio. The curves for the three expansion ratios are combined in Fig. 23 and the variation of C_F with $\frac{p_o}{p_c}$ for adiabatic conditions has been plotted for three values of the specific heat ratio. The experimental curves for the two higher expansion ratios cross the adiabatic curves sharply at lower pressure ratios. It is doubtful that such low specific heat ratios would exist if an adiabatic expansion was approximated. It may be that due to continued combustion after the nozzle throat is passed and to heat

added to the jet from the nozzle walls the expansion is closer to an isothermal process. Thus, a higher pressure prevailed at the exit section of the nozzle than adiabatic theory would indicate and a higher value of the thrust coefficient resulted.

The effect of under-expansion at the lower pressure ratios is shown by the curve for an expansion ratio of 2.00 and of over-expansion by the decrease in the thrust coefficient with increasing pressure ratio for an expansion ratio of 5.38.

In Fig. 23 values of C_F obtained by other experimentors are plotted together with the curves of Fig. 22 and an adiabatic curve for $\gamma = 1.2$. As p_o was not given by the other experimentors a value of 14.7 lb./sq.in. was chosen. When data was available the expansion ratio was calculated and placed beside the corresponding point in the figure.

On the basis of the faired results of C_m in Fig. 19 for a mixture ratio of 3.42 and the values of C_F in Fig. 22 for the three expansion ratios, the variation of the effective exhaust velocity c with $\frac{p_o}{p_c}$ has been computed and plotted in Fig. 24. The outside pressure p_o has been taken as the standard atmospheric pressure at sea level of 14.7 lb./sq.in.

Since the effective exhaust velocity is directly

proportional to the thrust coefficient and inversely proportional to the propellant flow coefficient it increases with decreasing pressure ratio and with increasing chamber pressure. The importance of the exhaust nozzle expansion ratio is clearly evident. An extropolation of the results to lower pressure ratios verifies Sängers reported exhaust velocity of about 10,000 ft./sec. at a chamber pressure of about 1500 lb./sq.in.

The curves in Fig. 25, Fig.26, and Fig. 27 show the variation of the thermal efficiency with pressure ratio for various mixture ratios for the three exhaust nozzle expansion ratios. The curves have been computed from Eq. (8) using C_m from Fig. 18 and C_F from Fig. 22 to determine the exhaust velocity c. Since the curves for C_F were faired in only for a mixture ratio of 3.42 the effect of mixture ratio on that coefficient is neglected in calculating the thermal efficiency.

The dependence of the specific propellant consumption on the pressure ratio is shown in Fig. 28 for p_o = 14.7 lb./sq.in. and r = 3.42

Conclusion

There had been some doubt expressed when this apparatus was constructed as to the usefulness of gas

propellant rocket experiments in predicting the characteristics of the liquid propellant rocket motor. The close agreement of the results herein described with those obtained with liquid propellants by other investigators seems, however, to justify the development of this type of testing technique.

The measurement of the rate of flow of the propellant components presented one of the most difficult problems. At first a Thomas type flow meter was tried. Its calibration was found to be uncertain in this set-up and its use was dropped following an explosion in the oxygen line. The explosion increased the respect of the experimenters for gases at high pressure and led to a careful re-design of the propellant supply lines.

Grateful acknowledgement is made to Dr. Theodore von Kármán for his interest and clarifying suggestions, and to Dr. E. E. Sechler and Mr. A.M.O. Smith for their aid in designing the apparatus.

References

1. Sänger, E. — Nuere Ergebnisse der Raketenflugtechnik, Flug, H. Pittner, Vienna, Vol.I, pp 1-22, 1934

   Der Verbrennungs-Raketenmotor, Schweizer Boutzeitung, Vol.107, pp 1-4, 1936.

2. Goddard, R. H. — Liquid-propellant Rocket Development, Smithsonian Miscellaneous Collections, Vol. 95, No.3, 1936

3. American Rocket — Society-John Shesta, Report on Rocket Tests, Astronautics, No.31, 1935
   Report of Motor Tests of June 2nd, Astronautics, No.32, 1935.
   John Shesta, H.Franklin Pierce and James H. Wyld- Report on the 1938 Rocket Motor Tests, Astronautics No. 42, pp. 2-6, 1939.

4. Truax, R. C. — Annapolis Motor Tests, Astronautics No. 42, pp 6-10, 1939.

5. Africano, A. — The Design of a Stratosphere Rocket Jour. of the Aero. Sciences, Vol.3, pp. 287-290, 1936.

6. Bartocci, A. — La Forza di Reazione Nell'efflusso di Gas, L'Aerotecnica, pp. 235-276, March 1938.

7. Uddenberg, R. — A Simplified Expression for Jet Reaction, Astronautics, No.34, pp. 19-20, 1936.

8. Malina, F. J. — Characteristics of the Rocket Motor Unit Based on the Theory of Perfect Gases, Ph.D. Thesis, California Institute of Technology, pp. 1-32, 1940.

FIG. 1

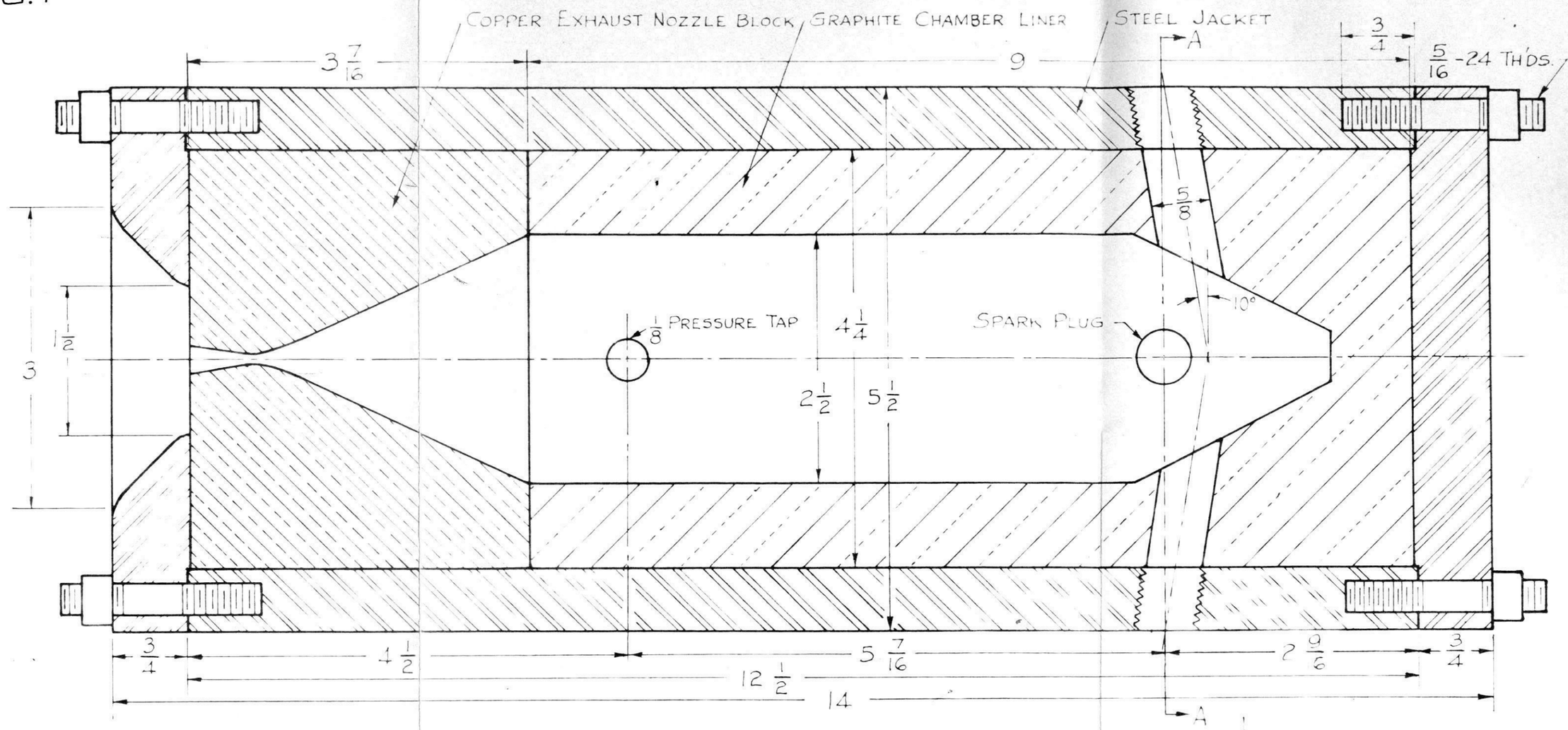

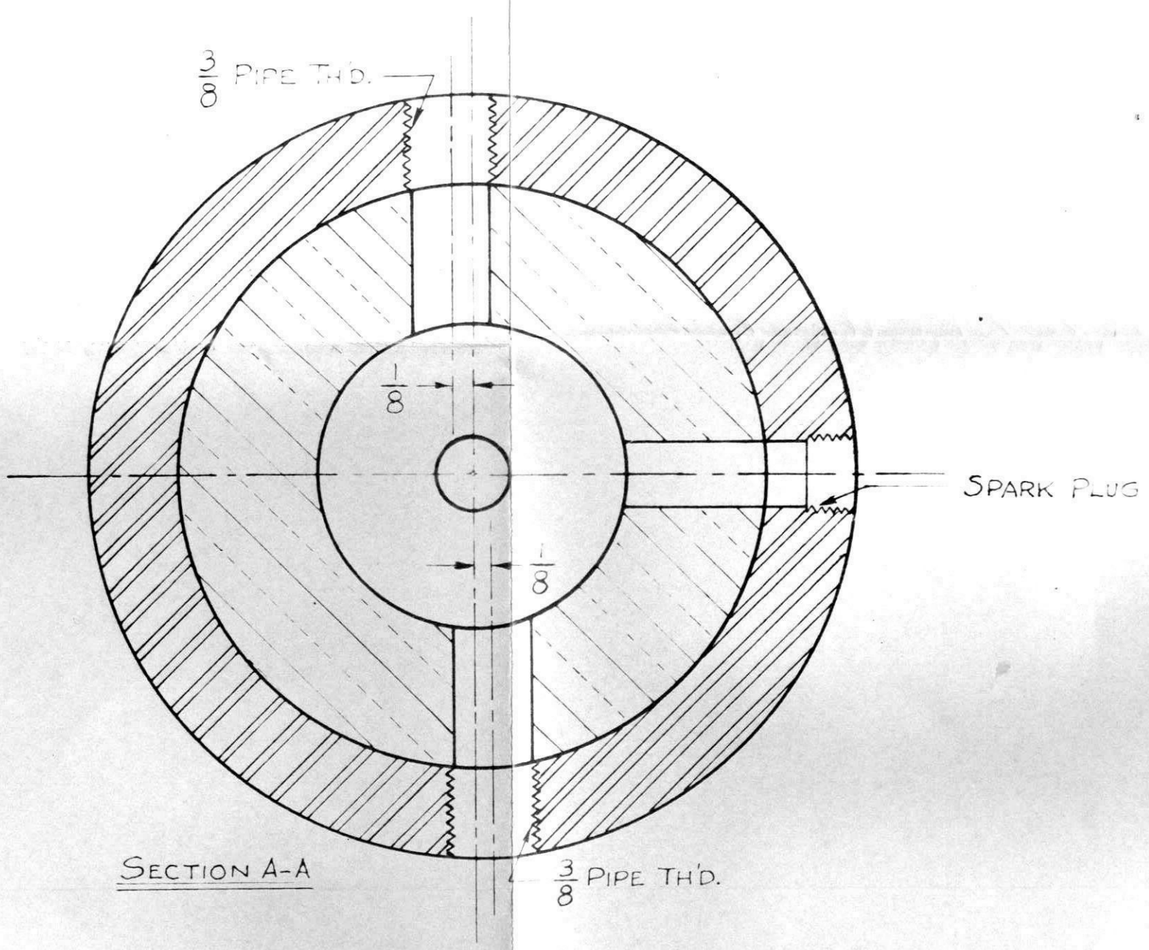

SECTION A-A

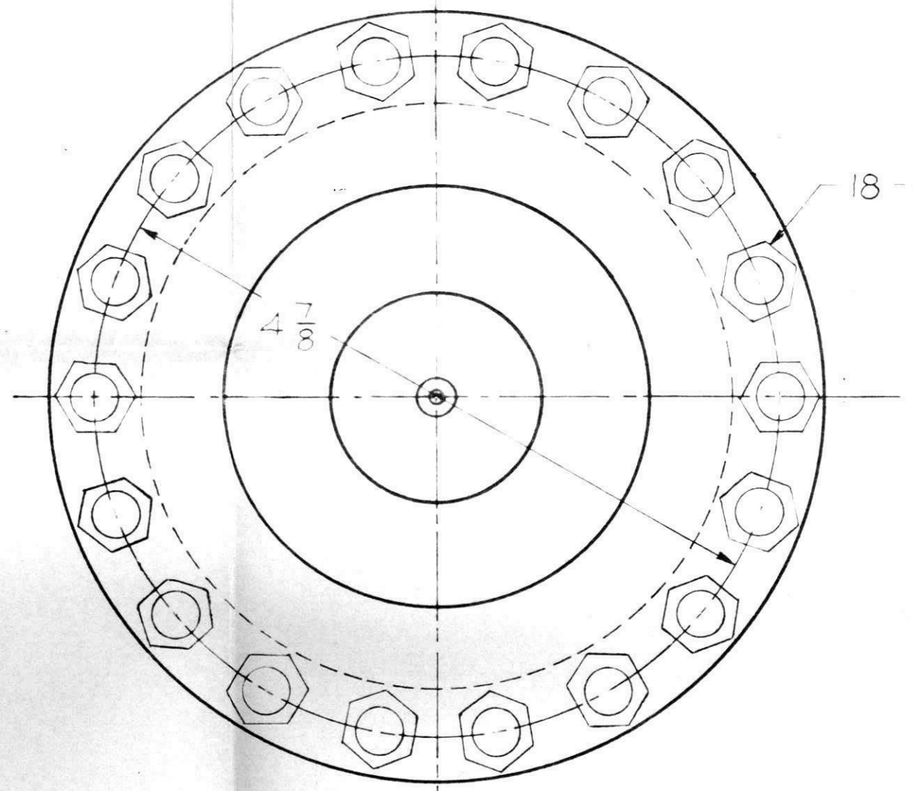

							TOLERANCES .010 OR ±, UNLESS OTHERWISE NOTED
							SCALE: 1"=1"
MATERIAL	FINISH	HEAT TREAT	DRAFTSMAN	CHECKED	APPROVED	ENGINEER	
GUGGENHEIM AERONAUTICAL LABORATORY CALIFORNIA INSTITUTE OF TECHNOLOGY			GAS PROPELLANT ROCKET MOTOR				
			NAME				DRAWING NO

FIG. 2

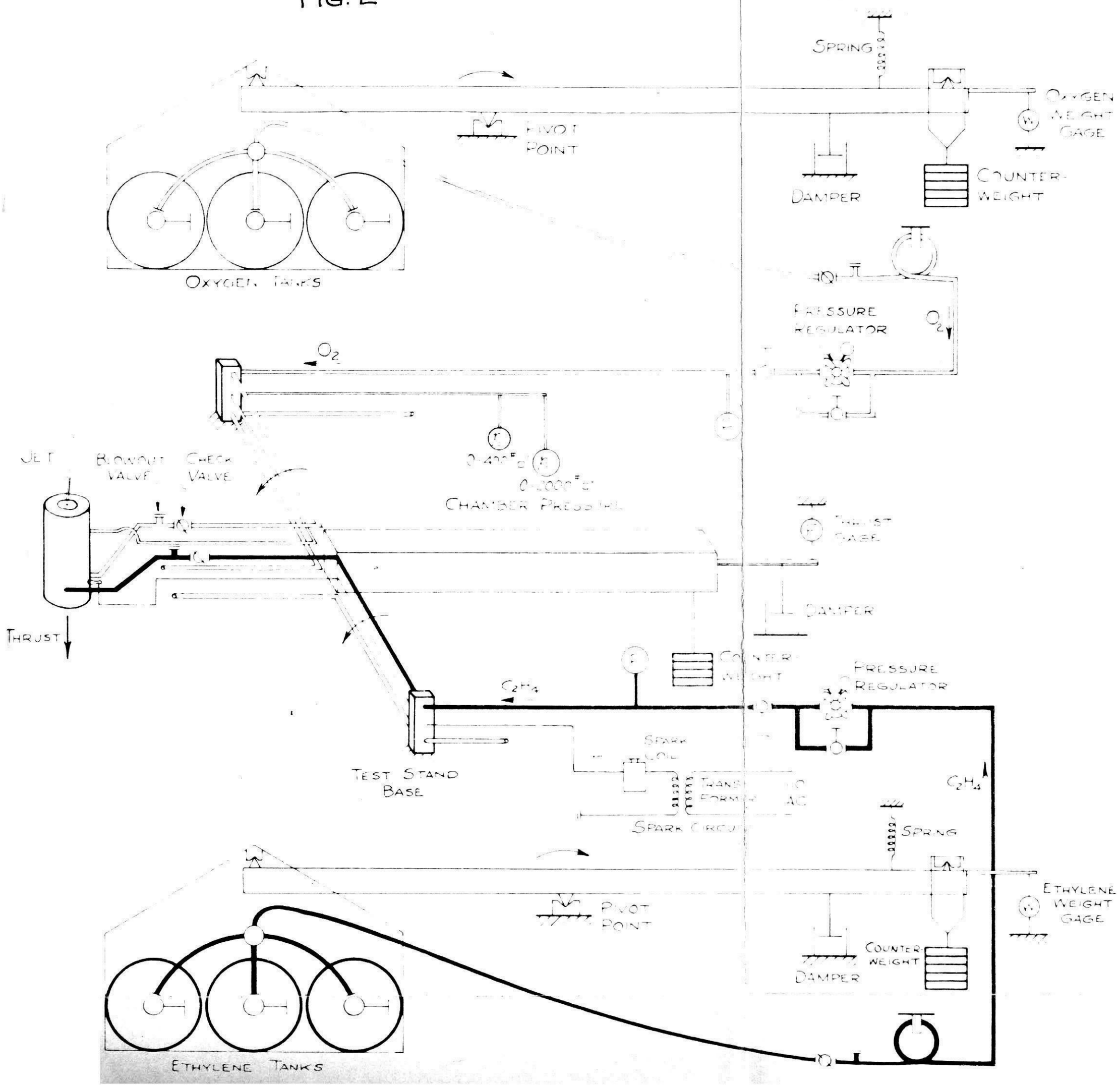
SPRING
OXYGEN WEIGHT GAGE
PIVOT POINT
DAMPER
COUNTER-WEIGHT
OXYGEN TANKS
PRESSURE REGULATOR
O_2
JET
BLOWOUT VALVE
CHECK VALVE
0-400 PSIG
0-2000 PSIG
CHAMBER PRESSURE
THRUST
C_2H_4
SPARK COIL
TRANSFORMER
AC
SPARK CIRCUIT
TEST STAND BASE
ETHYLENE WEIGHT GAGE
ETHYLENE TANKS

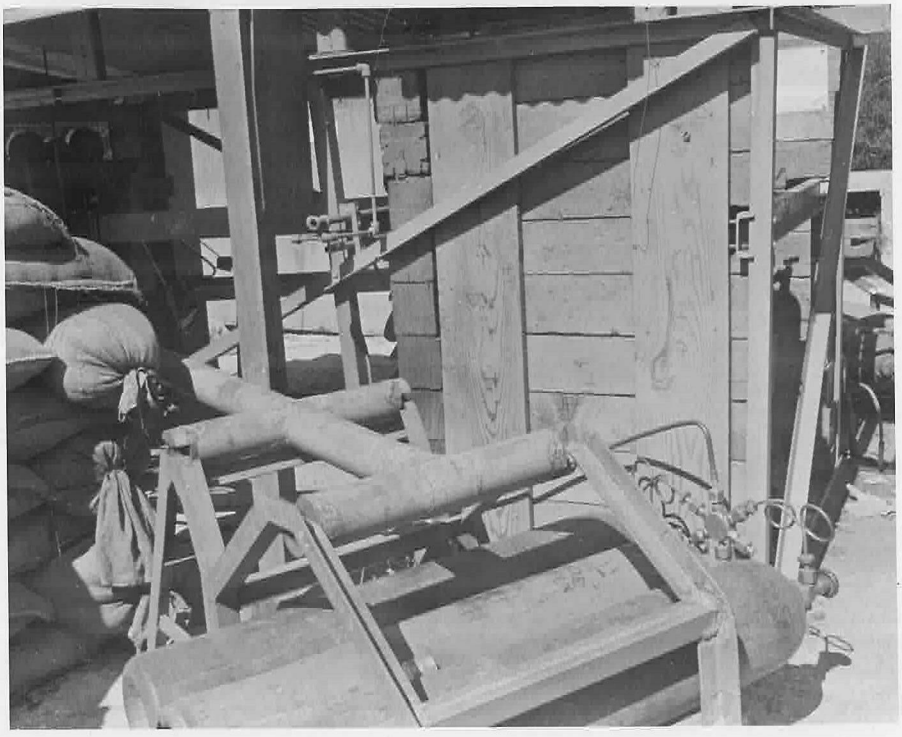

FIG. 3

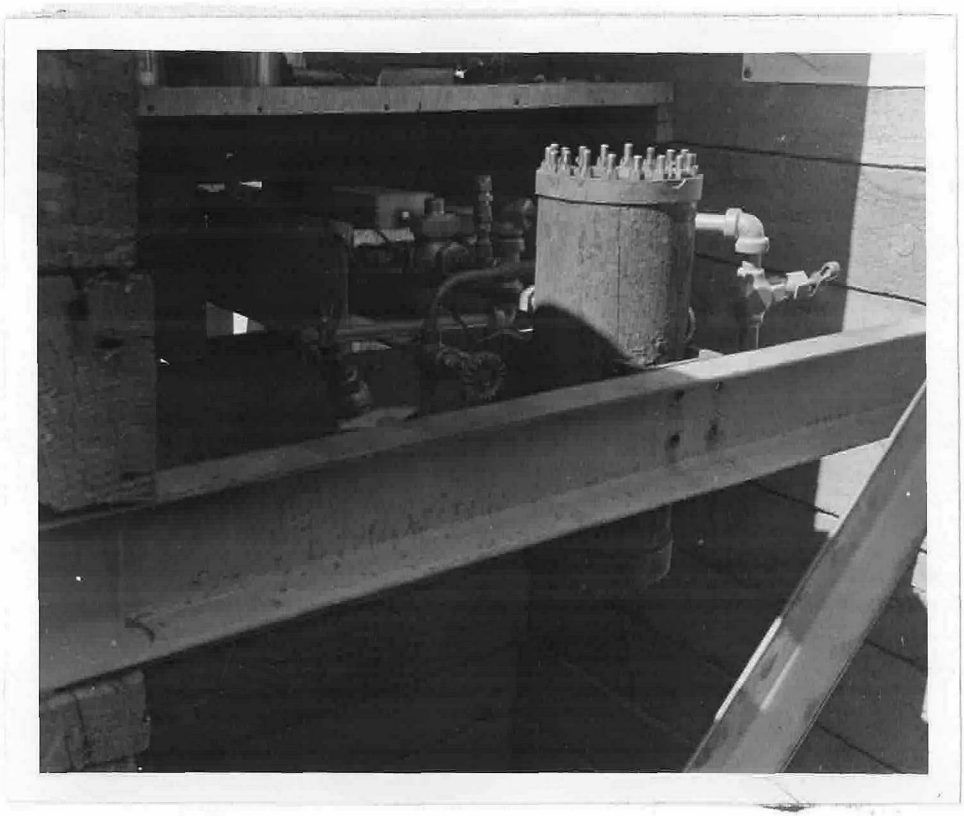

FIG. 4

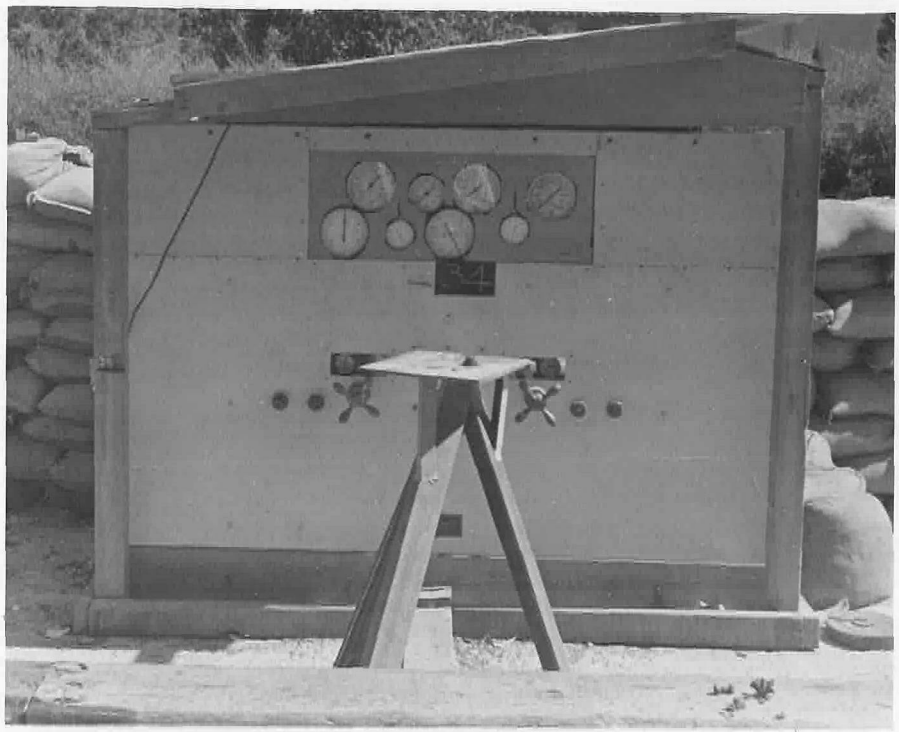

FIG. 5

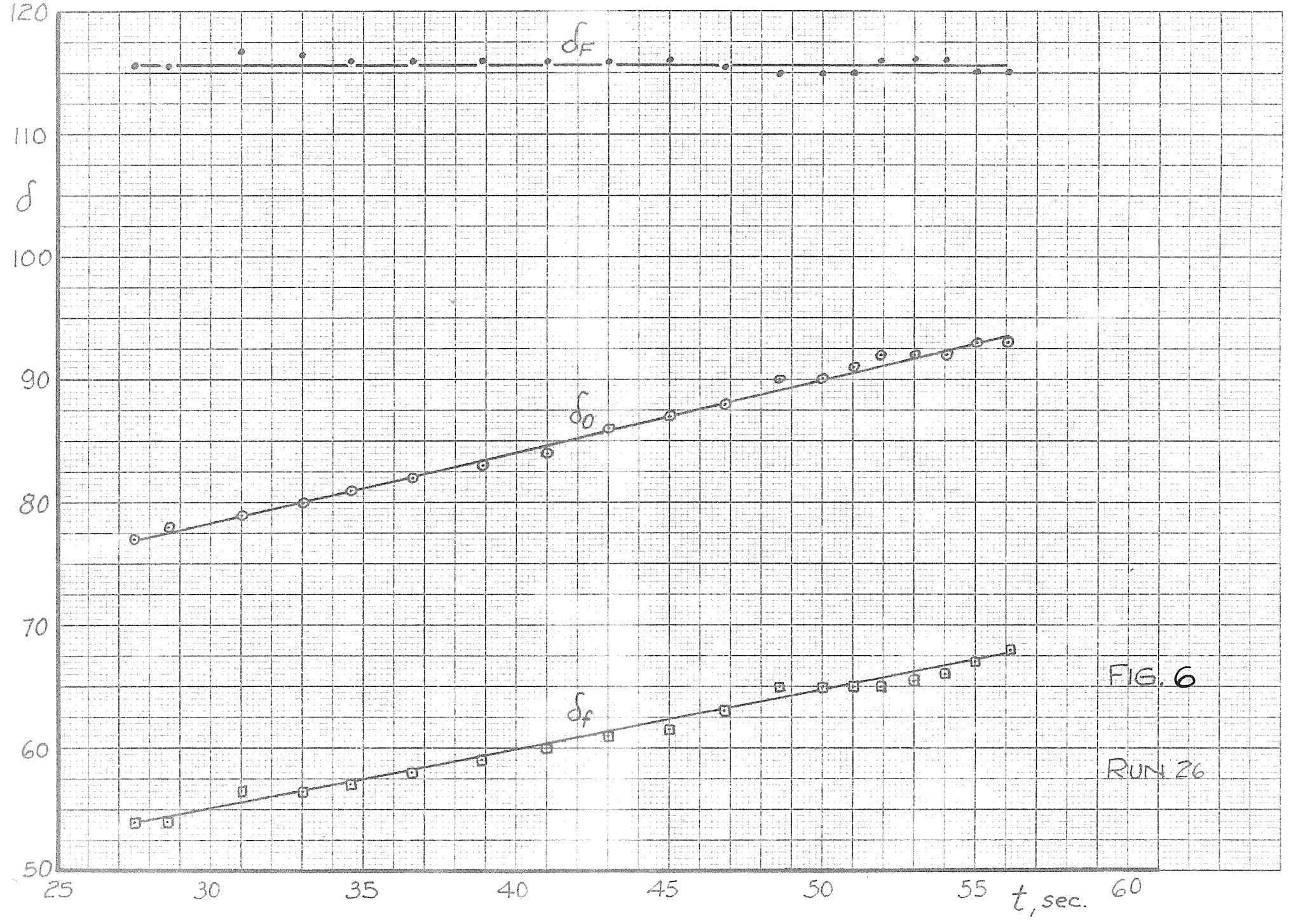
120
110
δ
100
90
80
70
60
50
δ_F
δ_o
δ_f
25
30
35
40
45
50
55
60
t, sec.

FIG. 6

RUN 26

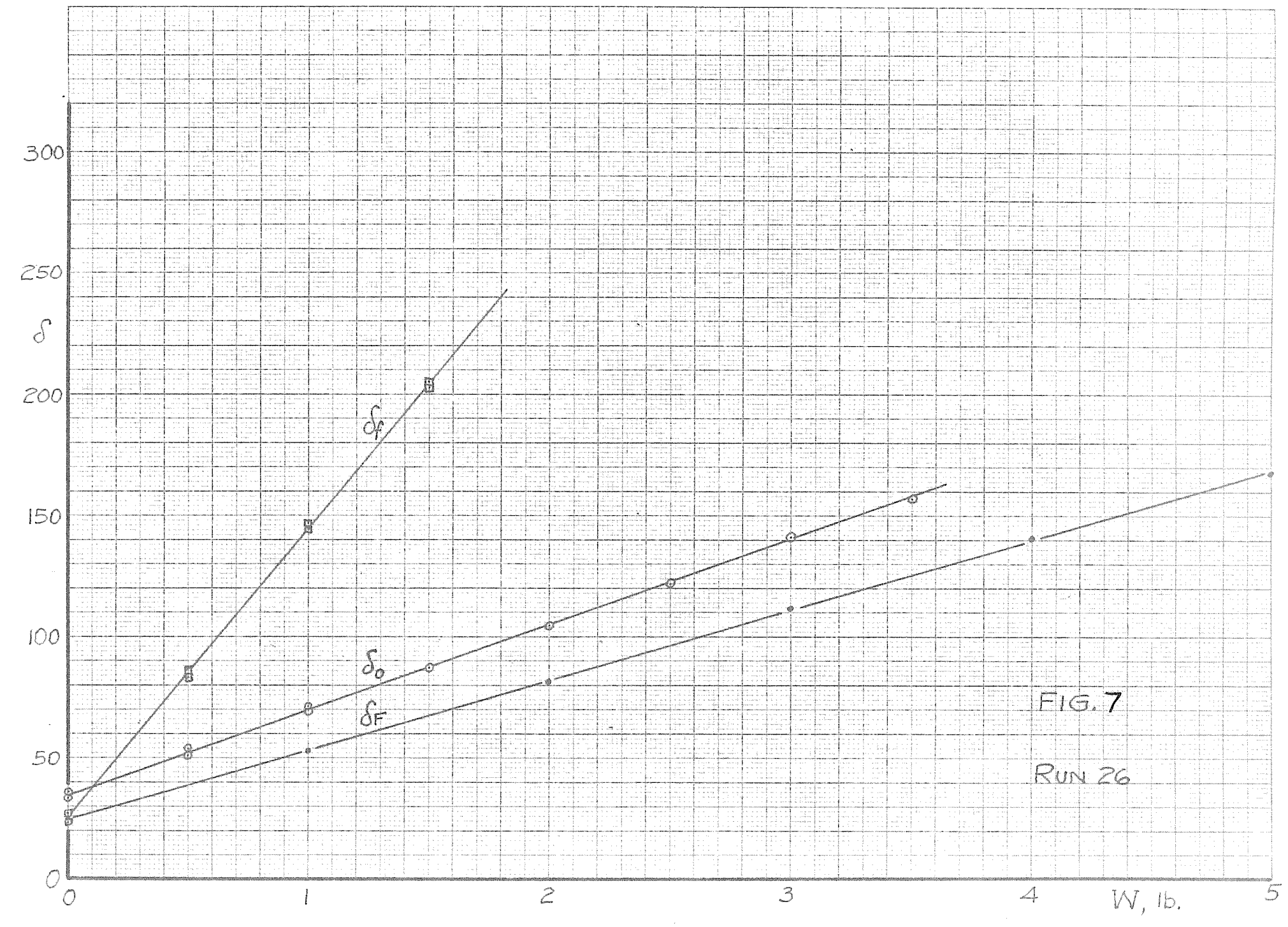

FIG. 7

RUN 26

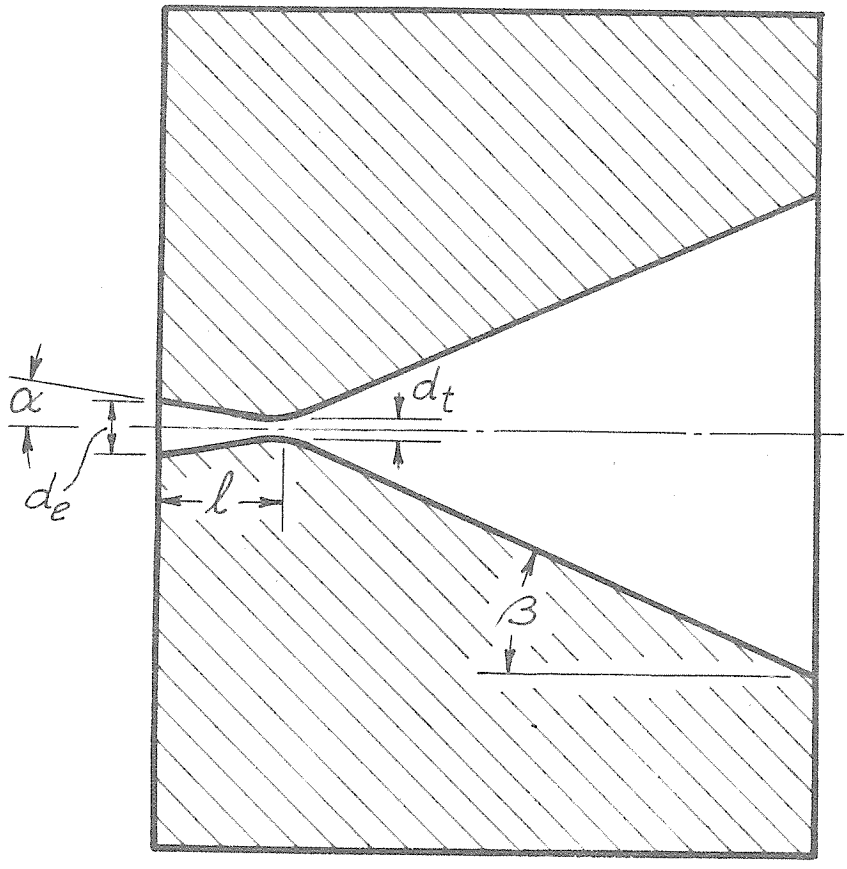

FIG. 8

TABLE II.

Run No.	Hot or cold thrust	p_o, lb/sq.in	T °F	p_c, lb/sq.in. (abs)	w_o lb/sec	F lb.	d_t in.	d_e in.	f_t sq.in.	f_e sq.in	ϵ	α	β	l in.	$p_c f_t$ lb.	p_o/p_c	C_{m_o}	C_F	ft/sec
1	cold	14.30	85.0	62.3	.0216	.61	.131	.328	.01350	.0845	6.26	5°	39°	1.125	.841	.229	.894	.725	919
2	"	"	"	64.3	.0215	.67	"	"	"	"	"	"	"	"	.868	.222	.861	.772	1003
3	"	"	"	64.3	.0339	.70	"	"	"	"	"	"	"	"	.868	.222	.958	.806	943
4	"	"	88.0	113.3	.0399	1.52	"	"	"	"	"	"	"	"	1.531	.126	.905	.992	1328
5	"	"	"	110.3	.0375	1.52	"	"	"	"	"	"	"	"	1.490	.130	.875	1.020	1305
6	"	"	"	114.3	.0412	1.56	"	"	"	"	"	"	"	"	1.545	.125	.927	1.010	1328
7	"	"	"	162.3	.0558	2.50	"	"	"	"	"	"	"	"	2.192	.088	.885	1.140	1445
8	"	"	"	60.3	.0215	.60	"	"	"	"	"	"	"	"	.815	.237	.917	.737	900
9	"	14.22	82.4	270.3	.0994	4.67	"	"	"	"	"	"	"	"	3.655	.053	.945	1.278	1510
10	"	14.30	"	459.3	.1700	8.37	"	"	"	"	"	"	"	"	6.200	.031	.953	1.350	1585
11	"	"	"	359.3	.1385	6.63	"	"	"	"	"	"	"	"	4.850	.040	.994	1.370	1543
12	"	"	88.0	34.3	.0116	.18	"	"	"	"	"	"	"	"	.463	.417	.871	.389	498

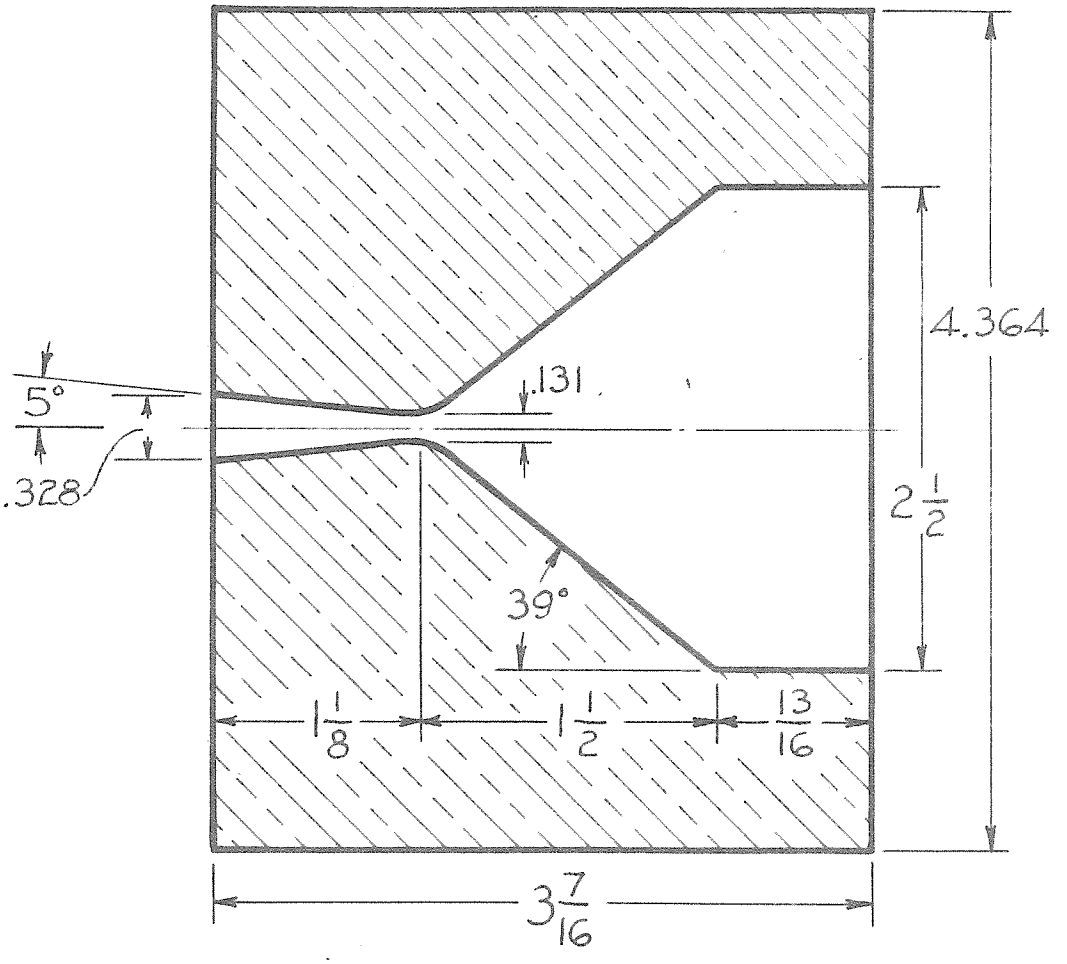

$\epsilon = 6.26$

(GRAPHITE)

FIG. 9

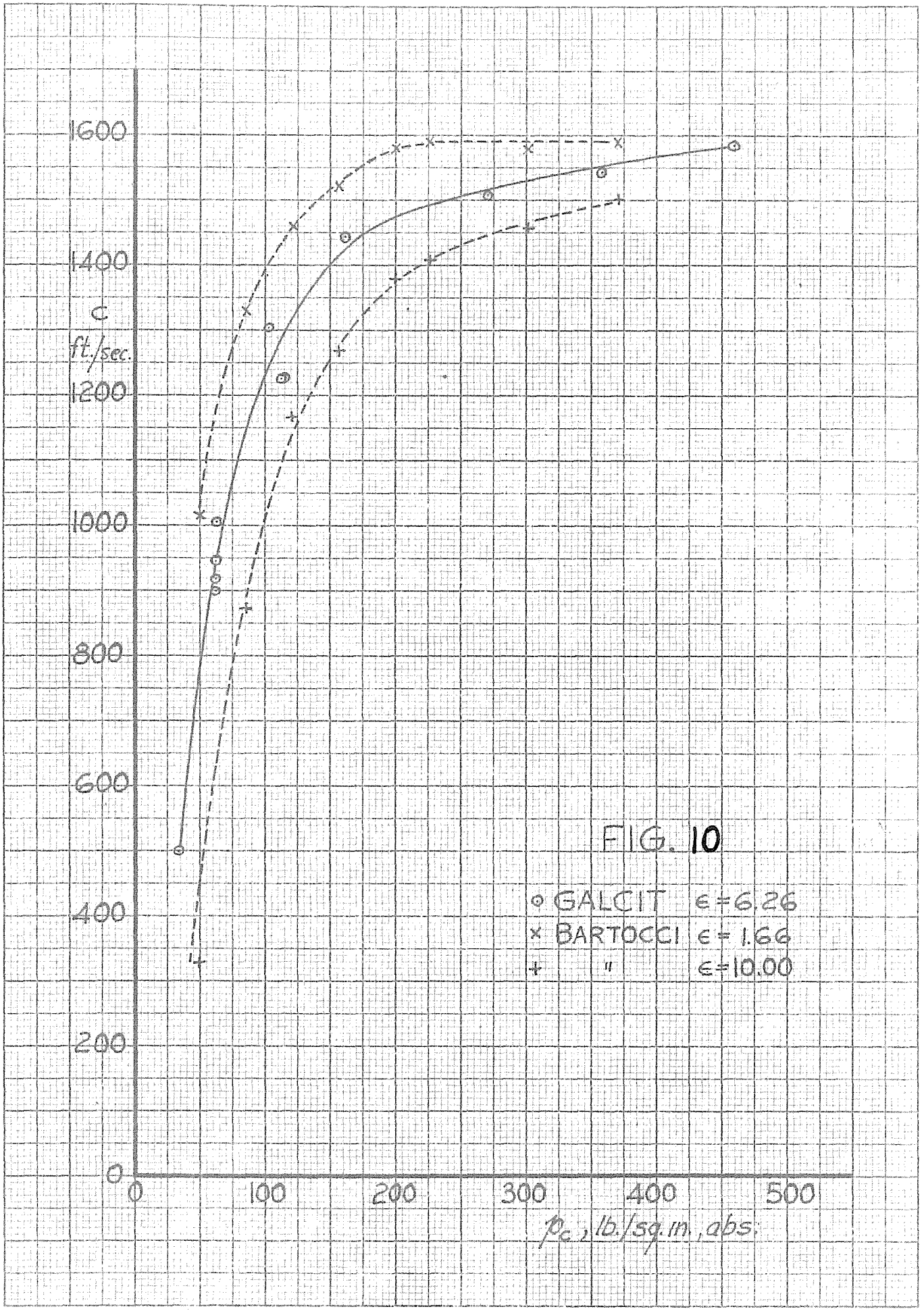
1600
1400
c
ft./sec.
1200
1000
800
600
400
200
0
0
100
200
300
400
500
p_c, lb./sq.in., abs.
o GALCIT ε=6.26
× BARTOCCI ε=1.66
+ " ε=10.00

FIG. 10

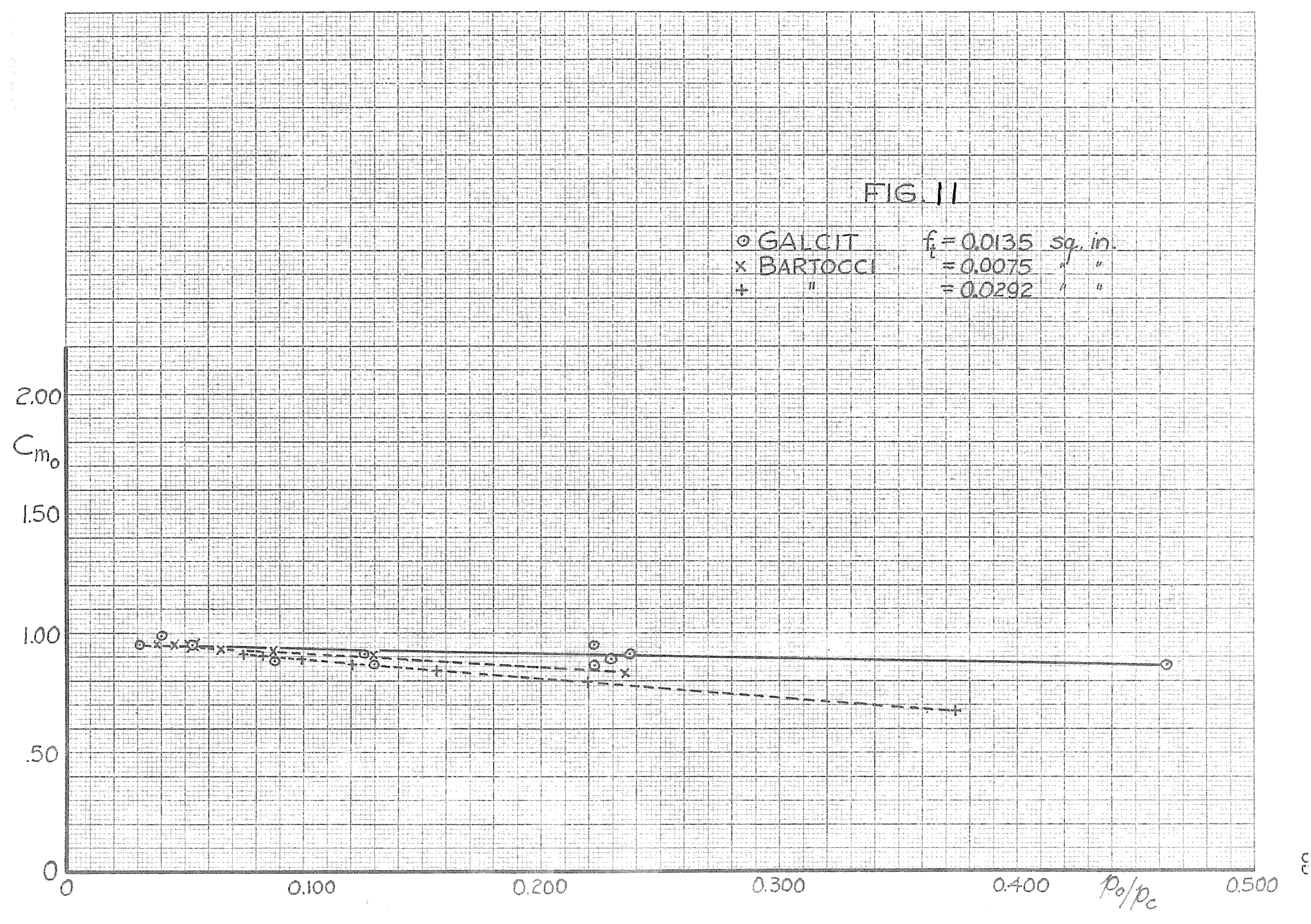
FIG. 11
⊙ GALCIT f_t = 0.0135 sq. in.
× BARTOCCI = 0.0075 " "
+ " = 0.0292 " "
2.00
C_{m_o}
1.50
1.00
.50
0
0
0.100
0.200
0.300
0.400
p_o/p_c
0.500

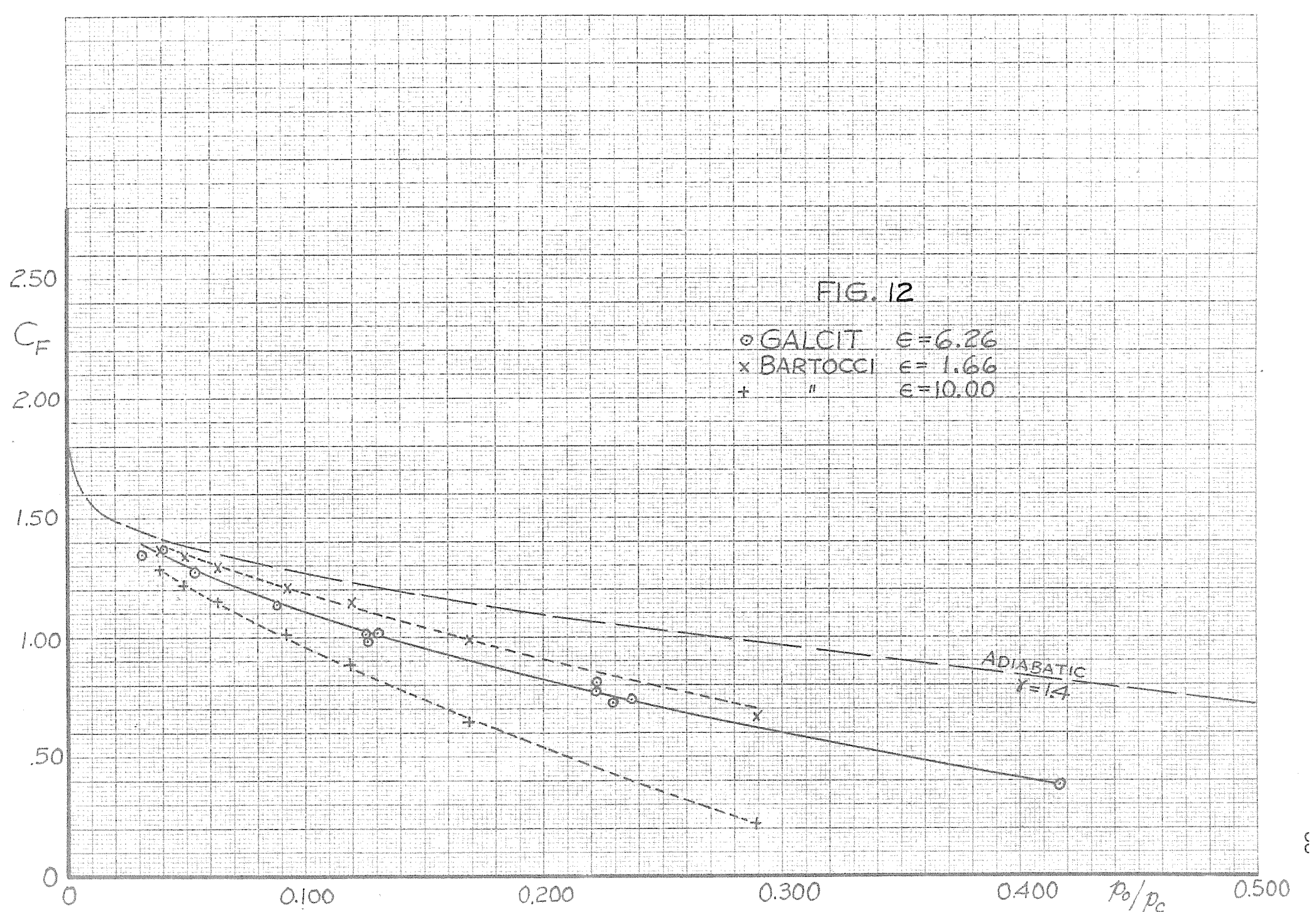
FIG. 12
⊙ GALCIT ε=6.26
× BARTOCCI ε= 1.66
+ " ε=10.00
ADIABATIC γ=1.4
C_F
2.50
2.00
1.50
1.00
.50
0
0
0.100
0.200
0.300
0.400
p_0/p_c
0.500

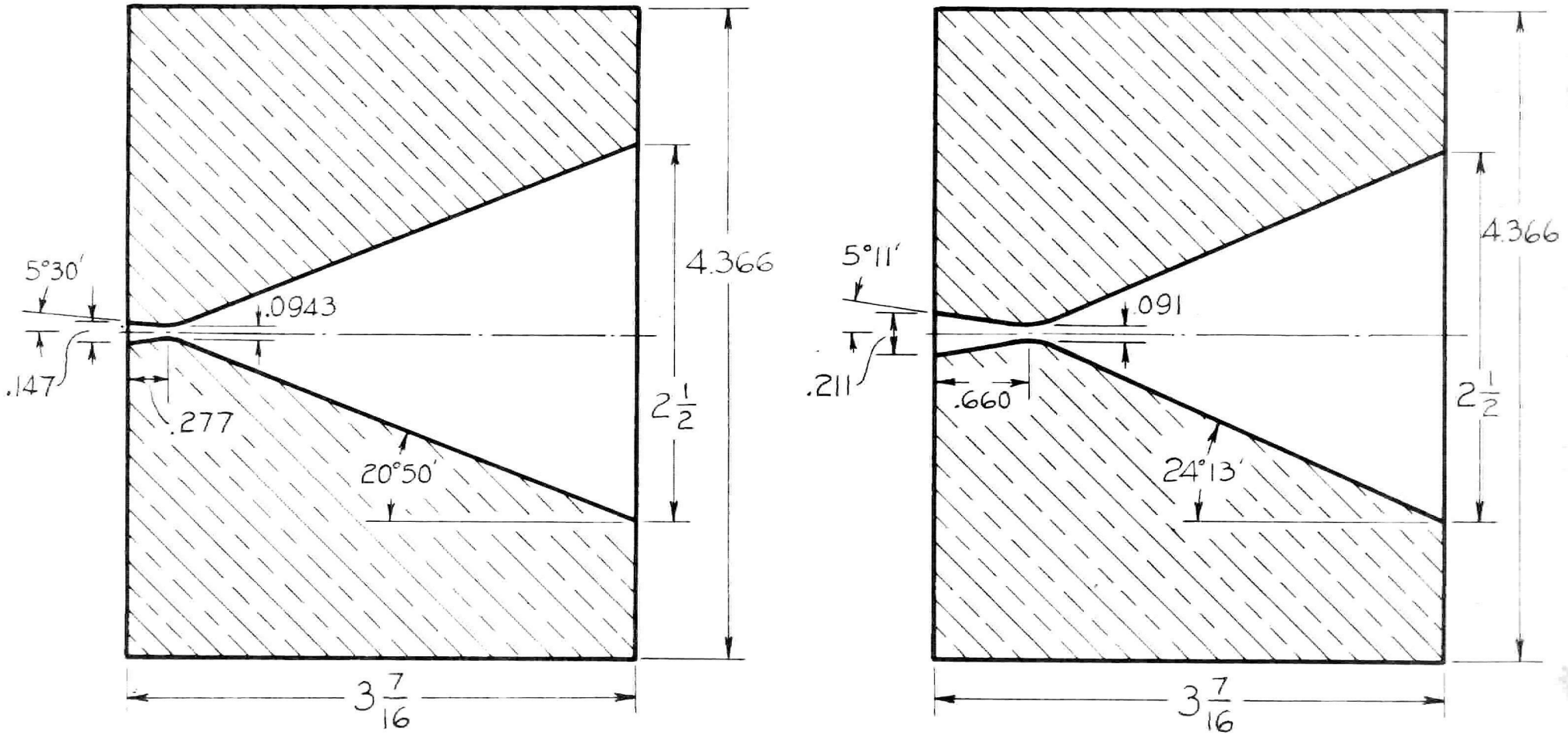

$\epsilon = 2.45$ (COPPER) $\epsilon = 5.38$

FIG. 13

TABLE III.

Run No.	Hot or cold thrust	p_o lb./sq.in	T °F	p_c, lb/sq.in (abs.)	w_f lb/sec	w_o lb/sec	w lb/sec	F lb.	d_t in.	d_e in.	f_t sq.in.	f_e sq.in.	ϵ	α	β	l in.	$p_c f_t$ lb.	p_o/p_c	r	C_{m_f}	C_{m_o}	C_m	C_F	c ft/sec.	η_{th} %	w_{sp} lb/sec/lb F
13	Hot	14.4	69.8	224.4	.00821	.00750	.01571	2.03	.0940	.1470	.00694	.01698	2.45	5°30'	30°50'	.277	1.559	.0641	.91	.1830	.1670	.3500	1.303	4160	3.30	.00773
14	"	"	69.0	320.4	.00406	.01560	.01966	3.21	"	"	"	"	"	"	"	"	2.226	.0448	3.84	.0633	.2440	.3073	1.440	5260	13.30	.00610
15	"	"	74.5	359.4	.01356	.01038	.02394	3.79	"	"	"	"	"	"	"	"	2.495	.0401	.77	.1890	.1440	.3330	1.518	5100	4.58	.00631
16	"	"	71.6	509.4	.02050	.01200	.03250	4.95	"	"	"	"	"	"	"	"	3.540	.0283	.59	.2010	.1180	.3190	1.400	4910	3.81	.00655
17	"	"	69.6	340.4	.00372	.01840	.02212	3.58	"	"	"	"	"	"	"	"	2.366	.0423	4.95	.0546	.2700	.3246	1.511	5210	16.10	.00617
18	"	"	64.8	371.4	.00722	.01444	.02166	3.70	"	"	"	"	"	"	"	"	2.580	.0388	2.00	.0972	.1940	.2912	1.436	5500	9.06	.00585
19	"	"	"	376.4	.02000	.00733	.02733	3.87	"	"	"	"	"	"	"	"	2.618	.0382	.37	.2660	.0973	.3633	1.480	4560	2.69	.00705
20	"	"	"	371.4	.00667	.01600	.02267	3.70	"	"	"	"	"	"	"	"	2.580	.0388	2.40	.0900	.2160	.3060	1.435	5250	9.35	.00614
21	"	"	"	366.4	.00334	.02135	.02469	3.68	"	"	"	"	"	"	"	"	2.542	.0393	6.39	.0457	.2920	.3377	1.445	4800	17.00	.00671
22	"	"	68.0	398.4	.03071	.00679	.02750	4.08	"	"	"	"	"	"	"	"	2.770	.0361	.33	.2600	.0852	.3452	1.475	4780	3.02	.00674
23	"	"	"	398.4	.00680	.01760	.02440	4.05	"	"	"	"	"	"	"	"	2.770	.0361	2.44	.0853	.2210	.3063	1.461	5350	9.80	.00602
24	"	"	"	389.4	.00429	.02380	.02809	4.10	"	"	"	"	"	"	"	"	2.703	.0370	5.55	.0551	.3060	.3611	1.516	4740	14.70	.00681
25	"	"	"	311.4	.01133	.01033	.02166	3.07	"	"	"	"	"	"	"	"	2.165	.0462	.91	.1820	.1660	.3480	1.418	4560	3.77	.00705
26	"	"	"	311.4	.00400	.01467	.01867	3.03	"	"	"	"	"	"	"	"	2.165	.0462	3.67	.0642	.2350	.2992	1.400	5230	12.80	.00615
27	"	"	"	310.4	.00225	.01975	.02200	2.96	"	"	"	"	"	"	"	"	2.155	.0463	8.78	.0363	.3180	.3543	1.374	4330	18.20	.00744
28	"	14.3	70.4	271.3	.01173	.00767	.01940	2.44	"	"	"	"	"	"	"	"	1.885	.0527	.65	.2160	.1420	.3580	1.293	4050	2.71	.00795
29	"	"	"	271.3	.00750	.01227	.01977	2.34	"	"	"	"	"	"	"	"	1.885	.0527	1.64	.1380	.2260	.3640	1.241	3810	3.83	.00845
30	"	"	"	261.3	.00317	.01573	.01890	2.44	"	"	"	"	"	"	"	"	1.815	.0547	4.97	.0607	.3020	.3627	1.345	4160	10.35	.00771
31	Hot	14.4	77.0	186.4	.00938	.00543	.01480	1.97	.1004	.1470	.00794	.01698	2.14		20°50'	.277	1.481	.0772	.58	.2300	.1270	.3470	1.330	4260	2.88	.00752
32	"	"	"	172.4	.00200	.01585	.01785	1.81	.1028	"	.00831	"	2.04	4°35'	"	"	1.433	.0835	7.93	.0485	.3840	.4325	1.263	3270	9.52	.00985
33	"	14.5	71.6	130.5	.00324	.00753	.01077	1.17	"	"	"	"	"	"	"	"	1.084	.1110	2.32	.1040	.2420	.3460	1.079	3500	4.05	.00930
34	"	14.4	69.8	538.4	.03500	.00951	.04451	6.08	.1032	"	.00836	"	2.03	4°30'	"	"	4.530	.0267	.27	.2690	.0732	.3422	1.345	4400	2.46	.00732
35	"	"	"	539.4	.01031	.03470	.03501	5.81	"	"	"	"	"	"	"	"	"	.0267	2.40	.0794	.1900	.2694	1.385	5340	9.64	.00605
36	"	"	68.0	253.4	.01016	.00856	.01872	2.77	.1053	"	.00873	"	1.95	4°19'	"	"	2.206	.0570	.84	.1600	.1350	.2950	1.255	4770	4.18	.00675
37	"	"	"	247.4	.00653	.01133	.01786	2.70	"	"	"	"	"	"	"	"	2.161	.0582	1.74	.1050	.1820	.2870	1.248	4580	6.51	.00660
38	"	"	"	246.4	.00413	.01107	.01520	2.60	"	"	"	"	"	"	"	"	2.154	.0583	2.68	.0668	.1790	.2458	1.205	5500	11.09	.00585

TABLE IV.

Run No.	Hot or cold thrust	p_o, lb./sq.in (abs)	T °F	p_c, lb/sq.in. (abs)	w_f lb./sec	w_o lb./sec	w lb./sec	F lb.	d_t in.	d_e in.	f_t sq.in	f_e sq.in.	ϵ	α	β	l in.	$p_c f_t$ lb.	p_o/p_c	r	C_{m_f}	C_{m_o}	C_m	C_F	c ft./sec.	η_{th} %	W_{sp} lb./sec/lb F
39	Hot	14.4	68.5	499.4	.01655	.02070	.03725	4.82	.091	.211	.00651	.03500	5.38	5° 11'	24° 13'	.660	3.250	.0289	1.25	.1770	.2220	.3990	1.482	4170	3.90	.00772
40	"	"	"	479.4	.00339	.02092	.02431	4.77	"	"	"	"	"	"	"	"	3.120	.0301	6.17	.0378	.2330	.2718	1.530	6310	28.40	.00510
41	"	"	"	369.4	.01080	.01030	.02110	3.51	"	"	"	"	"	"	"	"	2.400	.0390	.95	.1560	.1490	.3050	1.461	5350	5.55	.00601
42	"	"	"	364.4	.00827	.01408	.02235	3.40	"	"	"	"	"	"	"	"	2.372	.0395	1.70	.1210	.2060	.3270	1.432	4900	6.46	.00657
43	"	"	"	364.4	.00241	.02445	.02686	3.35	"	"	"	"	"	"	"	"	2.372	.0395	10.03	.0353	.3590	.3940	1.415	4030	17.80	.00798
44	"	"	"	296.4	.00574	.00778	.01352	2.30	"	"	"	"	"	"	"	"	1.930	.0486	1.35	.1035	.1401	.2440	1.190	5460	7.00	.00589
45	"	"	"	299.4	.00361	.01378	.01739	2.30	"	"	"	"	"	"	"	"	1.949	.0481	3.81	.0644	.2460	.3104	1.180	4260	8.72	.00755
46	"	"	"	296.4	.00317	.01312	.01629	2.30	"	"	"	"	"	"	"	"	1.930	.0486	4.13	.0571	.2365	.2936	1.190	4550	11.10	.00707
47	"	"	"	220.4	.00692	.00568	.01260	1.42	"	"	"	"	"	"	"	"	1.435	.0653	.82	.1680	.1380	.3060	.990	3630	2.40	.00886
48	"	"	"	216.4	.00535	.00507	.01042	1.42	"	"	"	"	"	"	"	"	1.410	.0665	.95	.1320	.1250	.2570	1.008	4380	3.73	.00734
49	"	"	"	214.4	.00150	.00650	.00800	1.42	"	"	"	"	"	"	"	"	1.396	.0672	4.23	.0373	.1620	.1993	1.018	5720	17.03	.00563
50	"	"	82.0	409.4	.00920	.01480	.02400	3.67	"	"	"	"	"	"	"	"	2.664	.0352	1.60	.1200	.1930	.3130	1.377	4920	6.27	.00653
51	"	"	"	409.4	.01083	.01521	.02604	3.64	"	"	"	"	"	"	"	"	2.664	.0352	1.40	.1410	.1980	.3390	1.365	4500	4.85	.00715
52	"	"	"	394.4	.00473	.02035	.02508	3.53	"	"	"	"	"	"	"	"	2.565	.0365	4.30	.0641	.2750	.3401	1.375	4530	10.73	.00710
53	"	"	"	392.4	.00866	.01317	.02183	3.42	"	"	"	"	"	"	"	"	2.555	.0367	1.52	.1180	.1790	.2970	1.338	5030	6.35	.00639
54	"	"	"	395.4	.01300	.00885	.02185	3.60	"	"	"	"	"	"	"	"	2.573	.0364	.68	.1780	.1200	.2960	1.400	5300	4.70	.00608
55	"	"	"	389.4	.01013	.01476	.02489	3.43	"	"	"	"	"	"	"	"	2.532	.0370	1.45	.1390	.3030	.3410	1.353	4440	4.81	.00725
56	"	"	"	379.4	.00696	.01160	.01856	3.35	"	"	"	"	"	"	"	"	2.466	.0379	1.67	.0980	.1630	.2610	1.358	5810	8.96	.00554
57	"	"	"	374.4	.00475	.01735	.02210	3.27	"	"	"	"	"	"	"	"	2.440	.0384	3.65	.0677	.2470	.3147	1.340	4760	10.50	.00676
58	"	"	"	369.4	.00635	.01556	.02191	3.17	"	"	"	"	"	"	"	"	2.402	.0390	2.45	.0918	.2250	.3168	1.318	4660	7.47	.00690

FIG. 14

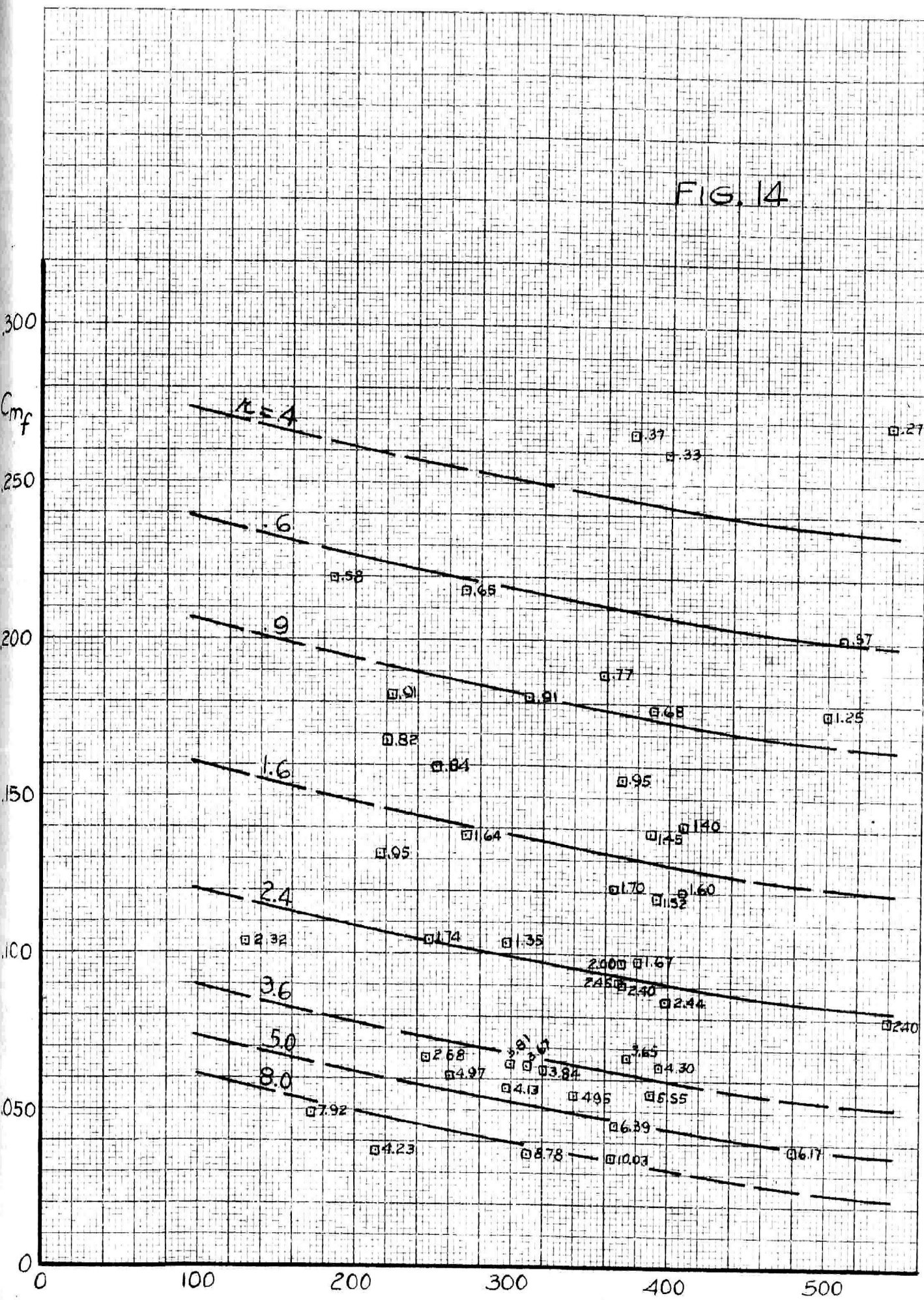
300
250
200
150
100
050
0
C_{mf}
0
100
200
300
400
500
lb/sq in abs
k = 4
.6
.9
1.6
2.4
3.6
5.0
8.0
.37
.33
.27
.58
.68
.37
.91
.91
.77
.68
1.25
.82
.84
.95
1.64
1.40
1.45
.95
1.70
1.60
1.52
2.32
1.74
1.35
2.00
1.67
2.40
2.44
2.40
2.68
4.97
4.13
3.84
4.96
6.55
4.30
7.92
4.23
8.78
10.03
6.39
6.17

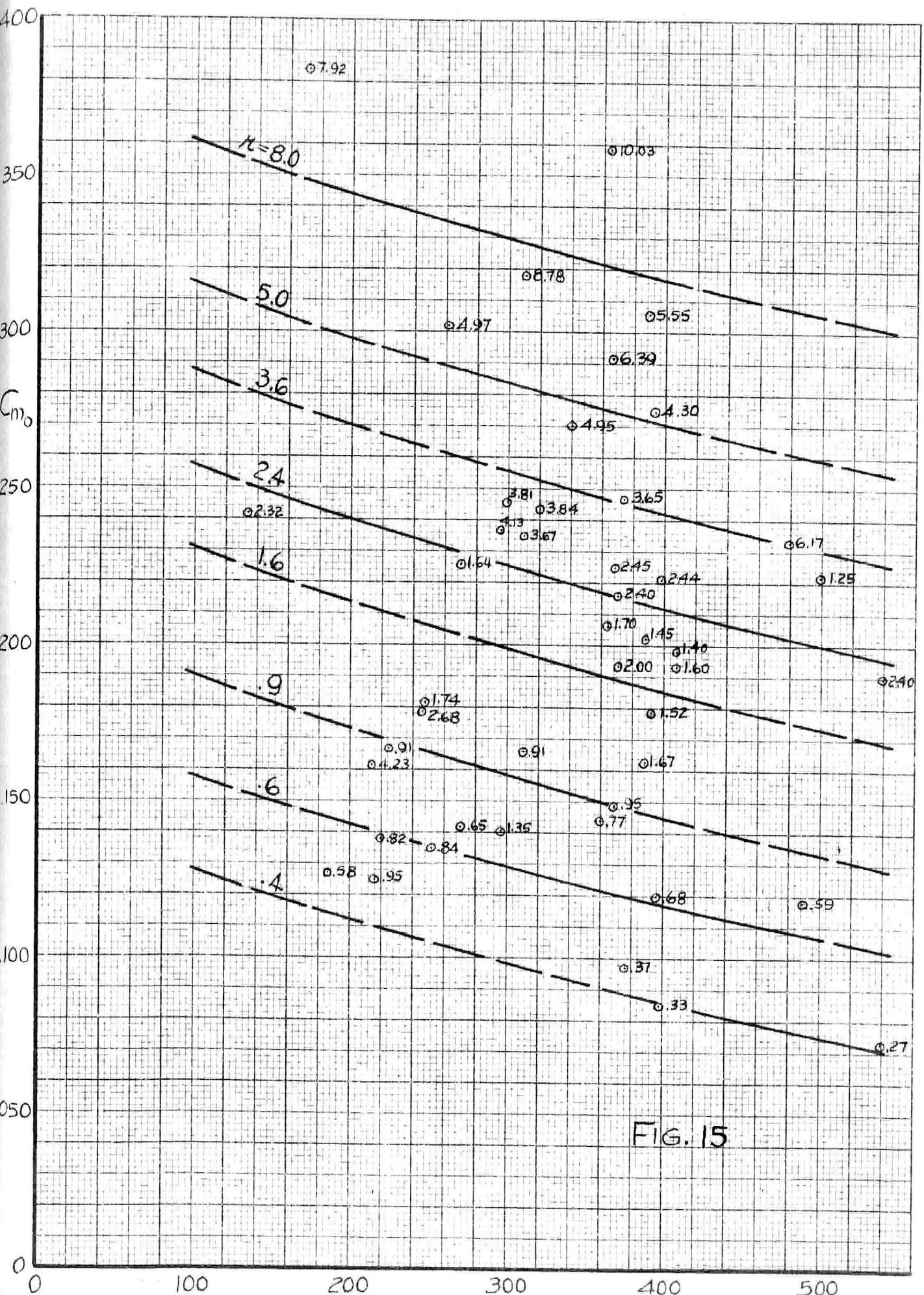
400
350
300
250
200
150
100
050
0
C_{m_o}
0
100
200
300
400
500
p_c, lb/sq.in., abs.
h=8.0
5.0
3.6
2.4
1.6
.9
.6
.4
7.92
10.03
8.78
5.55
4.97
6.39
4.30
4.95
3.65
6.17
3.81
3.84
2.32
4.13
3.67
1.64
2.45
2.44
1.25
2.40
2.40
1.70
1.45
1.40
2.00
1.60
1.74
2.68
1.52
.91
4.23
.91
1.67
.95
.77
.65
1.35
.82
.84
.58
.95
.68
.59
.37
.33
.27

FIG. 15

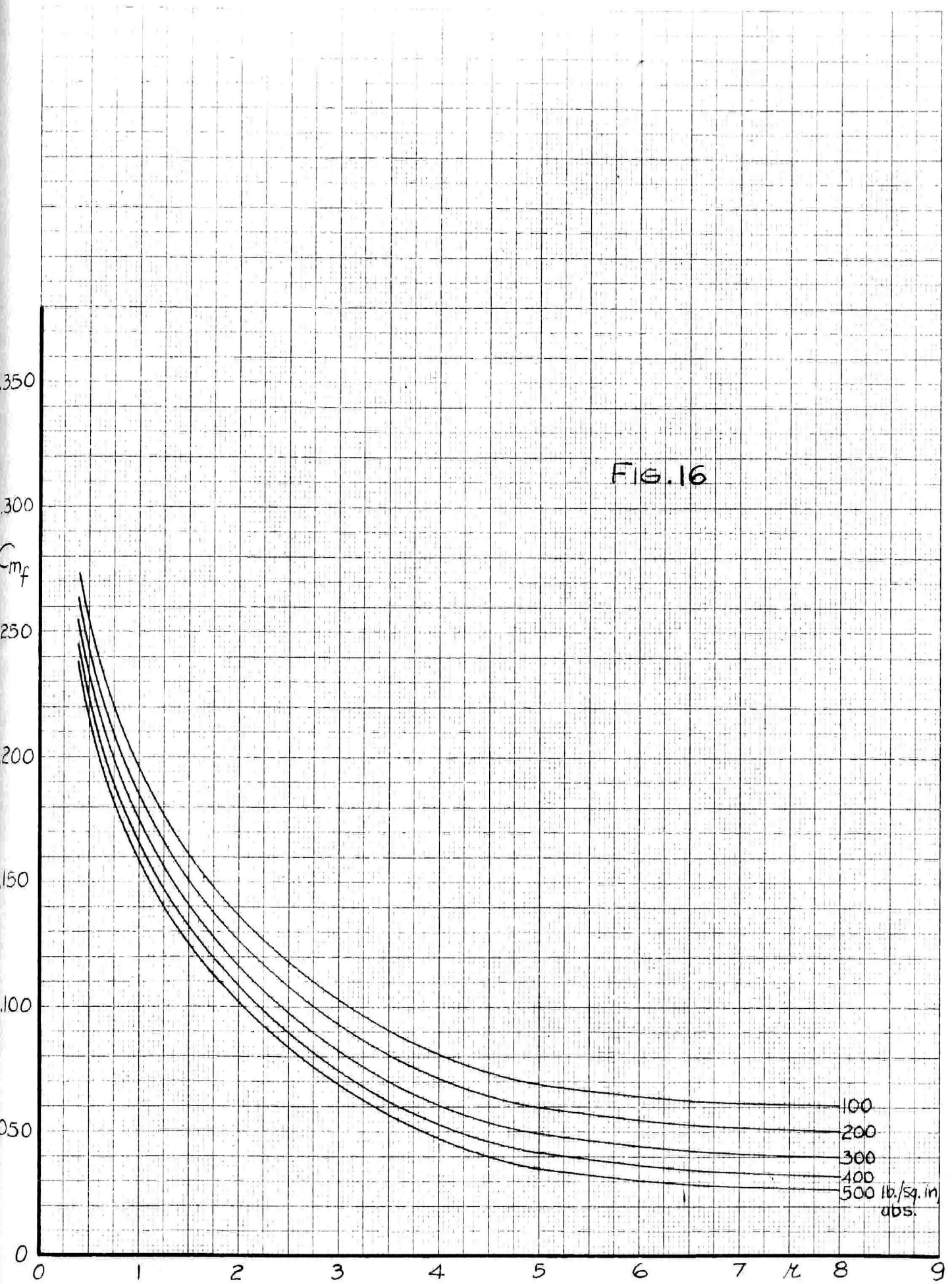
350
300
C_{m_f}
250
200
150
100
050
0
0
1
2
3
4
5
6
7
8
9
100
200
300
400
500 lb./sq. in. abs.

FIG. 16

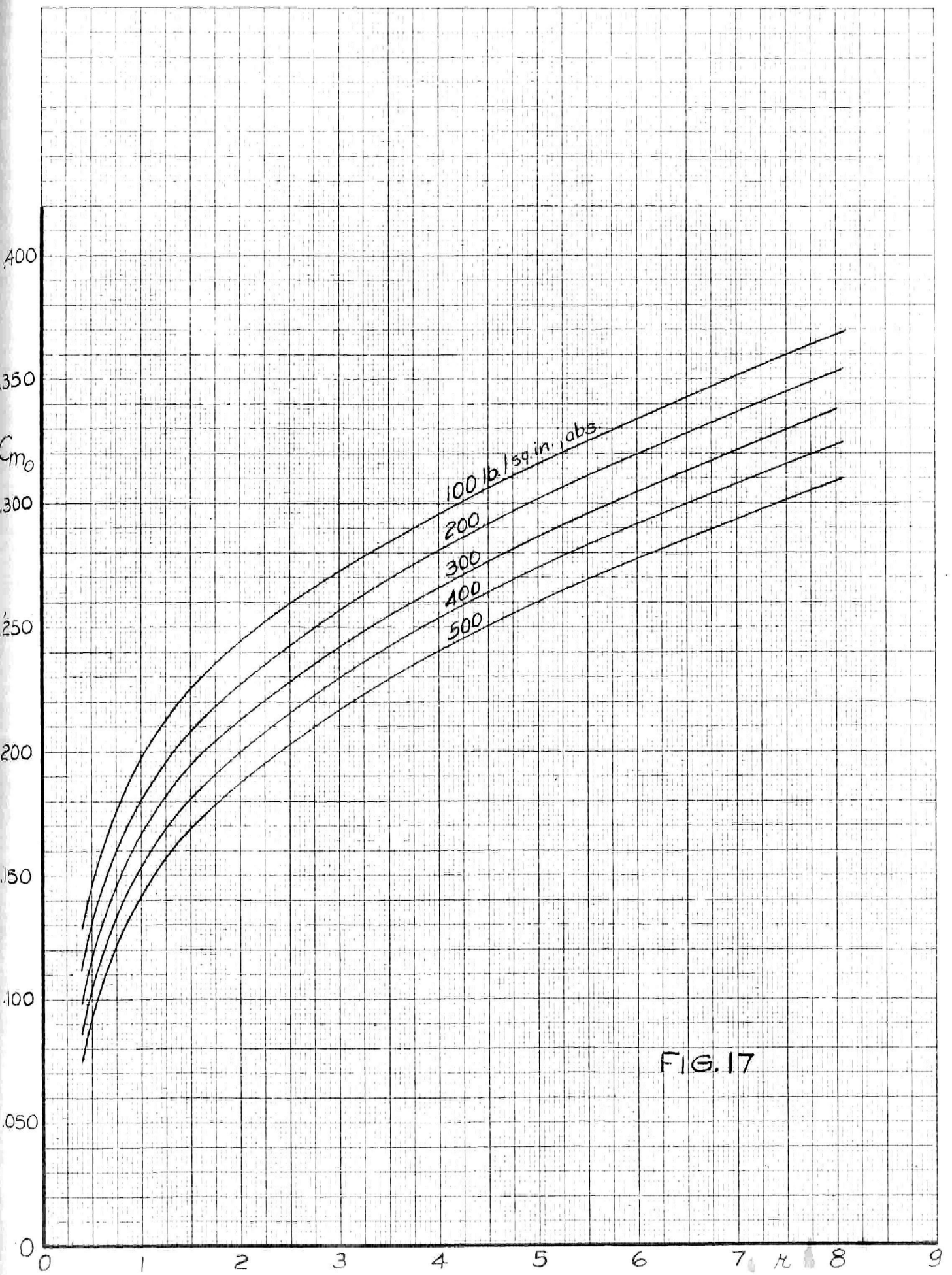
400
350
C_{m_o}
300
250
200
150
100
050
0
0
1
2
3
4
5
6
7
8
9
100 lb./sq.in. abs.
200
300
400
500

FIG. 17

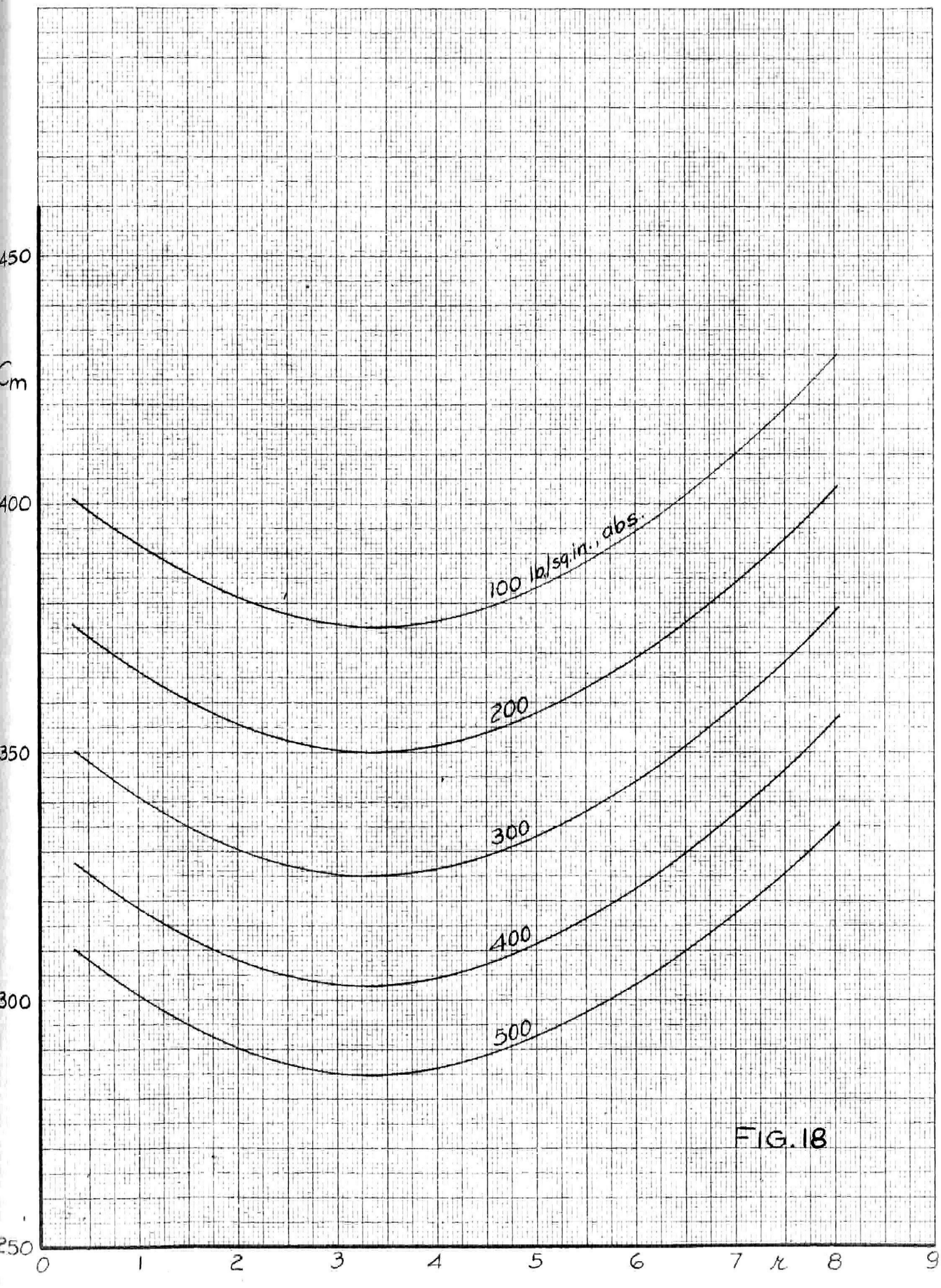
450
Cm
400
350
300
250
100 lb/sq.in., abs.
200
300
400
500
0
1
2
3
4
5
6
7
x
8
9

FIG. 18

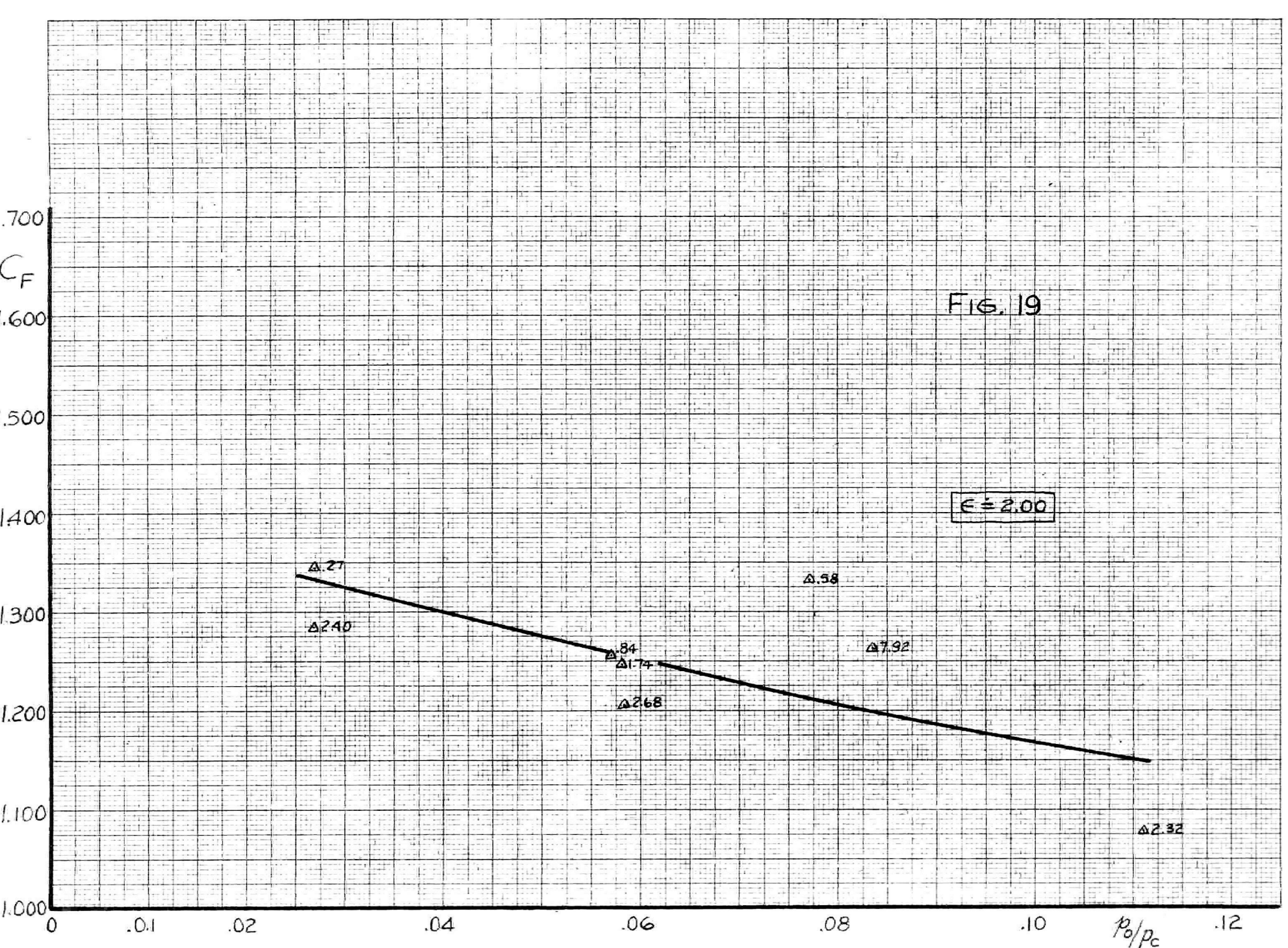
FIG. 19
$\epsilon = 2.00$
C_F
1.700
1.600
1.500
1.400
1.300
1.200
1.100
1.000
0
.01
.02
.04
.06
.08
.10
.12
p_0/p_c
Δ.27
Δ2.40
Δ.84
Δ1.74
Δ2.68
Δ.58
Δ7.92
Δ2.32

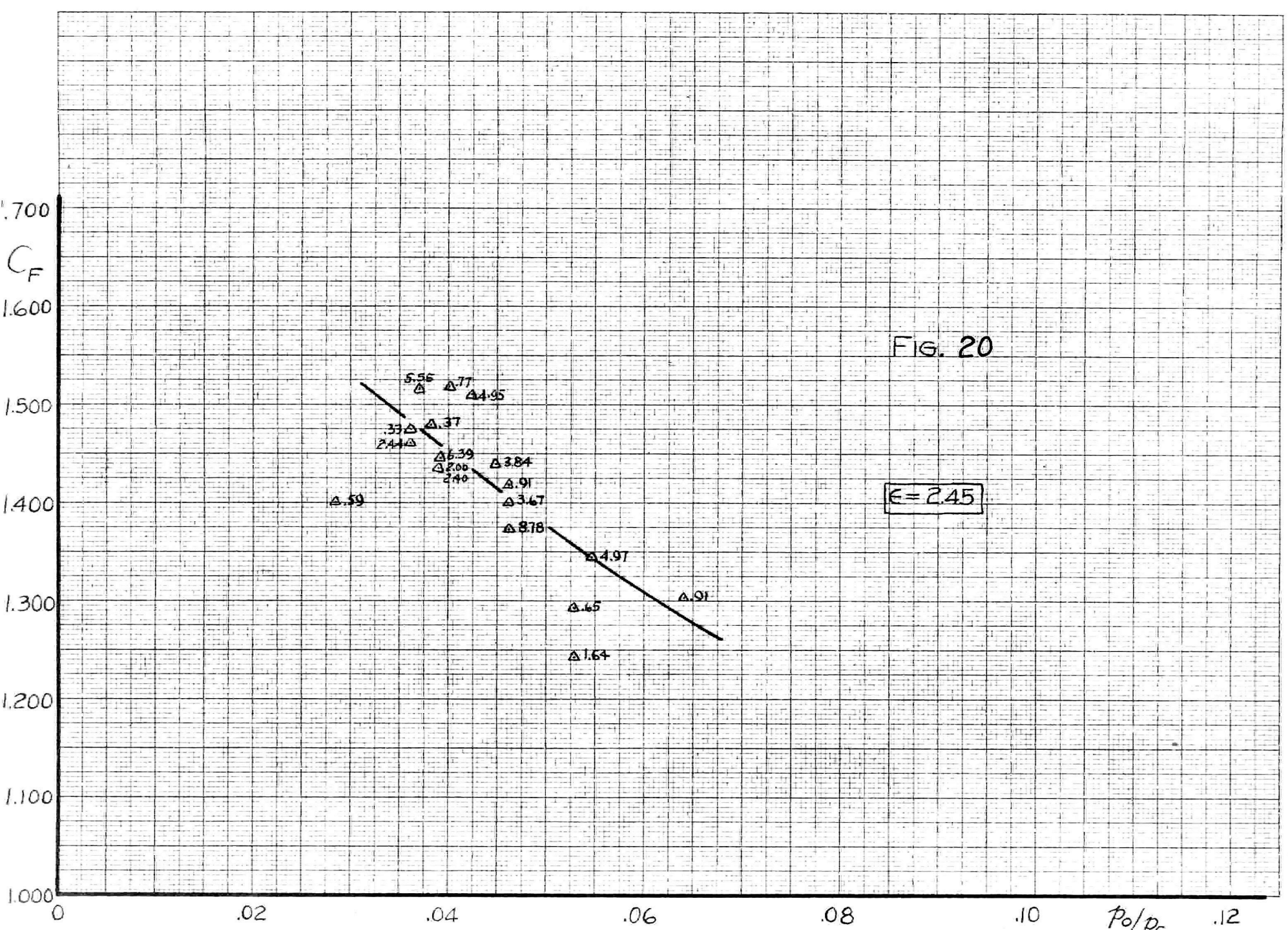
.700
C_F
1.600
1.500
1.400
1.300
1.200
1.100
1.000
0
.02
.04
.06
.08
.10
.12
p_o/p_-
5.56
.77
4.95
.33
.37
2.44
6.39
2.00
2.40
3.84
.91
.59
3.67
8.78
4.97
.91
.65
1.64
FIG. 20
$\epsilon = 2.45$

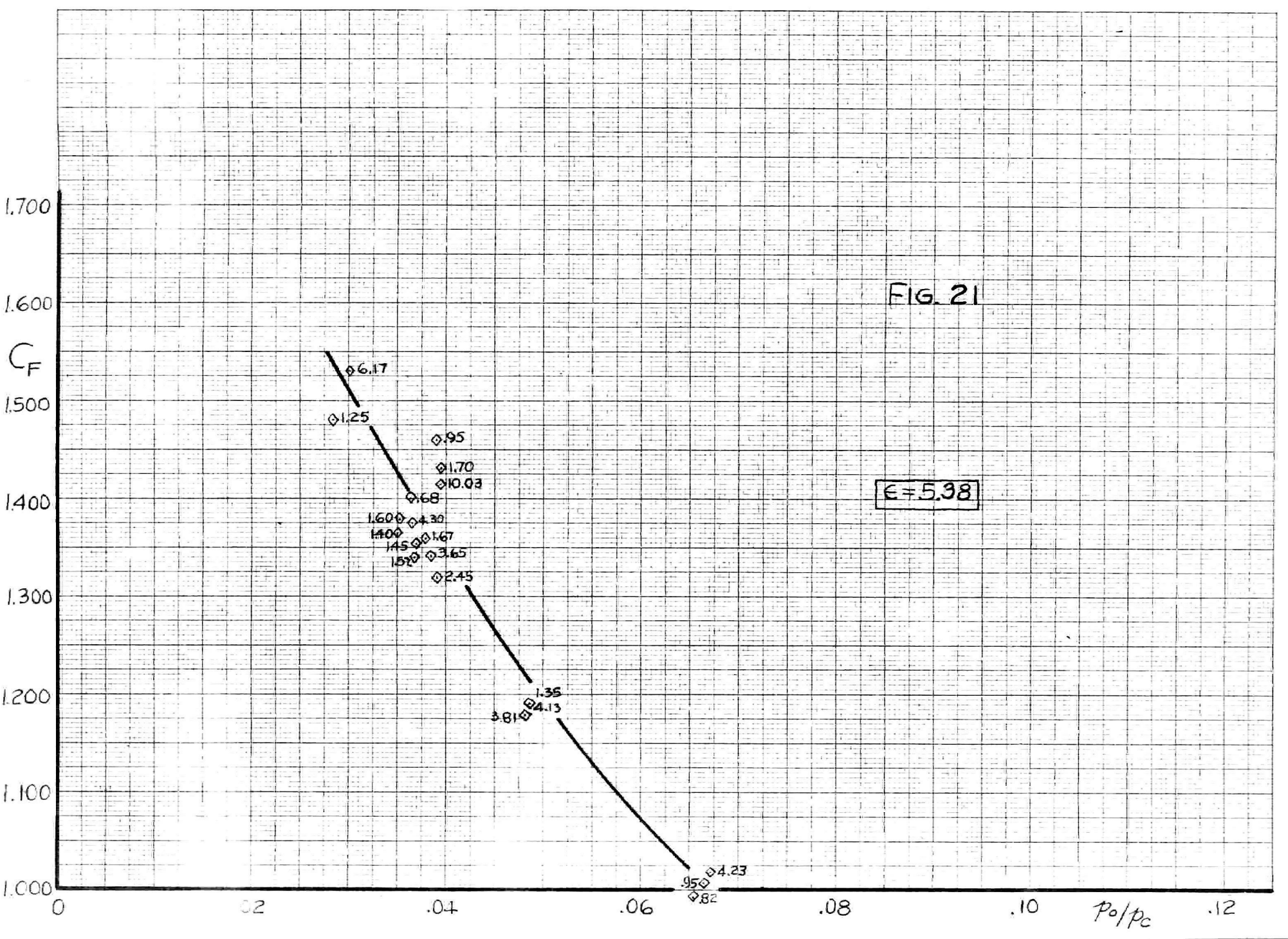
FIG. 21
ε=5.38
C_F
1.700
1.600
1.500
1.400
1.300
1.200
1.100
1.000
0
.02
.04
.06
.08
.10
.12
p_o/p_c
6.17
1.25
.95
1.70
10.03
1.68
1.60
4.30
1.40
1.67
1.45
1.52
3.65
2.45
1.35
4.13
3.81
4.23
.95
.82

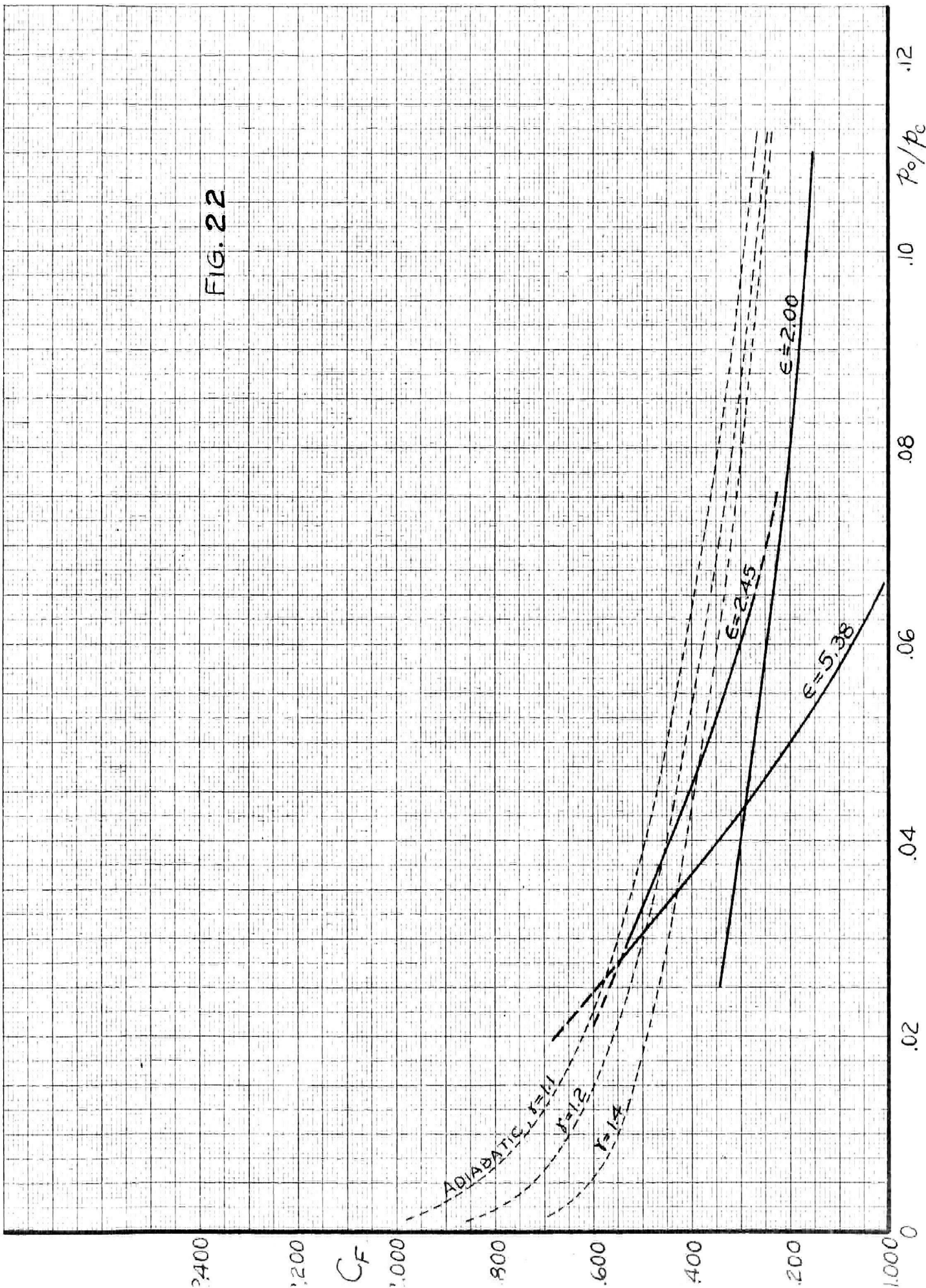
FIG. 22
C_F
2400
2200
2000
1800
1600
1400
1200
1000
0
.02
.04
.06
.08
.10
.12
p_o/p_c
ADIABATIC, $\gamma=1.1$
$\gamma=1.2$
$\gamma=1.4$
$\epsilon=2.00$
$\epsilon=2.45$
$\epsilon=5.38$

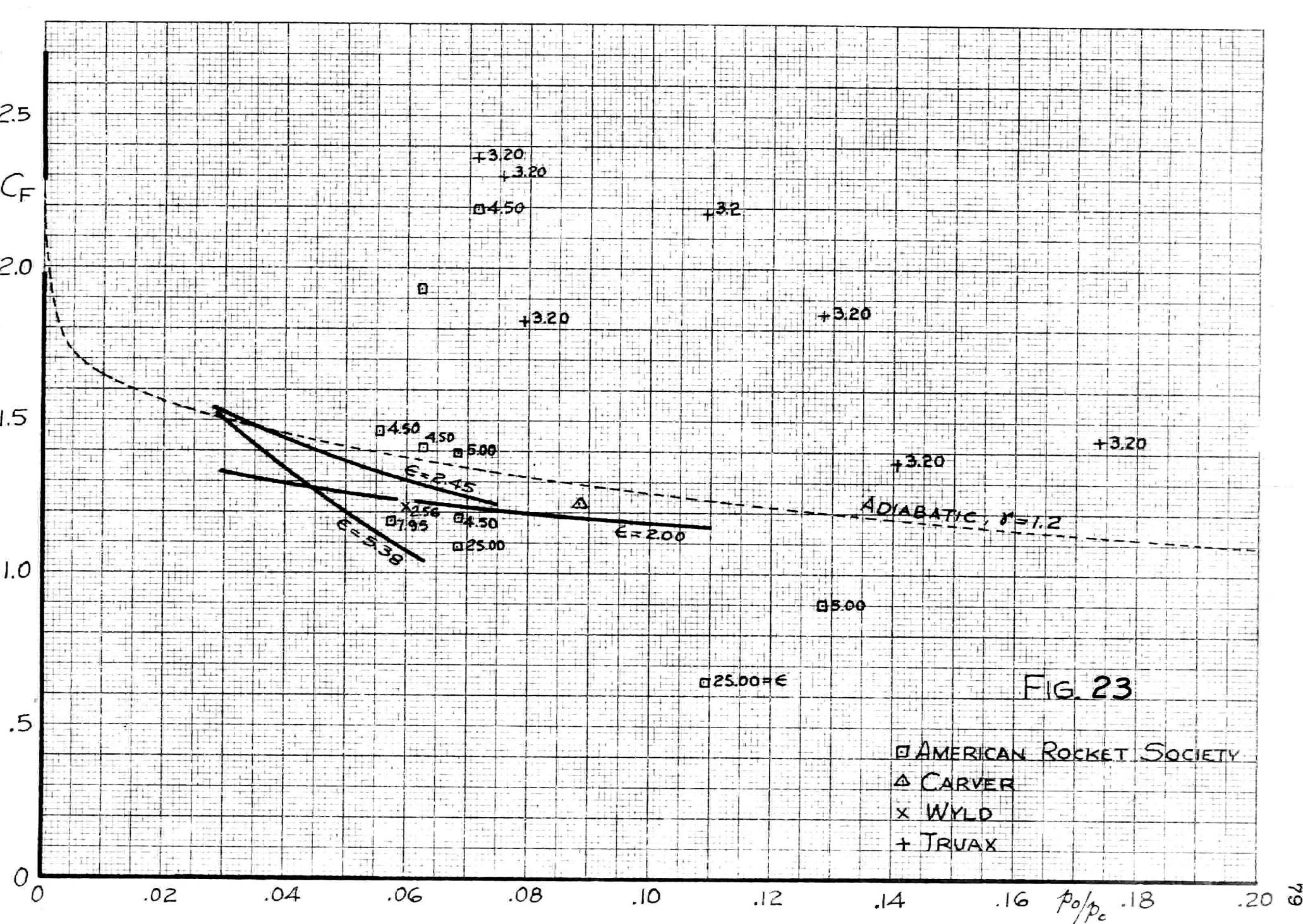
2.5
C_F
2.0
1.5
1.0
.5
0
.02
.04
.06
.08
.10
.12
.14
.16
p_o/p_c
.18
.20
+3.20
+3.20
□4.50
+3.2
+3.20
+3.20
□4.50
4.50
□5.00
+3.20
+3.20
ε=2.45
ADIABATIC, γ=1.2
×2.56
□7.95
□4.50
ε=5.38
ε=2.00
□25.00
□5.00
□25.00=ε
□ AMERICAN ROCKET SOCIETY
△ CARVER
× WYLD
+ TRUAX

FIG. 23

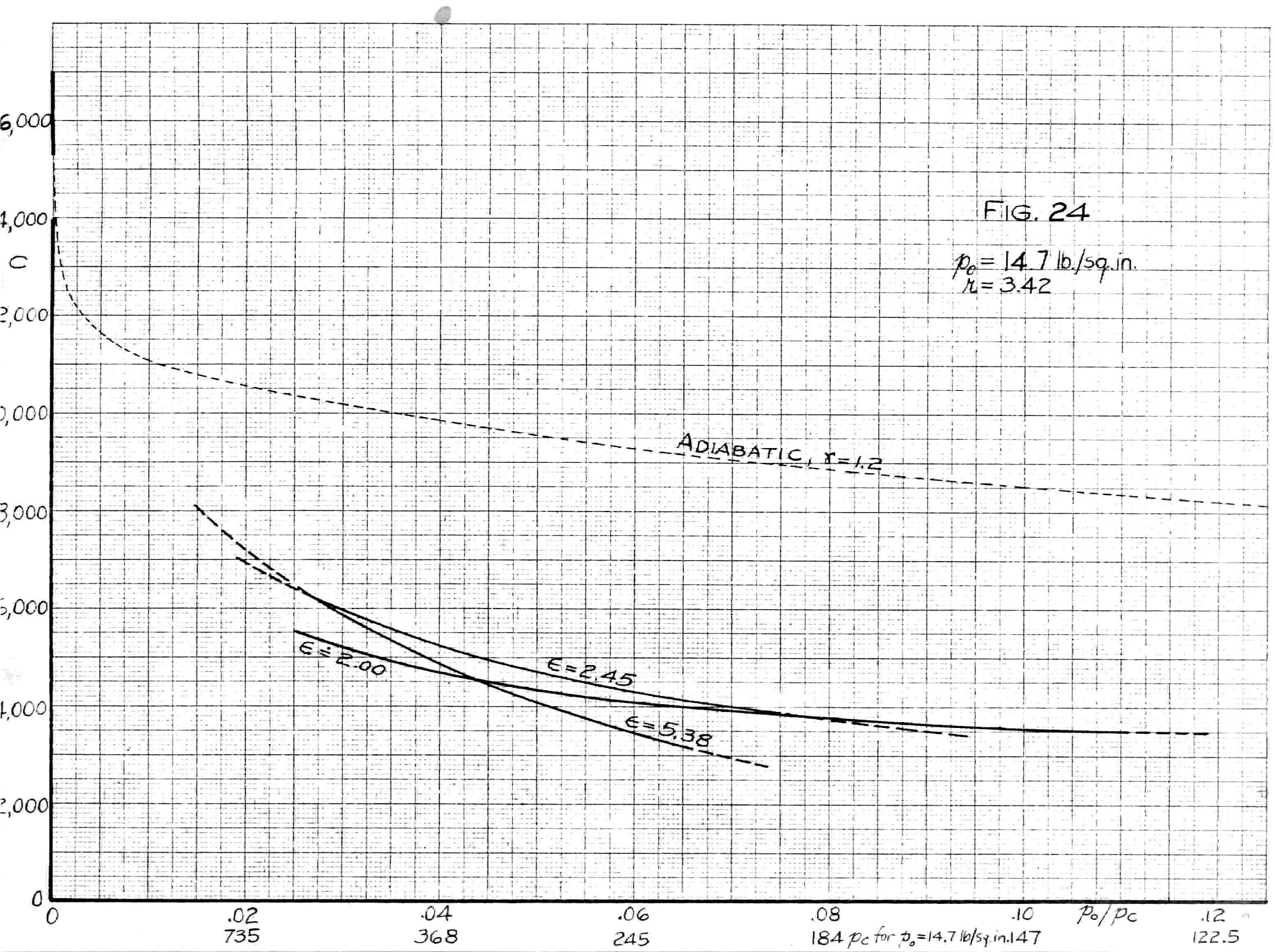
6,000
4,000
C
2,000
0,000
8,000
6,000
4,000
2,000
0
FIG. 24
p_o = 14.7 lb./sq.in.
γ = 3.42
ADIABATIC, γ=1.2
ϵ=2.00
ϵ=2.45
ϵ=5.38
0
.02
735
.04
368
.06
245
.08
184 p_c for p_o=14.7 lb/sq.in.
.10
147
p_o/p_c
.12
122.5

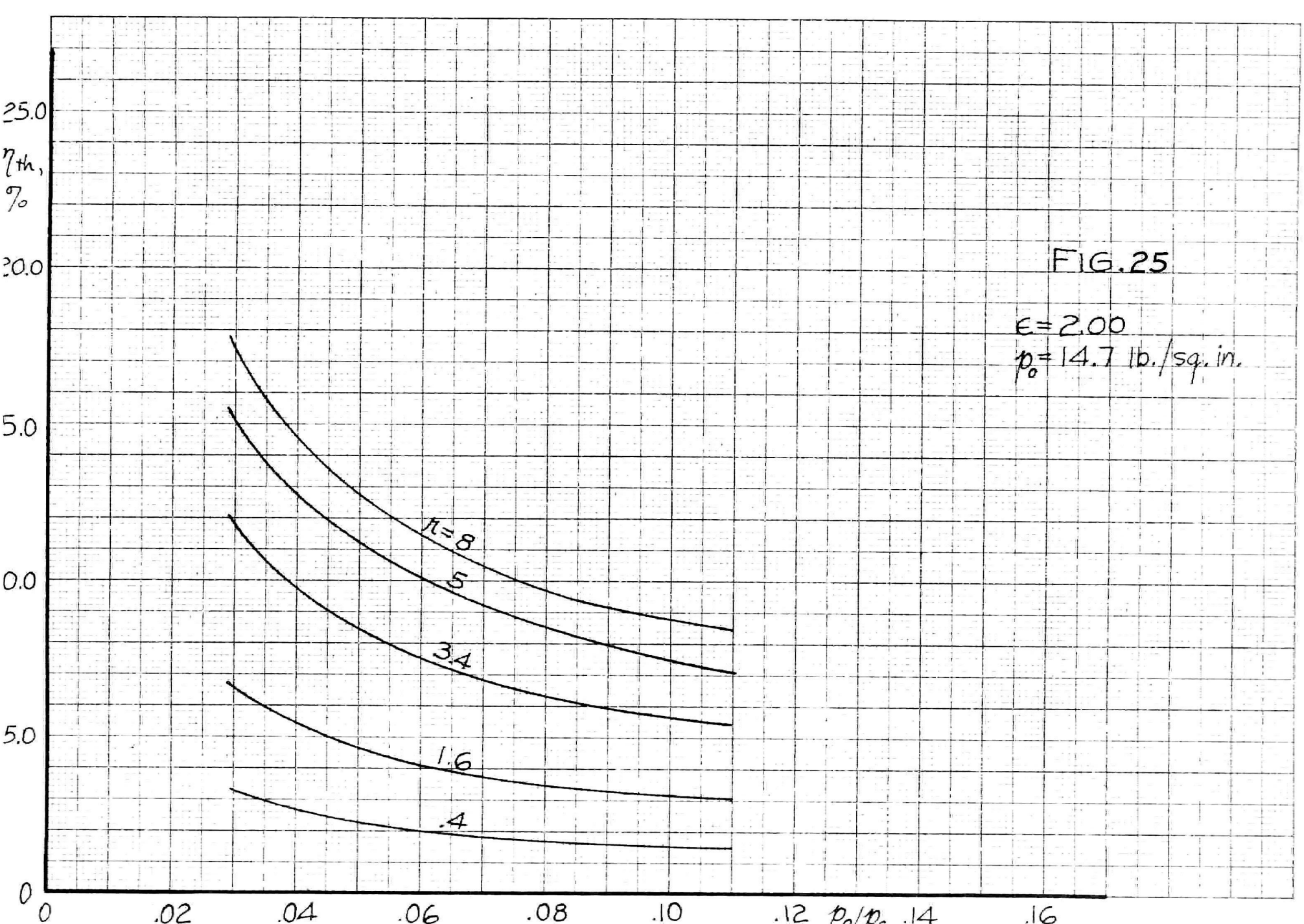

FIG. 25

$\epsilon = 2.00$

$p_o = 14.7$ lb./sq. in.

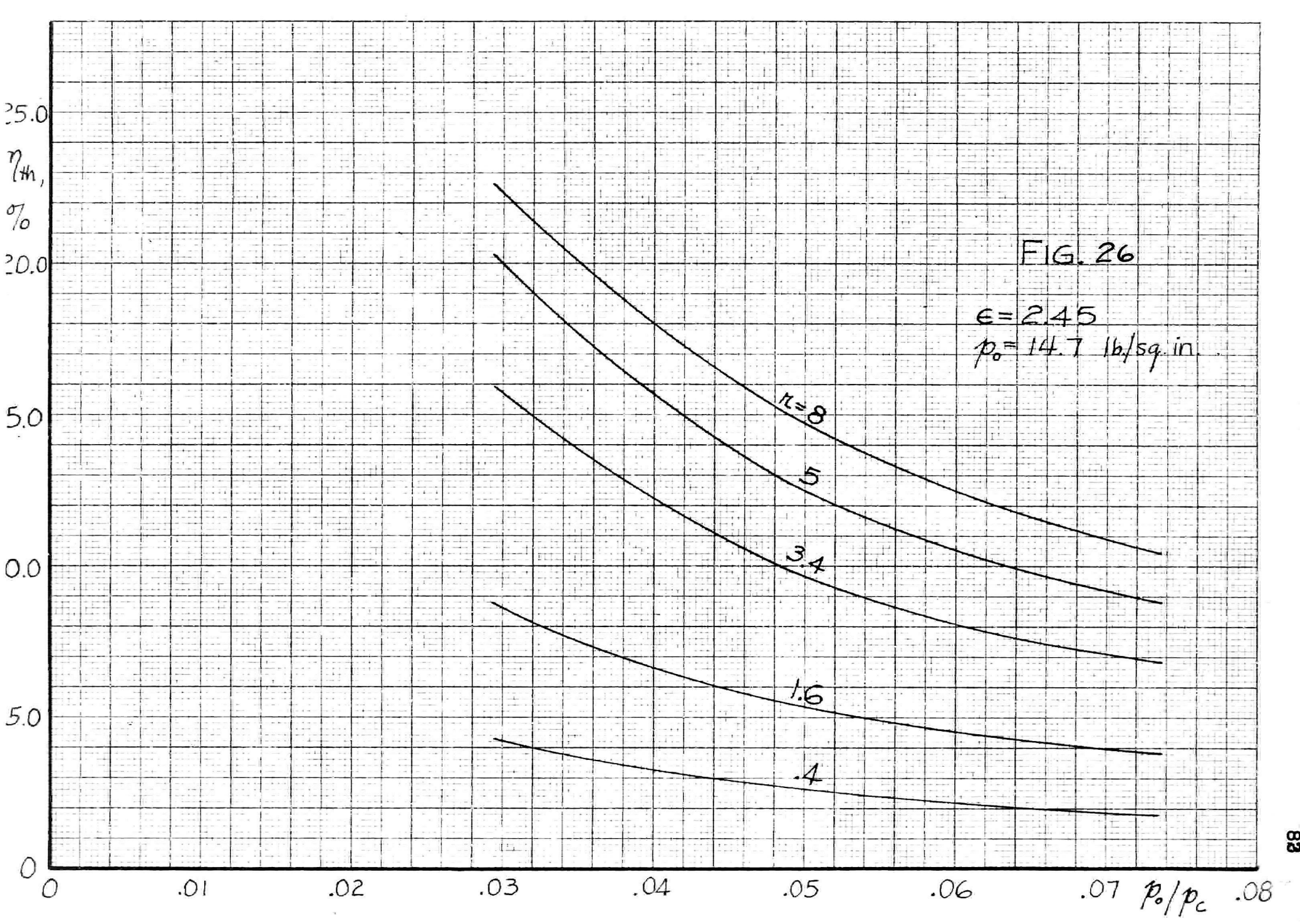
25.0
η_{th}, %
20.0
15.0
10.0
5.0
0.0
5.0
0
0
.01
.02
.03
.04
.05
.06
.07
.08
p_0/p_c
FIG. 26
$\epsilon = 2.45$
$p_0 = 14.7$ lb/sq. in.
$\pi = 8$
5
3.4
1.6
.4

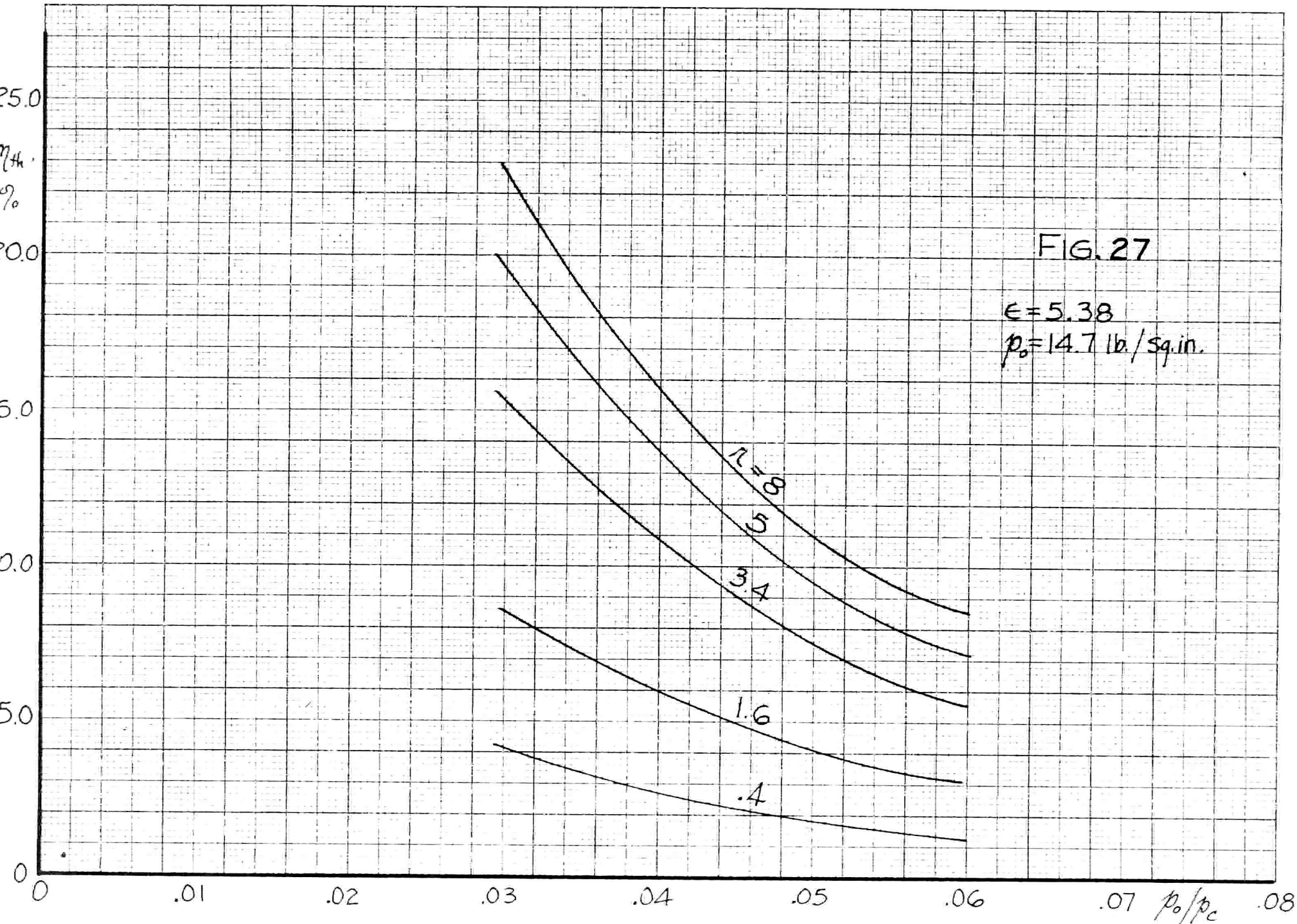
25.0
η_{th}, %
20.0
5.0
0.0
5.0
0
0
.01
.02
.03
.04
.05
.06
.07
p_o/p_c
.08
n = 8
5
3.4
1.6
.4
FIG. 27
$\epsilon = 5.38$
$p_o = 14.7$ lb./sq.in.

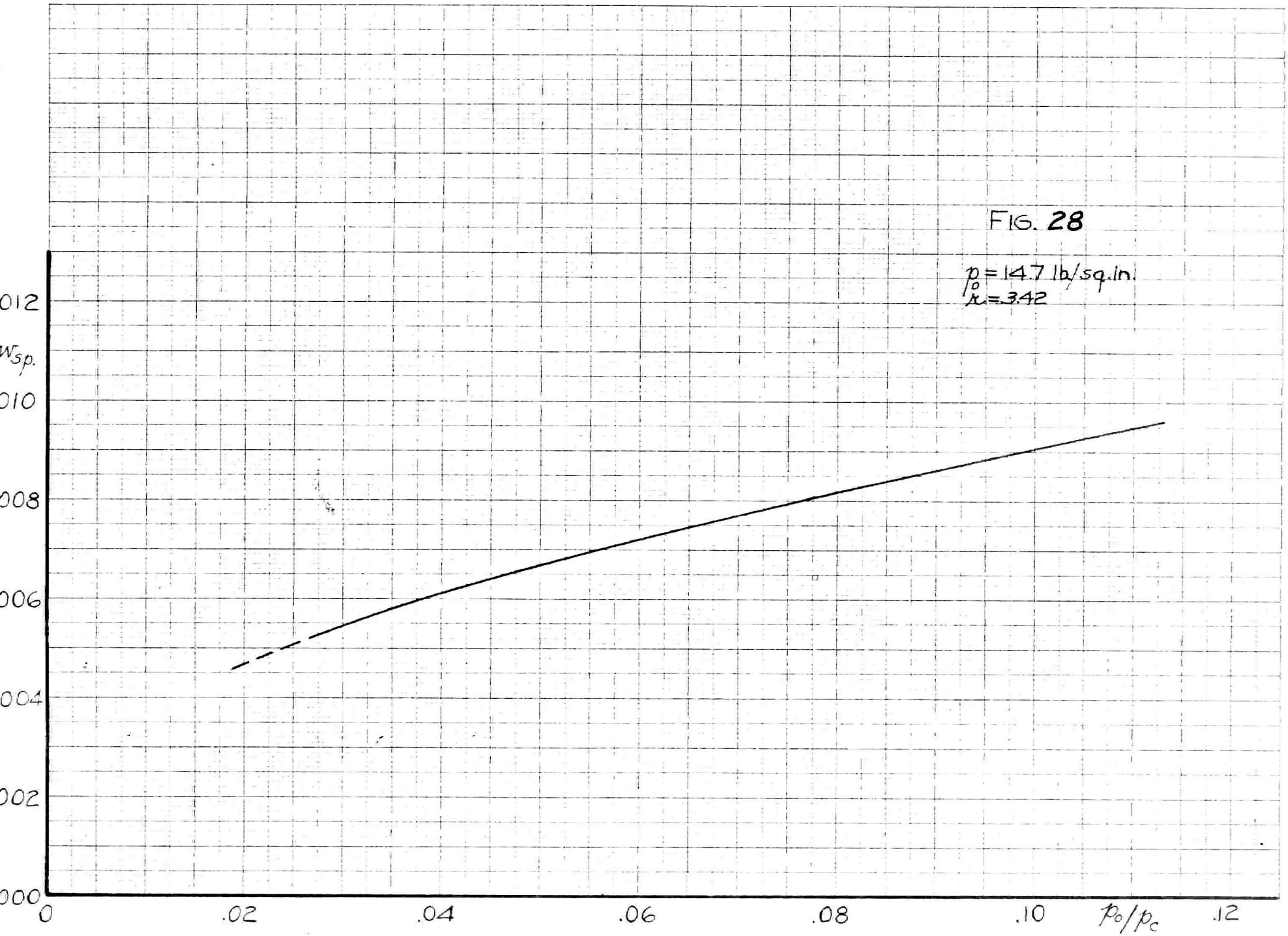
FIG. 28
p_o = 14.7 lb/sq.in.
γ = 3.42
012
$w_{sp.}$
010
008
006
004
002
000
0
.02
.04
.06
.08
.10
.12
p_o/p_c

MARCH, 1938 Reprinted from the JOURNAL OF THE AERONAUTICAL SCIENCES VOLUME 5, NO. 5

Flight Analysis of the Sounding Rocket

FRANK J. MALINA and A. M. O. SMITH, *California Institute of Technology*

Presented at the Aerodynamics Session, Sixth Annual Meeting, I. Ae. S. January 26, 1938

INTRODUCTION

IN ATTEMPTING to reach altitudes above those obtainable by sounding balloons, the rocket motor may be utilized to propel a suitable body. In this analysis a wingless shell of revolution will be considered in vertical flight.

It was felt that, before entering into practical experimentation, it was desirable to have a preliminary performance analysis based on simplified assumptions, using the most recent data for air resistance at high speeds. As a matter of fact, this analyis was completed without the knowledge of a similar investigation.[1] However, as this treatment is more general in discussing the influence of the design parameters and more suitable for application to particular cases, the authors believe it is worth while to present the analysis.

The equations of motion for flight *in vacuo* have been included to show the optimum performance and for comparison purposes. After developing similar expressions for flight with air resistance, a series of calculations was carried out using the method of step-by-step integration. The dimensions of the rocket chosen were felt to be feasible for practical construction. The motor efficiencies for the two cases were chosen to match closely the reported results of R. H. Goddard[2] and Eugen Sänger.[3]

The calculations have not been extended to further cases, as the amount of labor that would be required was not felt justified at the present time.

ASSUMPTIONS AND NOTATION

Throughout this analysis, the assumption will be made that the rocket motor supplies a thrust of constant magnitude for the period of powered flight. This means that the rate of flow of combustibles and the effective exhaust velocity remain constant. This assumption is of a conservative nature, as theoretical considerations show that the thermal efficiency of the rocket motor and, therefore, the thrust, will increase as the ratio between chamber pressure and exhaust pressure increases.

It has been assumed that the acceleration due to gravity remains constant. This assumption is also conservative.

The following notation has been used for the quantities involved:

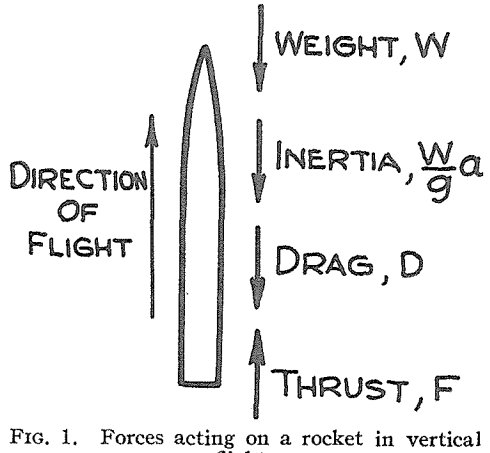

FIG. 1. Forces acting on a rocket in vertical flight.

F	=	thrust in lbs.
m	=	mass of exhaust gases flowing per second
c	=	F/m = effective exhaust velocity in ft./sec.
W_0	=	initial weight of rocket, lbs.
W	=	instantaneous weight of rocket, lbs.
W_{FO}	=	weight of fuel and oxidizer carried, lbs.
ζ	=	W_{FO}/W_0, ratio of weight of fuel plus oxidizer to initial weight of rocket
a_0	=	initial acceleration, ft./sec.^{2}
a	=	instantaneous acceleration, ft./sec.^{2}
g	=	acceleration of gravity, ft./sec.^{2}
V	=	instantaneous velocity, ft./sec.
V_s	=	velocity of sound, ft./sec.
h	=	altitude above sea level, ft.
t	=	time, sec.
A	=	largest cross-sectional area of rocket, sq. ft.
D	=	drag due to air resistance, lbs.
σ	=	air density ratio
ρ_0	=	mass density of air at sea level

In Fig. 1 the forces acting on the rocket in vertical flight are shown.

Summing the forces:

$$\Sigma \text{ Forces} = 0 = F - W - D - (W/g)a \qquad (1)$$

The thrust developed by the motor is expressed by

$$F = mc \qquad (2)$$

Then from Eqs. (1) and (2):

$$a = (mc - W - D)g/W \qquad (3)$$

If the rate of flow of combustibles is constant during powered flight, one can write:

$$W = W_0 - mgt \tag{4}$$

At the start of the flight,

$$W = W_0,\ a = a_0,\ V = 0,\ D = 0 \tag{5}$$

Then Eq. (3) becomes

$$a_0 = (mc - W_0)g/W_0 \tag{6}$$

and

$$m = W_0(a_0 + g)/cg \tag{7}$$

Eq. (3) can now be evaluated, using Eq. (4) and Eq. (7), and for the acceleration at any instant

$$a = -g + \frac{(a_0 + g)}{1 - \frac{t(a_0 + g)}{c}} - \frac{g}{1 - \frac{t(a_0 + g)}{c}} \frac{D}{W_0} \tag{8}$$

Flight *in Vacuo*

With no air resistance, the third term of Eq. (8) vanishes so that

$$a = \frac{dV}{dt} = -g + \frac{(a_0 + g)}{1 - \frac{t(a_0 + g)}{c}} \tag{9}$$

Integrating Eq. (9) one has, for the velocity at any instant:

$$V = \frac{dh}{dt} = -gt - c \log\left[1 - \frac{t(a_0 + g)}{c}\right] + V_0 \tag{10}$$

Integrating Eq. (10) one has, for the height at any instant:

$$h = -\frac{1}{2}gt^2 + ct + \left(\frac{c^2}{a_0 + g} - ct\right) \log\left[1 - \frac{t(a_0+g)}{c}\right] + V_0 t + h_0 \tag{11}$$

The maximum acceleration and maximum velocity will occur at the time that the fuel is exhausted. The time at which thrust ceases is expressed, using Eq. (4), by the relation

$$(1 - \zeta)W_0 = W_0 - mgt_p \tag{12}$$

Introducing Eq. (7) into Eq. (12), one obtains, for the duration of powered flight:

$$t_p = \zeta c/(a_0 + g) \tag{13}$$

If, at the start of the flight, $V_0 = 0$ and $h_0 = 0$, then

$$a_{max.} = -g + \frac{a_0 + g}{c - \zeta} \tag{14}$$

$$V_{max.} = -c\left[\frac{g\zeta}{a_0 + g} + \log(1 - \zeta)\right] \tag{15}$$

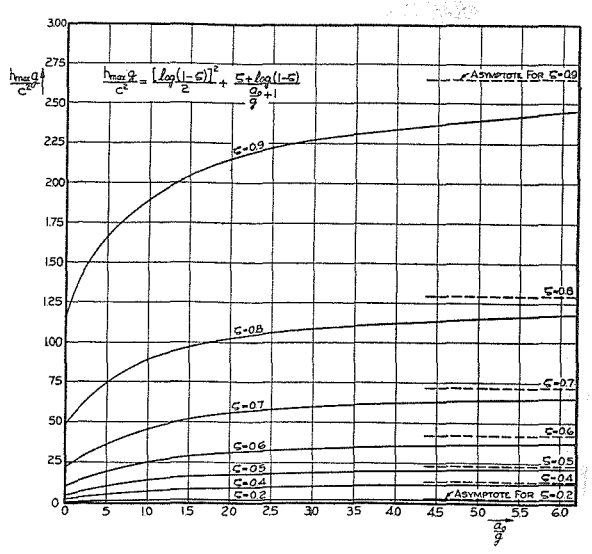

Fig. 2. Variation of $h_{max.}g/c^2$ with a_0/g for various ζ for flight *in vacuo*.

The maximum height reached will be the sum of the height at the time the fuel is exhausted and the height resulting from coasting. The height resulting from coasting is given by the expression:

$$h_c = V_{max.}^2/2g \tag{16}$$

Adding this to Eq. (11) and evaluating t_p from Eq. (13), the maximum height reached is

$$h_{max.} = \frac{c^2}{g}\left\{\frac{[\log(1 - \zeta)]^2}{2} + \frac{\zeta + \log(1 - \zeta)}{(a_0/g) + 1}\right\} \tag{17}$$

Eq. (17) shows that three parameters determine the rocket performance *in vacuo*. They are a_0, ζ, and c. In Fig. 2 the variation of $h_{max.}\,g/c^2$ is plotted for various values of a_0/g and ζ. The importance of having a large percentage of combustibles is clearly shown. The initial acceleration, a_0, is important until values in the neighborhood of $6g$ are reached.

Flight through a Resisting Medium

Considering flight through the air, the drag of the rocket can be expressed in the form

$$D = \rho_0 \sigma V^2 C_D A/2 \tag{18}$$

which, substituted in Eq. (8), gives

$$a = -g + \frac{(a_0 + g)}{1 - \frac{t(a_0 + g)}{c}} - \frac{g\rho_0\sigma V^2}{2\left[1 - \frac{t(a_0 + g)}{c}\right]} \cdot \frac{C_D A}{W_0} \tag{19}$$

This is the fundamental equation for vertical rocket flight. In addition to the performance parameters for flight *in vacuo*, the ratio $C_D A/W_0$ also has important significance in the construction of the sounding rocket. As it appears in a term which reduces the acceleration of the rocket, it should be as small as possible. A rocket

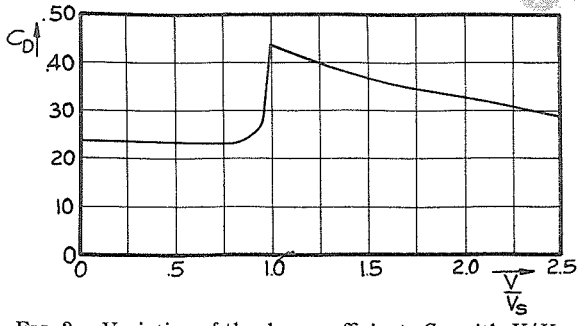

FIG. 3. Variation of the drag coefficient, C_D, with V/V_s.

of given initial weight should have as small a cross-section as possible and be of a shape that minimizes the drag coefficient.

As the density ratio, σ, and the drag coefficient, C_D, will be subject to great changes during flight, and are difficult to express accurately analytically, two ways of solving Eq. (19) are open. First, approximations can be made for the variation of σ and C_D to make an analytic solution possible, or second, a step-by-step method of integration of any degree of accuracy can be applied. The first method is quite likely to lead to extremely large errors, so that the second method has been chosen.

The variation of σ with height was obtained from references (4) and (5). The variation of C_D with the velocity of flight was taken from reference (6). It has been assumed, due to the lack of information, that the drag of the rocket was identical to the drag of a shell without a jet issuing at its base. The variation of the drag coefficient is reproduced from reference (6) in Fig. 3.

To describe the rocket flight, the following equations were used in the numerical calculations:

$$a_n = -g + \frac{(a_0 + g)}{1 - \frac{t_n(a_0 + g)}{c}} - \frac{g\rho_0\sigma_n V^2_{n-1}}{2\left[1 - \frac{t_n(a_0 + g)}{c}\right]} \cdot \frac{C_D A}{W_0} \qquad (20)$$

$$V_n = V_{n-1} + a_{n-1}\Delta t \qquad (21)$$

$$h_n = h_{n-1} + V_{n-1}\,\Delta t + (a_{n-1}/2)(\Delta t)^2 \qquad (22)$$

where

Δt = time interval under consideration
n = number of the interval in the r steps of the calculation

The acceleration during coasting is given by

$$a_{c_n} = \frac{F_c}{m} \qquad (23)$$

where

F_c = weight of the empty rocket plus air resistance or

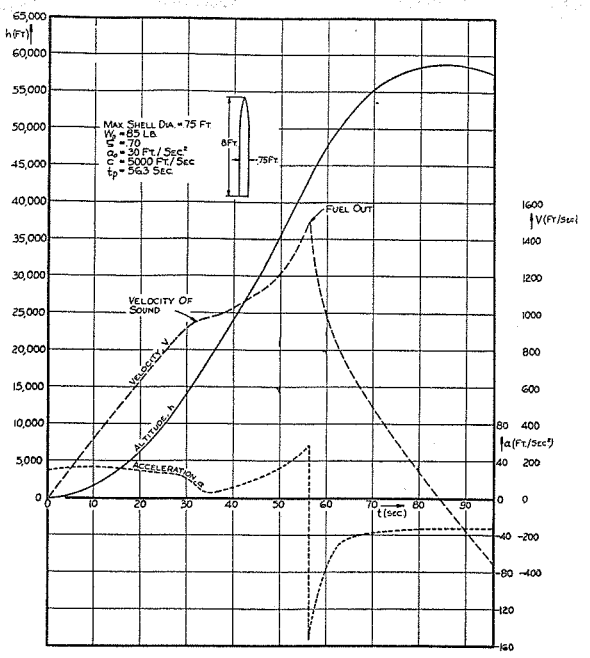

FIG. 4. Rocket performance for flight with air resistance, using a motor giving an effective exhaust velocity of 5000 ft./sec.

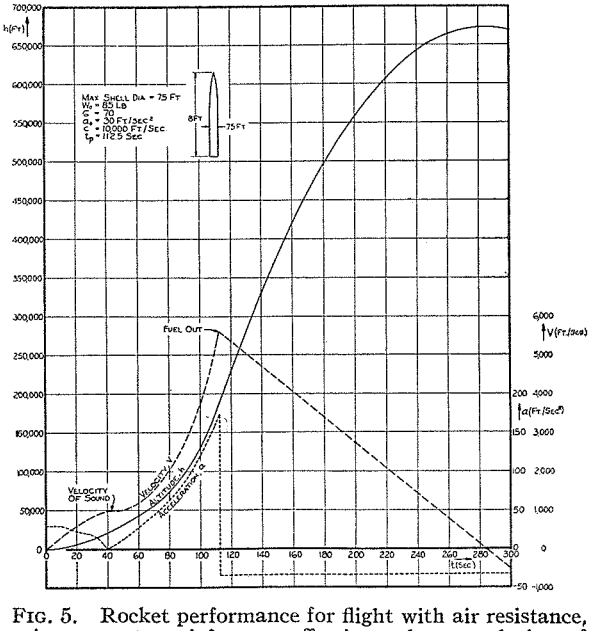

FIG. 5. Rocket performance for flight with air resistance, using a motor giving an effective exhaust velocity of 10,000 ft./sec.

$$a_{c_n} = -\left[g + \frac{\rho_0\sigma_n V^2_{n-1}\, g}{2(1 - \zeta)} \frac{C_D A}{W_0}\right] \qquad (24)$$

In the following results to be presented, it was necessary to select dimensions of what may be called a typical sounding rocket. Therefore, the results will apply only to rockets having the same value of the ratio $C_D A/W_0$. For rockets with a different value of the ratio, this analysis serves only as a guide to the performance to be expected.

In Fig. 4 are shown the performance curves of a rocket with $c = 5000$ ft./sec., $\zeta = 0.70$, and $a_0 = 30$ ft./sec.^{2}. The retarding influence of the air is made evident

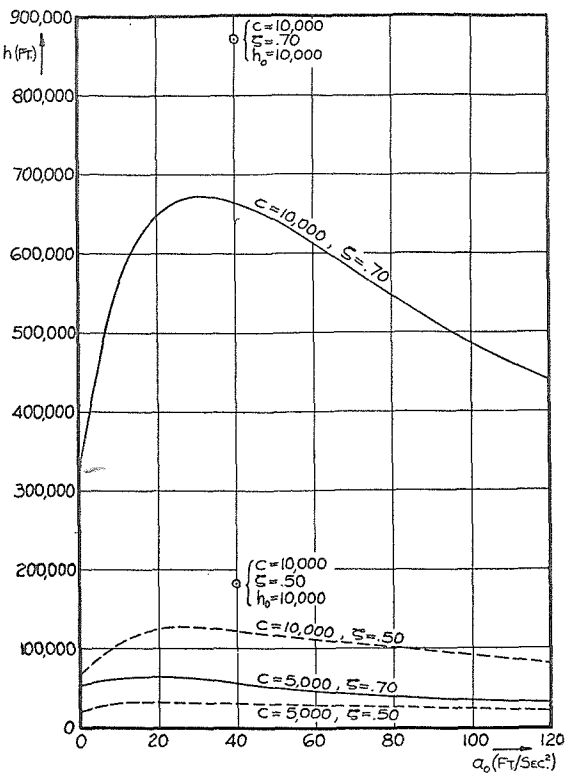

FIG. 6. Effect of a_0 on altitude to be reached for several performance parameter combinations.

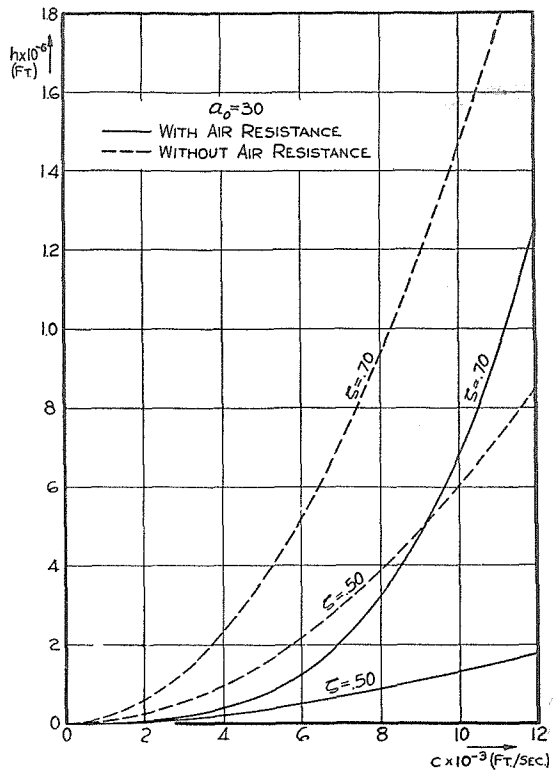

FIG. 7. Variation of altitude with c for $a_0 = 30$, with and without air resistance.

by the decrease in the acceleration as the velocity of sound is approached. The high density of the air at the time the fuel was exhausted prevented the rocket from coasting very high.

The performance curves shown in Fig. 5 are those for an identical rocket, but with a much more efficient motor which gives an exhaust velocity, c, of 10,000 ft./sec. For the same amount of thrust, the rate of flow of combustible is much smaller, so that the period of powered flight is greatly prolonged. This allows the rocket to get over the hump of the drag curve, and also to travel through less dense air. The velocity at the end of the powered flight will thus be much higher than before, causing the rocket to coast to a much higher altitude.

In Fig. 6 the variation of altitude with the initial acceleration is shown for the two cases. The importance of a high value of the exhaust velocity, c, is clearly evident. This shows that effort should be directed to develop a motor of high efficiency before flight attempts are made.

This figure also shows that there is a definite initial acceleration corresponding to the maximum possible height. This differs from flight *in vacuo* for which the height reached continually increases with the initial acceleration (see Fig. 2). A high velocity of flight through the dense lower levels of the atmosphere causes the combustibles to be rapidly "eaten up." The advantage to be gained by starting the rocket from a high point is shown in the figure by the calculated height for a rocket started from an initial altitude of 10,000 ft.

The variation of maximum height to be reached with the exhaust velocity, c, for flight *in vacuo* and in air, is shown in Fig. 7. This figure clearly illustrates the amount of height lost due to resistance of the air.

Higher altitudes may be reached by using the step-rocket. A rocket made up of three steps, respectively, of 600, 200, and 100 lbs., the lightest being fired last, with c of 10,000 ft./sec., a_0 of 40 ft./sec.^{2}, and ζ for each step of 0.70, starting from sea level, reaches a calculated altitude of 5,100,000 ft. and a maximum velocity of 11,000 m.p.h.

This analysis definitely shows that, if a rocket motor of high efficiency can be constructed, far greater altitudes can be reached than is possible by any other known means.

REFERENCES

[1] Ley, Willy, and Schaefer, Herbert, *Les Fusees Volantes Meteorologiques*, L'Aerophile, Vol. 44, No. 10, pp. 228–232, October, 1936.

[2] Africano, Alfred, *Rocket Motor Efficiencies*, Astronautics, No. 34, p. 5, June, 1936.

[3] Sänger, Eugen, *Neuere Ergebnisse der Raketenflugtechnik*, Flug, Special Publication No. 1, pp. 6–9, December, 1934.

[4] *Standard Atmosphere—Tables and Data*, N.A.C.A. Technical Report No. 218, 1925.

[5] Wood, K. D., *Technical Aerodynamics*, p. 8, McGraw-Hill, 1935.

[6] von Kármán, Th., and Moore, N. B., *Resistance of Slender Bodies Moving with Supersonic Velocities, with Special Reference to Projectiles*, A.S.M.E. Trans., p. 309, APM 54-27.

DECEMBER, 1938 Reprinted from the JOURNAL OF THE AERONAUTICAL SCIENCES VOLUME 6, NO. 2

Flight Analysis of a Sounding Rocket with Special Reference to Propulsion by Successive Impulses

HSUE-SHEN TSIEN and FRANK J. MALINA, *California Institute of Technology*

(Received July 6, 1938)

SUMMARY

In Part I of this paper an exact solution of the problem of determining the height reached by a body in vertical flight *in vacuo* propelled by successive impulses is presented. On the basis of this analysis it is concluded that a rocket propelled by successive impulses—the impulses being obtained, for example, from rapidly burning powder—can theoretically reach much greater heights than is possible by sounding balloons and, therefore, further experimental research is justified. In Part II the effect of the variation of the acceleration of gravity with height above sea level on the flight performance of a sounding rocket is analyzed. For a 1000 mile sounding rocket the decrease in gravitational pull accounts for a 25 percent increase in the maximum height reached over that calculated on the basis of a constant gravitational acceleration. In Part III the fundamental performance equation for flight of a sounding rocket in air is expressed in terms of dimensionless parameters and factors and their physical significance is discussed. Finally, in Part IV the theory of the preceding sections is applied to a specific case of a sounding rocket propelled by successive impulses which are supplied by a reloading type of powder rocket motor.

INTRODUCTION

IN 1919, R. H. Goddard[1] published the historically important paper which suggested the use of nitrocellulose powder as a propellant for raising a sounding rocket to altitudes beyond the range of sounding balloons. To determine the feasibility of this propellant, a series of experiments had been carried out and it was found that a thermal efficiency of 50 percent could be expected if the powder was exploded in a properly designed chamber and the resulting gases were allowed to escape at high velocity through an expanding nozzle. In 1931, R. Tilling used a mixture of potassium chlorate and naphthalene as propellant and actually reached an altitude of 6600 feet. More recently, L. Damblanc[2] made static tests with a slow burning black powder and from these estimated that a height of 10,000 feet could be reached using a two-step arrangement. The results so far reported offer an incentive to further analysis.

The propulsion obtained by the use of powder charges in a rocket motor, which are supplied by a reloading mechanism, is referred to in this paper as propulsion by successive impulses. This type of propulsion is essentially different from the type of propulsion made available by a rocket motor which continuously burns a combustible mixture at constant pressure. The thrust of the latter rocket motor is nearly constant, whereas in the former case, due to the rapidness of the combustion of the powder charges, the propulsion consists of a series of uniform impulses.

The effect of decreasing gravitational acceleration on the maximum height reached by a rocket has been considered by A. Bartocci.[3] However, he assumes that the rocket itself has a constant acceleration during powered flight. L. Breguet and R. Devillers[4] also considered the effect of the variation of g. To simplify the analysis, they assumed that the acceleration of the rocket was equal to a constant multiple of g. Since the sounding rocket will be propelled by a nearly constant thrust or a uniform rate of successive impulses, in Part II the authors have studied the problem anew according to this mode of propulsion.

When the sounding rocket is ascending through the air the maximum height reached is less than that reached for flight *in vacuo*. Recently, studies have been made of the problem by W. Ley and H. Schaefer[5] and by F. J. Malina and A. M. O. Smith.[6] On the basis of the latter study a group of new performance parameters and factors have been isolated from the general performance equation, and these are discussed in Part III.

NOTATION

Referring to Fig. 1, the following notation has been used throughout the paper:

w = weight of propellant and propellant container ejected per impulse, lbs.
k = ratio of propellant container weight to sum of container and propellant weight ejected per impulse.
λ = $(1 - k)$.
W_0 = initial weight of rocket, lbs.
M_0 = initial mass of the rocket, slugs.
W_r = instantaneous weight of rocket, lbs.
ζ = ratio of initial weight of propellants to initial total weight of a rocket propelled by constant thrust.
ζ_1 = ratio of initial weight of propellants to initial total weight of a rocket propelled by successive impulses.
ζ_1' = ζ_1/λ.
n = number of impulses per second.
N = total number of impulses occurring during powered flight.

t = time, sec.
Δt = interval between impulses, sec.
a_0 = initial acceleration imparted to rocket, ft. per sec.^{2}
g_0 = acceleration of gravity at the starting point of flight, ft. per sec.^{2}
g = acceleration of gravity above the starting point of flight, ft. per sec.^{2}
c = effective exhaust velocity of ejected propellant, ft. per sec.
v = instantaneous velocity, ft. per sec.
Δv_r = velocity imparted to rocket by the rth impulse, ft. per sec.
v_r' = velocity at end of the rth interval, ft. per sec.
v_{s_0} = velocity of sound corresponding to atmospheric conditions at the starting point of flight, ft. per sec.
v_s = velocity of sound corresponding to atmospheric conditions at height reached by the rocket at time t, ft. per sec.
B = Mach's number = v/v_s.
$V_{max.}$ = velocity of rocket at start of coasting flight, ft. per sec.
$V_{max._0}$ = velocity of rocket at start of coasting flight if g is constant and equal to g_0, ft. per sec.
h = altitude above sea level, feet.
h_r = height reached at the beginning of the rth interval, feet.
h_r' = height reached at the end of the rth interval, feet.
H_P = height traveled during powered flight, feet.
H_{P_0} = height traveled during powered flight, if g is constant and equal to g_0, feet.
H_C = height traveled during coasting flight, feet.
H_{C_0} = height traveled during coasting flight, if g is constant and equal to g_0, feet.
$H_{max.}$ = height traveled during powered flight and coasting flight, feet.
$H_{max._0}$ = height traveled during powered flight and coasting flight, if g is constant and equal to g_0, feet.
R = radius of earth, 2.088×10^8, feet.
D = drag on rocket due to air resistance, lbs.
C_D = drag coefficient of rocket.
C_D^* = drag coefficient of rocket at velocity of sound.
Λ = drag-weight factor (discussed in the section on the effect of air resistance).
ρ_0 = mass density of air at the starting point of flight, slugs per cu.ft.
σ = ratio of air density at altitude to air density at the starting point of flight.
T = absolute temperature of atmosphere at the height reached by the rocket at time t, °F.
T_0 = absolute temperature of atmosphere at the starting point of flight, °F.

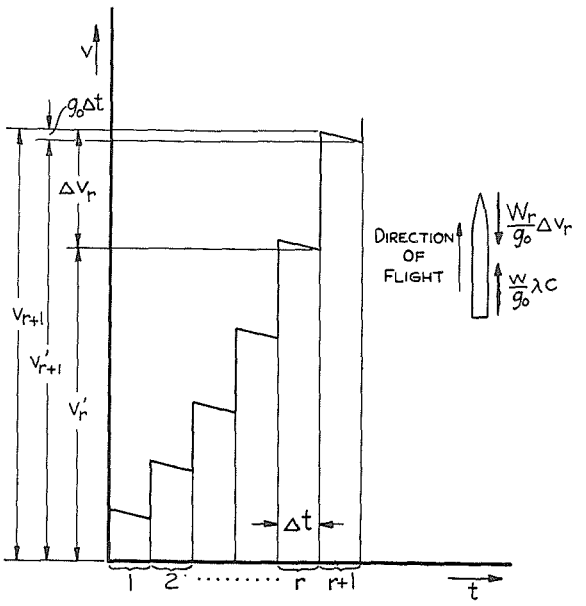

FIG. 1. Variation of the flight velocity v with the time t.

A = largest cross-sectional area of rocket shell, sq.ft.
d = largest diameter of rocket shell, ft.
l = length of rocket shell, ft.

I

An approximate method of calculating the maximum height reached by a rocket propelled by powder was developed by R. H. Goddard.[1] To simplify the analysis a continuous loss of mass was assumed and the problem was so stated, that a minimum mass of propellant necessary to lift one pound of mass at the end of the flight to any desired height was determined. However, if high-powered powder is used, the rate of burning is so rapid that the propulsive action is instantaneous. The rocket is thus acted upon by an impulse rather than by a constant thrust.

In the following analysis, it has, therefore, been assumed that the propulsive force is an impulsive force, *i.e.*, the force acts for such a brief interval of time that the rocket does not change its position during the application of the force, although its velocity and its momentum receive a finite change. If the combustion process of the propulsive unit takes place at constant volume this assumption is justified. Further, a study of interior ballistics of small arms reveals that the period between the ignition of the powder charge and the bullet's arrival at the end of a two-foot barrel is of the order of 14 ten-thousandths of a second. If the gases are not restrained and their travel through the burning chamber and the nozzle is of much shorter length, as is the case for the rocket motor, even shorter periods of duration of action can be expected.

Assuming that the propulsive force acts as an impulse, then the motion of the rocket can be calculated by Newton's third law, which states that

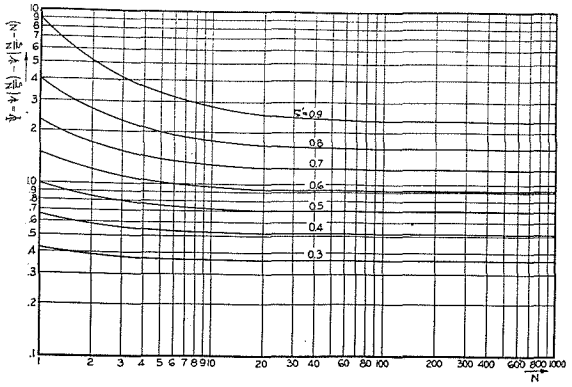

FIG. 2. Variation of Ψ with N for various values of ζ_1'.

impulses between two bodies are equal and opposite. Hence, equating the momentum of the exhaust gases to the momentum imparted to the rocket, using the quantities defined in the list of notation and referring to Fig. 1, the following relation can be written for flight *in vacuo:*

$$(\lambda w/g_0)c = (W_r/g_0)\,\Delta v_r \tag{1}$$

where

$$\lambda = (1 - k) \quad \text{and} \quad W_r = W_0 - rw \tag{2}$$

or

$$\Delta v_r = \frac{w\lambda c}{W_0 - rw} = \frac{\zeta_1'\lambda c}{N}\left(\frac{1}{1 - r\zeta_1'/N}\right) \tag{3}$$

where

$$\zeta_1' = wN/W_0 = \zeta_1/\lambda$$

During the interval between impulses, Δt, the velocity is reduced by the action of gravity so that at the end of the rth interval, the velocity of the rocket will be

$$v_r' = v_r - g_0\Delta t = v_{r-1}' + \Delta v_r - g_0\Delta t \tag{4}$$

Therefore

$$v_r' = \sum_{s=1}^{s=r} \Delta v_s - rg_0\Delta t \tag{5}$$

Substituting for Δv_s from Eq. (3)

$$v_r' = \frac{\zeta_1'\lambda c}{N}\sum_{s=1}^{s=r}\frac{1}{1 - s(\zeta_1'/N)} - rg_0\Delta t \tag{6}$$

or

$$v_r' = \frac{\zeta_1'\lambda c}{N} S_1 - rg_0\Delta t$$

where

$$S_1 = \sum_{s=1}^{s=r}\frac{1}{1 - s(\zeta_1'/N)}$$

The height gained during each interval will be represented by the area under the velocity curve in the interval, or

$$h_r' - h_r = v_r'\Delta t + \tfrac{1}{2}g_0(\Delta t)^2 \tag{7}$$

Therefore, at the end of the Nth interval which is the end of the powered flight, the height will be

$$H_{P_0} = \sum_{r=1}^{r=N} v_r'\Delta t + (N/2)g_0(\Delta t)^2$$

Substituting for v_r' its value in Eq. (6)

$$H_{P_0} = \sum_{r=1}^{r=N}\Delta t\left\{\frac{\zeta_1'\lambda c}{N}\sum_{s=1}^{s=r}\frac{1}{1 - s(\zeta_1'/N)} - rg_0\Delta t\right\} + \frac{N}{2}g_0(\Delta t)^2$$

$$= \frac{\zeta_1'\lambda c}{N}\Delta t\sum_{r=1}^{r=N}\frac{N + 1 - r}{1 - r(\zeta_1'/N)} - g_0(\Delta t)^2\sum_{r=1}^{r=N}(r - \tfrac{1}{2})$$

$$= \frac{\zeta_1'\lambda c}{N}\Delta t S_2 - \frac{N^2}{2}g_0(\Delta t)^2 \tag{8}$$

where

$$S_2 = \sum_{r=1}^{r=N}\frac{N + 1 - r}{1 - r(\zeta_1'/N)}$$

The maximum height reached will be the sum of the height at the end of powered flight and the height traveled during coasting or

$$H_{max.0} = H_{P_0} + H_{C_0} = H_{P_0} + V^2_{max.0}/2g_0 \tag{9}$$

To calculate the maximum height one has first to evaluate the sums S_1 and S_2.* Noting that

$$\frac{1}{1 - s(\zeta_1'/N)} = \int_0^\infty e^{-x\{1 - s(\zeta_1'/N)\}}dx$$

S_1 can be written in the form

$$S_1 = \int_0^\infty e^{-x}\sum_{s=1}^{s=r}(e^{x\zeta_1'/N})^s dx = \int_0^\infty e^{-x}\frac{e^{x\zeta_1'/N} - e^{(r+1)\zeta_1'/N}}{1 - e^{x\zeta_1'/N}}dx$$

Putting

$x = Ny/\zeta_1'$, the above intergral becomes

$$S_1 = -\frac{N}{\zeta_1'}\int_0^\infty e^{-Ny/\zeta_1'}\left(\frac{1 - e^{ry}}{1 - e^{-y}}\right)dy = \frac{N}{\zeta_1'}\left\{\psi\left(\frac{}{\zeta_1'}\right) - \psi\left(\frac{N}{\zeta_1'} - r\right)\right\} \tag{10}$$

where $\psi(z) = (d/dz)\{\log\Gamma(z)\}$. (The reader is referred to references 7 and 8 for detailed information on this function.) Similarly, S_2 can be summed as

$$S_2 = \frac{N}{\zeta_1'}\left\{N - \left[\frac{N}{\zeta_1'} - (N + 1)\right]\times\left[\psi\left(\frac{N}{\zeta_1'}\right) - \psi\left(\frac{N}{\zeta_1'} - N\right)\right]\right\} \tag{11}$$

Substituting Eqs. (10) and (11) into Eqs. (6) and (8), and then into Eq. (9)

$$H_{max.0} = \frac{\lambda^2c^2}{2g_0}\Psi^2 - \frac{\lambda c}{n}\left\{\left(\frac{N}{\zeta_1'} - 1\right)\Psi - N\right\} \tag{12}$$

* The authors wish to thank Prof. H. Bateman for his suggestion of this method of summing.

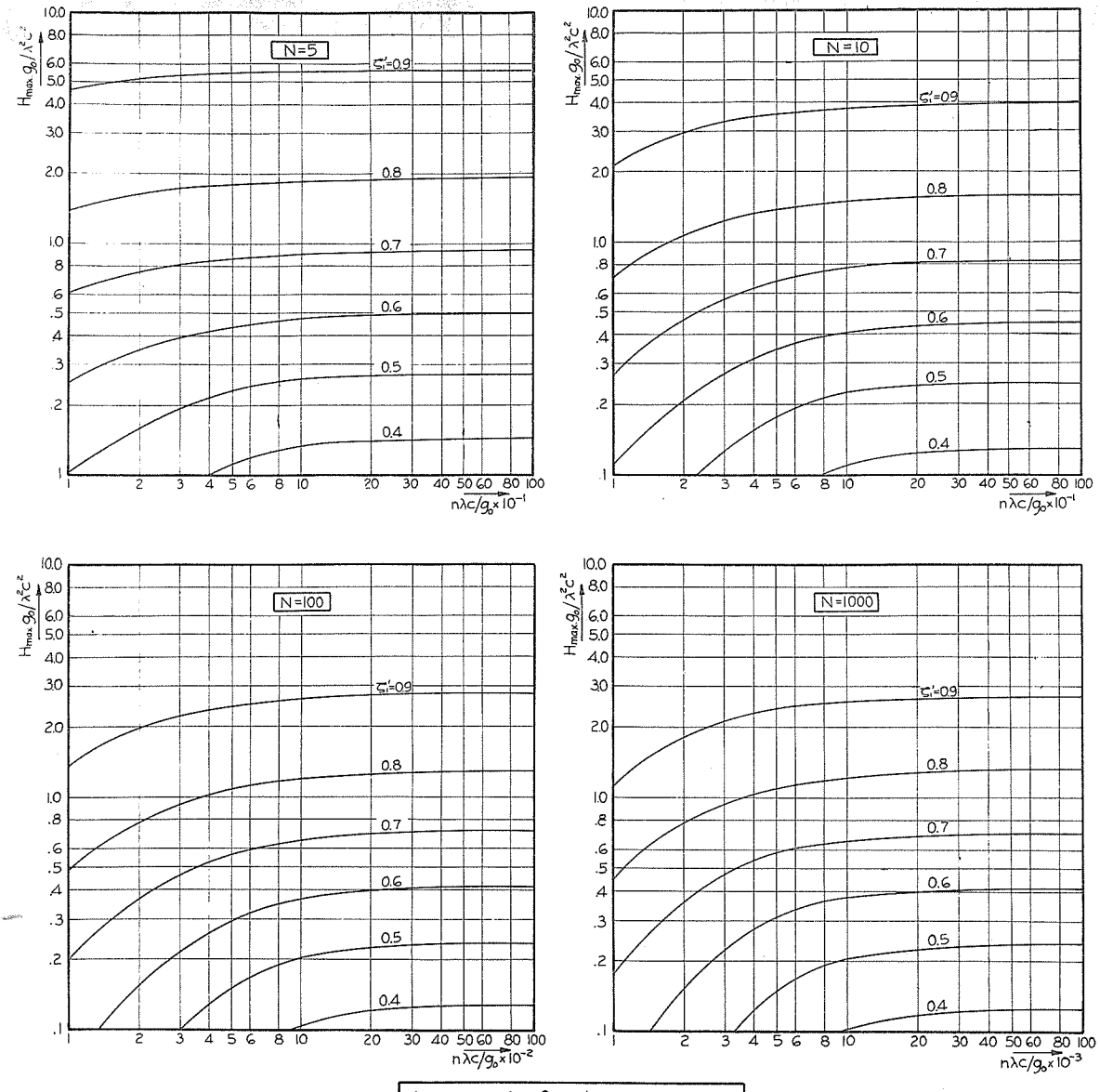

$$\frac{H_{max.}g_0}{\lambda^2c^2} = \frac{1}{2}\Psi^2 - \frac{1}{\frac{n\lambda c}{g_0}}\left[\left(\frac{N}{\zeta_1'}-1\right)\Psi - N\right]$$

FIG. 3. $H_{max_{.0}}g_0/\lambda^2c^2$ with nc/g_0 for various values of ζ_1'.

where $n = 1/\Delta t$, and $\Psi = \psi(N/\zeta_1') - \psi[(N/\zeta_1') - N]$.

For convenience of calculation in Fig. 2 the quantity Ψ is plotted against N for different values of ζ_1'.

It can easily be shown that when $N = 1$

$$\Psi = \zeta_1'/(1 - \zeta_1')$$

so that Eq. (12) reduces to

$$H_{max.0} = \frac{\lambda^2c^2}{2g_0}\left(\frac{\zeta_1'}{1 - \zeta_1'}\right)^2 \tag{12a}$$

Also, as $N \to \infty$, $\Psi \to -\log(1 - \zeta_1')$, thus Eq. (12) reduces to

$$H_{max.0} = \frac{\lambda^2c^2}{g_0}\left\{\frac{[\log(1 - \zeta_1')]^2}{2} + \frac{\zeta_1' + \log(1 - \zeta_1')}{(a_0/g_0) + 1}\right\} \tag{12b}$$

where

$$a_0 = \frac{\zeta_1'}{N}n\lambda c - g_0 = \frac{nw\lambda c}{W_0} - g_0 \tag{12c}$$

The quantity a_0 can be considered as the initial acceleration of the rocket if $N \to \infty$. It is interesting to notice that Eq. (12b) is the equation obtained by Malina and Smith (Ref. 6) for calculating the maximum height of a constant thrust rocket, as expected.

Fig. 3 shows the variation of $H_{max.0}g_0/\lambda^2c^2$ with $n\lambda c/g_0$ for different values of ζ_1' and for four values of N. These curves show that when the total number of impulses, N, becomes larger than 100, the maximum height reached is imperceptibly changed by increasing the number.

At this point it is necessary to discuss the similarity existing between a rocket propelled by successive

TABLE 1

Successive Impulses

$$H_{max._0} = \frac{\lambda^2 c^2}{g_0}\left\{ {}^1/_2\Psi^2 - \frac{1}{n\lambda c/g_0}\left[\left(\frac{N}{\zeta_1'} - 1\right)\Psi - N\right]\right\}$$

Case	λc Ft. per Sec.	ζ_1'	N	n Impulses per Sec.	$H_{max._0}$ Feet
1	10,000	0.70	326	3	1,472,000
2	10,000	0.70	10	0.092	1,686,000
3	7,000	0.70	326	3	560,000
4	7,000	0.70	10	0.092	676,000

Constant Thrust

$$H_{max._0} = \frac{c^2}{g_0}\left\{ {}^1/_2\,[\log(1-\zeta)]^2 - \frac{1}{a_0/g_0 + 1}\,[\log(1-\zeta) + \zeta\right\}$$

Case	C	ζ	a_0	$H_{max._0}$ Feet
1	10,000	0.70	32.2	1,468,000
2	10,000	0.70	32.2	1,468,000
3	7,000	0.70	12.9	555,000
4	7,000	0.70	12.9	555,000

impulses and a rocket propelled by constant thrust. The former loses not only the mass of the propellant, but also the containers for the individual charges. The difference in effect on the rocket between the propellant and its containers is that the propellant has an effective exhaust velocity, c, while the ejected containers leave the rocket without appreciable velocity. The propulsive action, however, will remain the same if the whole cartridge, that is, the propellant charge and its container, is considered wholly as propellant, but leaving the motor at a reduced effective exhaust velocity λc. The rocket propelled by constant thrust loses only the mass equal to the propellant carried; therefore, it can be said to be equivalent to the "successive impulses" rocket if its effective exhaust velocity and its total mass of propellant are equal, respectively, to the reduced exhaust velocity and to the sum of the masses of all the containers of the "successive impulses" rocket. In other words, c is equal to λc and ζ is equal to ζ_1'.

In Table 1 the heights for four cases have been calculated to illustrate the effect of the exhaust gas velocity and the total number of impulses given to a rocket whose weight ratio, ζ_1' is 0.70. It will be noticed that for flight *in vacuo* a greater height will be reached if a smaller number of impulses is employed. The lower portion of the Table shows the maximum height reached by an equivalent "constant thrust" rocket for the same four cases with the initial acceleration given by Eq. (12c). The close agreement between the maximum height reached by use of successive impulses, when the total number of impulses exceeds 100, and that reached by the use of constant thrust simplifies the solution of the problem of decreasing acceleration of gravity with height, and enables prediction for flight with air resistance to be based on the results obtained for a rocket propelled by constant thrust (cf. reference 6). These problems are considered in the following sections.

II

It is well known that the acceleration of gravity decreases with the height above the earth's surface according to the following relation:

$$g = g_0[R/(R + h)]^2 \tag{13}$$

At an altitude of 1000 miles the acceleration is only 0.64 times that at sea level. Therefore, for flights up to such altitudes the assumption that g is approximately constant is no longer valid. It was shown by Malina and Smith[6] that a three-step rocket could theoretically reach such an altitude. Thus it is interesting to see how the decrease of g will increase the maximum height reached by the rocket.

First, the effect on powered flight *in vacuo* will be considered and then on coasting flight *in vacuo*. For powered flight the analysis is based on the assumption that the thrust is constant. However, the results can be applied to the case of propulsion by successive impulses if the total number of impulses, N, exceeds 100 as was justified in the previous section.

The equivalent mass of gas flowing per second continuously for the case of successive impulses is

$$wn/g_0 = m \tag{14}$$

Assuming that the rocket starts from rest at sea level, the equation of motion *in vacuo* is

$$\frac{d^2h}{dt^2} = -g_0\left(1 + \frac{h}{R}\right)^{-2} + \frac{mc/M_0}{1 - (m/M_0)t} \tag{15}$$

This is a non-linear differential equation which cannot be solved by usual means. However, for all practical purposes the ratio h/R during powered flight is much smaller than 1, therefore, only first order terms in h/R occurring in the expansions need to be retained. This approximation linearizes the equation to the form

$$\frac{d^2h}{dt^2} = g_0\left(\frac{2h}{R} - 1\right) + \frac{mc/M_0}{1 - (m/M_0)t} \tag{16}$$

The solution of this equation with the initial condition that $h = 0$ and $dh/dt = 0$ when $t = 0$ is

$$h = \frac{R}{2}\left\{1 - \cosh\sqrt{\frac{2g_0}{R}}\,t\right\} + \frac{c}{2\sqrt{2g_0/R}}\left\{e^{\xi u}\int_{\xi}^{\xi u}\frac{e^{-x}dx}{x} - e^{-\xi u}\int_{\xi}^{\xi u}\frac{e^{x}dx}{x}\right\} \tag{17}$$

where $\xi = \sqrt{2g_0/R}\ M_0/m$ and $u = 1 - (m/M_0)t$. At the end of the powered flight, the time is

$$t = t_P = M_0\zeta/m \tag{18}$$

Therefore, the height at the end of the powered flight is

$$H_P = \frac{R}{2}\left\{1 - \cosh\sqrt{\frac{2g_0}{R}}\,\frac{M_0\zeta}{m}\right\} + \frac{c}{2}\sqrt{\frac{R}{2g_0}}\left\{e^{\xi(1-\zeta)}\int_{\xi}^{\xi(1-\zeta)}\frac{e^{-x}dx}{x} - e^{-\xi(1-\zeta)}\int_{\xi}^{\xi(1-\zeta)}\frac{e^{x}dx}{x}\right\} \tag{19}$$

If the hyperbolic cosine term and the integrals are expanded and only first order terms in $1/R$ are retained in consistency with the linearization of Eq. (15), the equation reduces to

$$H_P = -\left\{\frac{\zeta^2 g_0}{2}\left(\frac{W_0}{w}\right)^2 + \frac{\zeta^4 g_0^2}{12R}\left(\frac{W_0}{w}\right)^4\right\} + c\,\frac{W_0}{w}\left\{(1-\zeta)\log(1-\zeta) + \zeta\right\} +$$

$$\frac{cg_0}{18R}\left(\frac{W_0}{w}\right)^3\left\{6(1-\zeta)^3\log(1-\zeta) + \zeta(11\zeta^2 - 15\zeta + 6)\right\}$$

$$= H_{P_0} + \frac{g_0}{6R}\left(\frac{W_0}{w}\right)^3\left\{\frac{c}{3}\left[6(1-\zeta)^3\log(1-\zeta) + \zeta(11\zeta^2 - 15\zeta + 6)\right] - \frac{\zeta^4 g_0}{2}\left(\frac{W_0}{w}\right)\right\} \tag{20}$$

Differentiating Eq. (17), and substituting the relation of Eq. (18), the maximum velocity at the end of powered flight is

$$V_{max.} = -\sqrt{\frac{Rg_0}{2}}\sinh\sqrt{\frac{2g_0}{R}}\,\frac{M_0\zeta}{m} - \frac{c}{2}\left\{e^{\xi(1-\zeta)}\int_{\xi}^{\xi(1-\zeta)}\frac{e^{-x}dx}{x} + e^{-\xi(1-\zeta)}\int_{\xi}^{\xi(1-\zeta)}\frac{e^{x}dx}{x}\right\} \tag{21}$$

Again expanding and retaining only first order terms in $1/R$, Eq. (21) reduces to

$$V_{max.} = -\left\{\left(\frac{W_0}{w}\right)\zeta + \frac{1}{3}\,\frac{\zeta^3 g_0^2}{R}\left(\frac{W_0}{w}\right)^3\right\} - \left\{c\log(1-\zeta) + \frac{cg_0}{2R}\left(\frac{W_0}{w}\right)^3\left[2(1-\zeta)^2\log(1-\zeta) + 2\zeta - 3\zeta^2\right]\right\}$$

$$= V_{max.0} - \frac{g_0(W_0/w)^2}{R}\left\{\frac{\zeta^3 g_0(W_0/w)}{3} + \frac{c}{2}\left[2(1-\zeta)^2\log(1-\zeta) + 2\zeta - 3\zeta^2\right]\right\} \tag{22}$$

It is seen that the second terms of Eq. (20) and (22) are the corrections to be applied to H_{P_0} and $V_{max.0}$ to account for the variation of the acceleration of gravity. Since both corrections are first order approximations they can be expected to apply approximately also to the case of successive impulses, even when the total number of impulses is less than 100.

The coasting height reached by the rocket due to its velocity at the end of powered flight can be obtained by equating the increase of potential energy during coasting flight to the kinetic energy at the end of powered flight. Thus,

$$\frac{1}{2}\,V_{max.}^2 = g_0\int_{H_P}^{H_P+H_C}\frac{dh}{[1 + (h/R)]^2}$$

or

$$H_C = (H_P + R)\left\{\frac{1}{1 - \dfrac{V_{max.}^2}{2g_0\,[R/(H_P+R)]^2(H_P+R)}} - 1\right\} \tag{23}$$

Putting $V_{max.}^2/2g_0[R/(H_P+R)]^2 = H_{C_0}$, which is the coasting height obtained by assuming a constant gravitational acceleration of the value equal to that at the height H_P, *i.e.*, the height where coasting starts, then Eq. (23) can be written

$$H_C = (H_P + R)\left\{\frac{1}{1 - H_{C_0}/(H_P+R)} - 1\right\}$$

Upon expanding the second term, this equation becomes,

$$H_C = H_{C_0}\left\{1 + \left(\frac{H_{C_0}}{H_P+R}\right) + \left(\frac{H_{C_0}}{H_P+R}\right)^2 + \left(\frac{H_{C_0}}{H_P+R}\right)^3 + \cdots\right\} \tag{24}$$

This equation shows that if the coasting flight starts from sea level, and if the maximum height reached is about 1000 miles, the increase due to the decrease in g is over 25 percent.

III

When the sounding rocket is ascending through the atmosphere instead of *in vacuo*, air resistance comes into play, causing the acceleration of the rocket to be reduced, which decreases the maximum height reached. Since air resistance increases with the air density and with the square of the flight velocity, it is desirable to keep the rocket from ascending too rapidly through the lower layers of the atmosphere where the air density is high. For this reason the optimum initial acceleration will no longer be infinite as shown by Eq. (12b). For the case of constant thrust Malina and Smith[6] have found that the optimum acceleration is around 30 ft. per sec.[2] For a total number of impulses greater than 100, the difference between propulsion by successive impulses and by constant thrust is very small, so one may expect the above optimum value of initial acceleration to hold for both cases of propulsion.

The actual amount of reduction in maximum height due to air resistance can be calculated by the method of step-by-step integration, if fair accuracy is desired. This integration is carried out by using the fundamental equation for vertical rocket flight which, as given in the previous paper (Ref. 6) is

$$\frac{d^2h}{dt^2} = a = -g + \frac{a_0 + g_0}{1 - t(a_0 + g_0)/c} - \frac{g_0\rho_0\sigma v^2}{2\left[1 - \dfrac{t(a_0 + g_0)}{c}\right]}\frac{C_DA}{W_0} \tag{25}$$

The significance of the ratio C_DA/W_0 was discussed in that paper.[6] Greater significance can, however, be attached to the various terms in the equation if it is transformed into the non-dimensional form

$$\frac{a}{g_0} = -\frac{g}{g_0} + \frac{\dfrac{a_0}{g_0} + 1}{1 - \dfrac{g_0t}{c}\left(\dfrac{a_0}{g_0} + 1\right)} - \frac{\left(\sigma\dfrac{T}{T_0}\right)\left(\dfrac{C_D}{C_D{}^*}B^2\right)\Lambda}{1 - \dfrac{g_0t}{c}\left(\dfrac{a_0}{g_0} + 1\right)} \tag{26}$$

where

$$\Lambda = \frac{\dfrac{\rho_0}{2}C_D{}^*Av_{s_0}{}^2}{W_0}$$

In Eq. (26) appear two types of significant quantities. First, quantities, called "factors," which are constant for any given family of rockets, and second, two quantities called "parameters," one of which is characteristic for a given family of rockets but changes in value along the flight path, and one which depends on the physical properties of the atmosphere. Thus there are the following factors:

a_0/g_0 = ratio of initial acceleration to g_0 ~ "initial acceleration factor," a motor characteristic.

c = exhaust velocity in ft. per sec. ~ "exhaust velocity factor," a motor characteristic.

Λ = "drag-weight factor."

ζ = ratio of weight of combustibles to total initial weight of the rocket ~ "loading factor."

The first two factors, *i.e.*, the "initial acceleration factor" and the "exhaust velocity factor," determine the characteristics of the propelling unit for a given family of rockets while the "drag-weight factor" and the "loading factor" determine the physical dimensions of the rockets. The "drag-weight factor" is a ratio of the drag of the rocket at sea level when traveling with the velocity of sound to the initial weight of the rocket. Since for any given family of rocket shapes the only terms in the factor which can be varied are the maximum cross-sectional area, A, and the initial weight, W_0, it is clear that if the initial weight is doubled then the cross-sectional area must also be doubled to keep the factor the same. The "loading factor" needs to be discussed in some detail as it does not appear explicitly in Eq. (26). Eq. (26) is a differential equation of the flight path which is satisfied at every point along the flight path. The loading factor ζ comes in only when this equation is integrated and the limits of integration are put in. For example, consider two rockets with identical performance factors and parameters, with the exception that one has a ζ of 0.90 and the other has a ζ of 0.50. The flight path of the two rockets will be identical up to the time that 0.50 times the initial weight of the rockets is used up as combustibles. At this point the rocket having a ζ of 0.50 will begin to decelerate while the one having a ζ of 0.90 will continue to accelerate until the remaining combustibles are used up. It is thus seen that the value of ζ controls the maximum height reached.

The two performance parameters are:

$\sigma T/T_0$ ~ physical properties of the atmosphere called the "atmosphere parameter."

$C_D/C_D{}^*$ ~ aerodynamic properties of the rocket called the "form parameter."

The "atmosphere parameter" for the earth's atmospheric layer will, of course, be the same for all rockets if standard conditions are assumed and its value depends only on the height the rocket has reached above the starting point of the flight. The "form parameter" is determined by the shape of the curve of C_D against B. This curve will be altered chiefly by the geometrical shape of the shell although it is also effected by the change in skin friction coefficient due to the change in Reynolds Number. As long as the rocket belongs to a family that has the same geometrical shape, which implies the same nose shape and the same l/d ratio, that is, the ratio of the length of the shell to the maximum diameter, the "form parameter" can be assumed to remain constant.

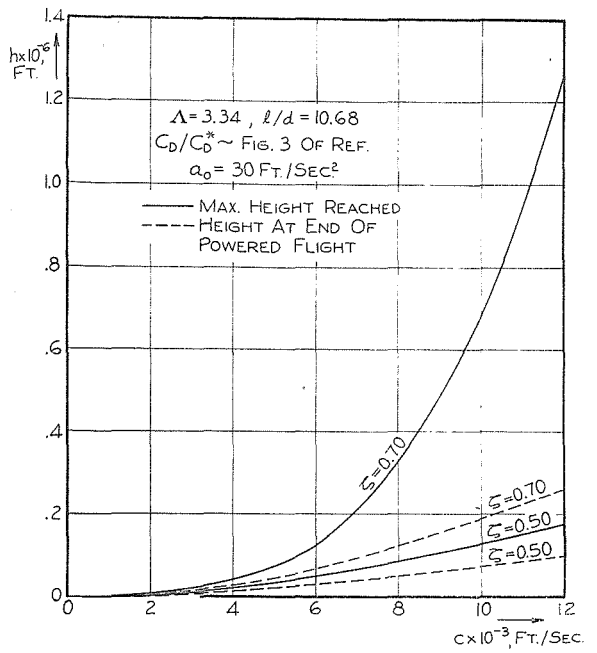

FIG. 4. Height reached in air at the end of powered flight and maximum height reached versus the exhaust velocity, c, for ζ of 0.50 and 0.70.

It is thus seen that the performance curves calculated for a typical rocket will also hold for a whole family of rockets determined by the values of the "factors" and of the "parameters" of the typical rocket and the design of a rocket to meet certain prescribed requirements is greatly simplified. Furthermore, for a good design of rocket form the variation of $C_D/C_D{}^*$, the form parameter, at the same values of B is small. Also, the deviation from standard atmospheric characteristics cannot be very large. Then, in view of the fairly accurate but not exact basic assumption of constant thrust, it is justified to use the same data for these two parameters for all cases. Thus, the performance problem is further simplified and depends only upon the four performance factors a_0/g_0, c, Λ, and ζ.

IV

The use of the results of the analysis developed in the preceding parts of this paper is illustrated in this section by the calculation of the performance of a rocket propelled by successive impulses, *e.g.*, a powder rocket. The performance of the powder rocket can be predicted from the results obtained for an equivalent rocket propelled by constant thrust, provided the powder rocket is acted upon by more than 100 impulses.

In making use of the equivalence existing between the two methods of propulsion it is necessary that the following quantities discussed in Part I and Part III be identical for the two cases: initial acceleration factor, a_0/g_0; exhaust velocity factor, c, for constant thrust and λc for successive impulses; drag-weight factor, Λ; loading factor, ζ, for constant thrust, and ζ_1' for successive impulses; atmosphere parameter $\sigma T/T_0$; form parameter, $C_D/C_D{}^*$; and slenderness ratio l/d.

For the example the following characteristics of the powder rocket are assumed:

POWDER ROCKET

W_0 = 85 lbs.	c = 7000 ft./sec.
ζ_1 = 0.658.	λc = 6580 ft./sec.
weight of powder per shot = 0.108 lbs.	$\zeta_1' = \zeta_1/\lambda$ = 0.70.
	d = 0.75 ft.
weight of cartridge = 0.007 lbs.	ν = 3.34.
	$C_D/C_D{}^* \sim$ Fig. 3 of reference 6.
m = 0.115 lbs. per shot.	
k = 0.06.	l/d = 10.68.
$\lambda = (l - k)$ = 0.94.	$\sigma T/T_0 \sim$ standard atmosphere, starting point —sea level.
n = 7.	
N = 518.	

EQUIVALENT CONSTANT THRUST ROCKET

W_0 = 85 lbs.	Λ = 3.34.
ζ = 0.70.	$C_D/C_D{}^* \sim$ Fig. 3 of reference 6.
c = 6580 ft./sec.	
$a_0 = (\zeta_1' n\lambda c/N) - g_0$.	l/d = 10.68.
= 30.0 ft. per sec.²	$\sigma T/T_0 \sim$ standard atmosphere, starting point —sea level.
d = 0.75 ft.	

The data for the equivalent rocket are now complete and it is found from Fig. 4 that $H_{max.}$ = 162,000 feet.

This is the maximum height reached by the rocket assuming that the acceleration of gravity does not vary with height. This assumption was shown in the preceding section to be practically valid for maximum heights up to about 800,000 feet.

Since the sounding rocket at the end of powered flight does not reach heights at which the acceleration of gravity is appreciably decreased, the heights calculated by Malina and Smith[6] can be used. In Fig. 4 the height at the end of powered flight is plotted against the exhaust velocity c for ζ = 0.70 and 0.50 for flight with air resistance. If the height at the end of powered flight is subtracted from the maximum height reached, the coasting height is obtained. This height may be perceptibly affected by the decreasing acceleration of gravity. Using Eq. (24) the corrected coasting height can be calculated. For a sounding rocket propelled by constant thrust of the same dimensions as above but with an exhaust velocity of 12,000 ft. per sec. it is found from Fig. 4 that

$$H_{max._0} = 1{,}270{,}000 \text{ feet}$$

From Fig. 4

$$H_P = 265{,}000 \text{ feet}$$

so that

$$H_{C_0} = H_{max._0} - H_P = 1{,}005{,}000 \text{ feet}$$

Using Eq. (24) the corrected coasting height is

$$H_C = 1{,}005{,}000\left[1 + \frac{1{,}005{,}000}{2.098 \times 10^8}\right] = 1{,}010{,}000 \text{ feet}$$

So that the maximum height with the coasting height corrected for decreasing acceleration of gravity is

$H_{max._0} = H_P + H_C = 265{,}000 + 1{,}010{,}000 =$ 1,275,000 feet

Conclusion

This study shows that a sounding rocket propelled by successive impulses can theoretically reach heights of much use to those interested in obtaining data on the structure of the atmosphere and extra-terrestrial phenomena if a propelling unit gives an exhaust velocity of 7000 ft. per sec. or more.

The possibility of obtaining such exhaust velocities depends upon two factors: first, the ability of the motor to transform efficiently the heat energy of the fuel into kinetic energy of the exhaust gases, and, second, the amount of heat energy that can be liberated from the fuel. In an actual motor which burns its fuel at constant volume by igniting a powder charge in the combustion chamber the ratio of the chamber pressure to the outlet pressure drops from a maximum at the beginning of the expansion to zero at the end of the process. It is not possible to design a nozzle that will expand the products of combustion smoothly during the whole process. Therefore, the attainable efficiency must be less than that of a corresponding "constant pressure" motor which has a mixture of combustibles, *e.g.*, gasoline and liquid oxygen, fed continuously into the combustion chamber at a constant pressure equal to the maximum pressure of the "constant volume" motor. However, very high maximum chamber pressures (up to 60,000 lbs. per sq. in. can be developed in a motor using constant volume burning, while the chamber pressure of a motor using constant pressure burning is limited to much lower pressures by the difficulty of feeding the combustibles. Therefore, the efficiency that can be obtained from motors using either of these processes should not be very different. As to the heat that can be liberated per unit mass of fuel, the present fuel, such as nitrocellulose powder for a constant volume motor, is much lower than the liquid combustibles such as gasoline and oxygen for a constant pressure motor.

These considerations indicate that the attainable exhaust velocity of a "constant volume" motor for propulsion by successive impulses will probably be lower than that of a "constant pressure" motor for supplying a continuous thrust. This is the reason why many experimenters abandoned the "constant volume" motor and turned to the "constant pressure" motor, the so-called liquid propellant motor. Theoretically, this defect of the "constant volume" motor can be compensated if a small total number of impulses (cf. Fig. 3) is used. However, the use of few impulses is of doubtful practical value because the resulting extreme accelerations will be harmful to instruments carried and will necessitate a heavier construction of the rocket.

However, even with the lower exhaust velocities of the "constant volume" motor it is shown by the analysis in this paper that with the exhaust velocity of 7000 ft. per sec. obtained experimentally by R. H. Goddard[1] it should be possible to build a powder rocket capable of rising above 100,000 feet. Thus it seems to the authors that a rocket propelled by successive impulses has useful possibilities and further experimental work is justified.

References

[1] Goddard, R. H.: *A Method of Reaching Extreme Altitudes*, Smithsonian Miscellaneous Collections, Vol. 71, No. 2, 1919.

[2] Damblanc, L.: *Les fusées autopropulsives à explosifs*, L'Aérophile, Vol. 43, pages 205–209 and pages 241–247, 1935.

[3] Bartocci, A.: *Le éscursioni in altezza col motore a reazione*, L'Aerotecnica, Vol. 13, pages 1646–1666, 1933.

[4] Breguet, L. and Devillers, R.: *L'Aviation superatmosphérique les aérodynes propulsées par reaction directe*, La Science Aérienne, Vol. 5, pages 183–222, 1936.

[5] Ley, W. and Schaefer, H.: *Les fusées volantes météorologiques*, L'Aérophile, Vol. 44, pages 228–232, 1936.

[6] Malina, F. J. and Smith, A. M. O.: *Analysis of the Sounding Rocket*, Journal of the Aeronautical Sciences, Vol. 5, pages 199–202, 1938.

[7] Whittaker and Watson: *Modern Analysis*, pages 246–247, 4th Edition, Cambridge, 1927.

[8] Davis, H. T.: *Tables of the Higher Mathematical Functions* Vol. 1, pages 277–364, Principia Press, 1st Edition, 1933